APPLICATIONS OF MODIFIED LOG-WAKE LAW IN SEDIMENT-LADEN FLOWS

MAY MYAT HLA

NATIONAL UNIVERSITY OF SINGAPORE

2003

APPLICATIONS OF MODIFIED LOG-WAKE LAW IN SEDIMENT-LADEN FLOWS

BY

MAY MYAT HLA

(B.Eng(Civil),YTU)

A THESIS SUBMITTED

FOR THE DEGREE OF MASTER OF ENGINEERING

DEPARTMENT OF CIVIL ENGINEERING

NATIONAL UNIVERSITY OF SINGAPORE

2003

ACKNOWLEDGEMENTS

The author would like to express her sincere appreciation and gratitude to her supervisor, Assistant Professor Dr. Guo Junke, John, for his constant advice, guidance and supervisions during the course of this research at the Department of Civil Engineering, National University of Singapore.

The author would like to extend her gratitude towards her colleagues and also to her friends for their invaluable help and contribution to her study.

The author would also like to express her appreciation for the assistance provided by the hydraulics and environmental laboratory staff of Department of Civil Engineering during the course of this study.

The author will forever be indebted to National University of Singapore for the award of Research Scholarship during the period of candidature.

Finally, the author is highly indebted to her parents and teachers, who had brought her to this level and hence her special thanks are due to them.

TABLE OF CONTENTS

SUMMARY

The objective of the present study is to investigate the effect of suspended sediment on velocity and concentration profiles in open channel flow. The modified log-wake law which can represent the entire vertical velocity profile of the open channel flow was presented. The investigations were then extended to turbulent flows over smooth bed forms using measurements reported in the limited literature.

The modified log-wake law examines the effects of secondary currents and free surface on velocity profile in smooth rectangular open channels. It consists of three components: the effect of channel bed, the effect of secondary currents that result from the sidewalls; and the effect of gravity that is due to the free surface. Therefore, the sediment laden flow in an open channel could be represented using this law postulated by Guo(2002).

The first part of this study reveals the effect of sediment on the velocity profile in open channel. Where, the effect of suspended sediment could be thought of as a factor that made von Karman constant of sediment water lower than that of clear water. Moreover, the increase in sediment concentration reduces the turbulence transfer coefficient under defined condition and in turn reduces the resistance of the flow. This effect causes the sediment-laden water to flow more rapidly than clear water in the outer region.

The second part suggests the structure of general concentration profile equation that completely describes the distribution of sediment concentration over the whole depth. The suspended concentration is presented in terms of the normalized suspended concentration. The behavior of the proportionality coefficient (β) that relates with the sediment transfer mechanism is investigated. Then the other parameters in the model are also determined and discussed.

Finally, all the results provide strong evidence that the application of the modified log-wake law in the sediment-laden flow is suitable for measuring velocity and concentration profile under a defined condition.

NOTATIONS

The following symbols are used in this study:

A	integration constant
b	open-channel width
C	integration constant
F_b	channel bed function
F_s	free surface function
F_w	sidewall function
F_r	Froude number,$V/\sqrt{gh}$
g	gravitational acceleration
h	flow depth of open-channel
R	pipe radius or hydraulic radius
Re	global Reynolds number
S	channel slope
u	time-averaged velocity in the downstream direction
u_{max}	maximum velocity in the flow direction
u_*	shear velocity in pipes or two-dimensional boundary layers
u_{*b}	average bed shear velocity
u_{*w}	average sidewall shear velocity
V	cross-sectional average velocity in Froude number
v	time-averaged velocity in the lateral direction
$W(\xi)$	wake function
w	time-averaged velocity in the upper direction
x	coordinate of the downstream direction

y	coordinate of the lateral direction
z	coordinate of the upward direction that is perpendicular to x-y plane
δ	boundary layer thickness at the channel centerline
κ	von Karman constant
λ	free surface factor
υ	kinematic viscosity of water
υ_t	kinematic eddy viscosity
ξ	normalized distance z relative to the boundary layer thickness δ
Π	wake strength
ρ	mass density of water
τ_{bc}	centerline bed shear stress
$\overline{\tau_b}$	average bed shear stress
τ_w	sidewall shear stress
$\overline{\tau_w}$	average sidewall shear stress
$\tau_{yx,}\tau_{zx},\tau_{yy},\tau_{zy}=\tau_{yz},\tau_{zz}$	shear stress, 1st subscript denotes the normal direction of a differential surface and 2nd the stress direction.
ε_s	sediment transfer coefficient
ε_m	momentum transfer coefficient
β	proportionality coefficient
κ_0	von Karman constant in clear water
κ	von Karman coefficient in sediment laden flow
d	diameter of sediment

ρ	mass density of water
ρ_s	mass density of sediment
ρ_m	average sediment-water mixture density
μ_0	dynamic viscosity of water at zero degree celcius
μ_w	dynamic viscosity of water at a given temperature
T	temperature at given degree celcius
T_k	temperature at kelvin
C	concentration at distance y from the channel bed
C_a	concentration at distance y = a from the channel bed
C_{avg}	volumetric suspended sediment concentration
ω	settling velocity of sediment
y_t	total flow depth
S_e	energy gradient
S_w	water surface slope

LIST OF FIGURES

Page no.

LIST OF TABLES

Chapter 1

INTRODUCTION

1.1 Statement and significance of the problem

Since the time of the previous investigations, the transportation of sediment has been regarded as a significant factor of flood control and channel maintenance. Sediment may be transported by flowing water in essentially two different ways, i.e., by rolling or sliding along the bed of the stream channel or in suspension in the body of the fluid. Material transported by the former method is called the bed-load of the stream, or simply bed-load, while that carried in the latter way is called the suspended load. In the neighborhood of the bed a continual interchange of material is occurring between the bed and the overlying fluid. Hence, it is obviously difficult to distinguish between the bed-load and suspended load at this point. Naturally, the two types of transportation are by no means independent, but they are separated only for convenience in studying and referring to them.

As developing methods of reducing accelerated erosion on lands are concerned about the important aspect of the suspended load of sediment, this study was undertaken on suspended load. The author examined the effect of suspended load on the velocity and concentration profile of flow by using modified log-wake law (Guo, 2002). The author investigated the parameters which were influenced the suspended load in the flow. This study could be useful for various hydraulic and some environmental engineering problems. In addition, the results of this study may provide an explanation for the rising of erosion problems.

1.2 Objectives

The main objectives of the present study are:

(1) to apply the modified log-wake velocity profile model for clear water to sediment laden flow by changing the value of von Karman constant

(2) to investigate the behavior of von Karman coefficient with respect to the sediment concentration gradient

(3) to establish the physical law for the distribution of suspended sediment in turbulent open-channel flow and

(4) to verify the theoretical concentration distribution law with the experimental data conducted by Coleman(1986).

1.3 Outlines

This dissertation consists of six chapters.

Chapter 1 introduces the subject of significance and the objectives of this study.

Chapter 2 reviews the information and knowledge established by previous researchers regarding velocity and concentration profiles in open channel turbulence flows.

Chapter 3 gives the details of experimental data used in this study.

Chapter 4 explains the method of analysis and discussion about the velocity profile in sediment-laden flow.

Chapter 5 also describes the method of analysis and discussion about the concentration profile in sediment-laden flow.

Lastly Chapter 6 draws a conclusion from the results of this study.

Chapter 2

Review of literature

This chapter reviews the detailed literature survey of existing velocity and concentration profile in open channel flow. Firstly, the velocity profile in clear water is reviewed in Section 2.1. Then, a review of the sediment-laden velocity profiles is followed in Section 2.2. After that, Section 2.3 describes the early developed concentration profiles in sediment laden flow and finally Section 2.4 summarizes the previous major results and weaknesses described in this chapter.

2.1 Velocity Profile in Clear Water

The existing velocity profile formula for the study condition can be classified into three groups: the logarithmic law, the log-wake law and the entropy law. The entropy law was proposed by Chiu(1987) and is still in its early stage of development, hence, is not discussed herein.

2.1.1 Background of logarithmic law

In the studied of the velocity profile, based on experimental studies on two-dimensional wall turbulence, turbulent shear flows are usually divided into two regions (White 1991): (1) an inner region where the wall shear stress dominates the flow, and (2) an outer region where the wall shear stress only indirectly affects the flow and is more influenced by the surface of the flow. The inner region can be further divided into a viscous sub-layer, a buffer layer, and a log layer. Prandtl in 1930 (Schlichting 1979),

using his momentum mixing length hypothesis, proposed the law of the wall for the inner region. It states that the velocity profile is a linear law in the viscous sub-layer and a log law away from the wall. In 1967, Spalding (White 1991) proposed a smooth transition between the linear law and the log law.

$$\frac{u}{u_{*b}} = \left(\frac{1}{\kappa} \ln \frac{z u_{*b}}{\upsilon} + A \right) \tag{2.1}$$

in which κ = Karman coefficient = 0.4 , and A = integration constant = 5.5. This equation smoothly merges the linear and the log laws and fits experimental data excellently. Therefore, Spalding's law of the wall can be regarded as a great success in the inner region. But the only weakness is its implicit functional relation.

2.1.2 Background of log-wake law

The fact that the departure from the logarithmic velocity profiles was observed as the distance from the boundary increases.

This phenomenon was first noticed by Laufer (1954) regarding with his experiment for pipe flow in the outer region. In his study, he found that the experimental data near a pipe axis systematically deviate from the log law. As the same results, Coles (1956) pointed out that similar deviations exist near the upper boundary of all boundary-layer flows including open-channel flows.

Then, Coles called this deviation a wake function W(ξ). Hinze (1975) further described the wake function by the following empirical equation.

$$W(\xi) = \frac{2\Pi}{\kappa} \sin^2 \frac{\pi \xi}{2} \tag{2.2}$$

In which Π is Coles' wake strength, $\kappa = (0.4 \sim 0.43)$ is the von Karman constant, and $\xi = \frac{z}{\delta}$ is a normalized distance z relative to the boundary layer thickness δ.

The log law was improved by adding the wake function (2.2) to result in the log-wake law as shown below.

$$\frac{u}{u_{*b}} = \left(\frac{1}{\kappa} \ln \frac{z u_{*b}}{\upsilon} + A \right) - \frac{\Delta u}{u_*} + \frac{2\Pi}{\kappa} \sin^2 \left(\frac{\pi \xi}{2} \right) \tag{2.3}$$

in which the first term represents the law of the wall, the second term is called the channel bed roughness function and the last term is also called wake flow function. In other words, for smooth bed boundary condition, the above equation becomes like that:

$$\frac{u}{u_{*b}} = \left(\frac{1}{\kappa} \ln \frac{z u_{*b}}{\vartheta} + A \right) + \frac{2\Pi}{\kappa} \sin^2 \frac{\pi \xi}{2} \tag{2.4}$$

in which u is time-averaged velocity at z or ξ, u_{*b} is the shear velocity at the channel bed, υ is the kinematics viscosity of water, and A is an integration constant.

In determining model parameters, Tominaga and Nezu(1992) experimentally showed that A is about 5.29 for sub-critical flow while it decreases with Froude number for supercritical flow. As for the wake strength Π, Coles(1956) suggested a value of 0.55 for flat plate boundary layers. However, the previous investigators proposed the various values of Π. Coleman(1981,1986) obtained Π =0.19; Nezu and Rodi(1986) found Π = 0.2; Kirkgoz(1989) reported a value of Π = 0.1; Cardoso etal.(1989) observed Π = -0.077 in a flow over smooth bed; Kironoto and Graf(1994) stated that Π = -0.08 ~ 0.04 for flows over gravel bed; and Wang and Plate(1996) got Π = -0.06 ~ 0.2. Moreover, they recommended the von Karman constant $\kappa = 0.33 \sim 0.4$ for non-Newtonian fluid.

Therefore, from this point of views we can infer that the multiple values of Π might be due to the effects of secondary currents and free surface. It can also say that the log-wake law (2.4) cannot replicate the velocity dip phenomena in narrow channels.

In fact, recently Lyn (2000) systematically tested the log-wake law (2.4) in view of statistics, together with two other versions of wake function. He showed that all three types of the log-wake law were found inadequate in exhibiting to a greater or lesser degree systematic structure in the residuals. On the other hand, he concluded that the most widely accepted log-wake law (2.4) consistently performed the poorest in terms not only of exhibiting a clear structure in the residuals but also of being associated with the largest residual mean square.

Therefore we can deduce that a refined velocity profile model is still needed for both clear water and sediment suspension water flows.

2.2 Velocity Profiles in Sediment-Laden Flows

The velocity profile of an open channel flow can be affected by several factors, such as the existence of secondary flow, suspended sediment concentration, density gradient, flow resistance, etc. In this section, the extension of the log law, the log-wake law and the power law will be reviewed to define the velocity profile in sediment-laden flow.

2.2.1 Application of logarithmic law in sediment-laden flows

The effect of suspended sediment on the velocity profile of logarithmic law has been studied experimentally by Vanoni (1964) , Einstein and Chien (1955), Vanoni and

Nomicos (1960) and Elata and Ippen (1961).Their results led to a view that the Karman constant, κ, of the logarithmic law equation decreases as sediment concentration increases. While, Imamoto, Asano and Ishigak (1977) found κ increases with increasing sediment concentration. Furthermore, Einstein and Chien (1955) proposed a graphical relation to predict the von Karman constant κ based on an energy concept. They also pointed out that the main effect of sediment suspension occurs near the bed. Later, Vanoni and Nomicos (1960) modified the Einstein and Chien parameter with the averaged volumetric concentration near the bed. Barton and Lin (1955) discussed the variation of the von Karman constant κ from the view of density gradient. Chien and Wan (1983) unified various arguments with a Richardson number. However, their study could not explain Elata and Ippen's (1961) neutral particle experiments. To explain his neutral particle experiments, Ippen (1971) argued that suspended sediment affects the velocity profile mainly by changing water viscosity. A good summary of this type of research can be found in the literature (Vanoni, 1975, Chien and Wan, 1983, Hu and Hui , 1995).

Almost at the same time as Einstein and Chien (1955), Kolmogorov(1954) and Barenblatt(1953,1996)also analyzed the effect of sediment suspension on the log law from a view of complete similarity. They considered the momentum equation, the sediment concentration equation and the turbulent energy equation simultaneously and concluded that the log law is still valid in sediment-laden flows except that the von Karman constant becomes smaller. This is exactly the same conclusion as that drawn by Einstein and Chien(1955). Barenblatt(1996) further pointed out that the application of the log law in sediment-laden flows, as it in clear water, is limited to the overlap zone. In the other words, the log law could not be valid in the wake layer and near the water surface.

Certainly a better model regarding velocity profiles in sediment-laden flow is still needed.

2.2.2 Application of Log-wake law in sediment-laden flows

One of the different forms of logarithmic law, the log-wake law, was introduced by Coleman (1981,1986).

$$\frac{U}{U_*} = \left[\frac{2.303}{\kappa}\log\frac{U_* y}{\upsilon} + A\right] - \frac{\Delta U}{U_*} + \frac{\prod}{\kappa}\omega\left(\frac{y}{\delta}\right) \qquad (2.5)$$

where the velocity U is the time-mean local velocity at y, κ is the Karman coefficient, and A is an integration constant. The term $\Delta U / U_*$ is the channel roughness velocity reduction function and $\upsilon = \frac{\mu}{\rho} = \frac{\mu_w\left(1 + 2.5\phi + 6.25\phi^2 + 15.62\phi^3\right)}{\rho_w + \left(\rho_s - \rho_w\right)\phi}$ = kinematics viscosity. The term $\frac{\pi}{\kappa}\omega\left(\frac{y}{\delta}\right)$ is the wake region velocity augmentation function. It contains the wake strength coefficient $\prod$, and the boundary layer thickness δ . The symbol ω is merely a functional symbol.

The part of Eq.(2.5) in square brackets is the original logarithmic law of the wall resulting from the familiar PRANDTL-KARMAN derivation. The velocity reduction and augmentation terms included in Eq.(2.5), with proper choice of numerical values of κ ,A, $\prod$, a proper definition of the functions $\Delta U / U_*$ and $\omega\left(\frac{y}{\delta}\right)$, will describe the entire velocity profile inside the boundary layer thickness δ in an open channel flow, except of case for any thin viscous sub-layer which may exist immediately at the channel bed. From the definition of υ , an effect of sediment in suspension is explicitly included in

Eq (2.5). In addition, implicit applied to sediment-laden effects may change the numerical values of κ, A and $\prod$ when the equation is applied to sediment-laden flows in contrast to clear water flows. The occurrence of these changes is subject to Coleman's experimental determination.

For the wake region velocity augmentation function, COLES (1956) found the empirical form:

$$\omega\left(\frac{y}{\delta}\right) = 2\sin^2\left(\frac{\pi}{2}\frac{y}{\delta}\right) \tag{2.6}$$

for a variety of flows ranging from boundary layer flows in air to water flows over an ogee spillway. Eq.(2.6) has the limit 2 at (y/δ = 1)and the limit zero at (y/δ = 0) . Using the upper limit of Eq.(2.6) and evaluating Eq.(2.5) at ($U = U_m$, $y = \delta$) gives:

$$\frac{U_m}{U} = \frac{2.303}{\kappa}\log\frac{U_*\delta}{\upsilon} + A - \frac{\Delta U}{U_*} + 2\frac{\prod}{\kappa} \tag{2.7}$$

where U_m is the maximum flow velocity in the channel, and δ is taken as the value of y at which U_m is observed to exist. Subtracting Eq.(2.7) from Eq.(2.5) gives the velocity defect law:

$$\frac{U_m - U}{U_*} = \left\{\left[-\frac{2.303}{\kappa}\log\frac{y}{\delta}\right] + 2\frac{\prod}{\kappa}\right\} - \frac{\prod}{\kappa}\omega\left(\frac{y}{\delta}\right) \tag{2.8}$$

Like Eq.(2.5), Eq.(2.8) will represent the entire velocity profile up to ($y = \delta$)except for the viscous sub-layer. The part of Eq.(2.8) in square brackets is the original form of the PRANDTL-KARMAN velocity defect law, and the part of the equation in curly brackets is the logarithmic part of the defect law in its later form, including an additive intercept term $2\prod/\kappa$. Since $\omega\left(\frac{y}{\delta}\right)$ disappears only at (y/δ = 0), the logarithmic part of Eq.(2.8)

is only an asymptote which the complete velocity defect law approaches as y/δ diminishes.

Then Coleman studied the effect of suspended sediment on the parameters κ and Π. He argued that if the log-wake law is applied, the von Karman constant κ remains the same as that in clear water but the wake strength coefficient Π increases with a Richardson number. He further pointed out that the previous conclusion by other researchers, i.e., κ decreases with sediment suspension, was obtained by incorrectly extending the log law to the wake layer. Coleman's argument was supported by Clioffi and Gallerano(1991) . Itakura and Kishi (1980) and Nezu and Rodi(1986) also found κ is constant and the effects of sediment concentration is reflected on the Monin-Obukhov length scale or wake strength.

Coleman's conclusion was actually an analogy to the effect of pressure-gradient on boundary-layer flows. However, the pressure equation of a boundary layer flow in the normal direction is not similar to the sediment concentration equation in a sediment-laden flow. The pressure or pressure-gradient is regarded as a constant at a certain cross-section in a boundary layer flow while the sediment concentration is usually not uniform in the vertical direction. In other words, the von Karman constant κ is not necessarily constant in sediment-laden flow.

Contrary to Coleman's finding, Lyn (1986,1988) believed that the effect of sediment suspension mainly occurs near the bed. That means the von Karman constant may decrease with sediment suspension while the wake strength coefficient Π may be independent of sediment suspension and kept about 0.2, the same as that in clear water. Recently, Kereselidze and Kutauaia(1995) , from their own experiments, deduced that both κ and Π vary with sediment suspension.

Besides the log-wake law, some other wake function forms can be found in literature. Ni and Hui(1988) proposed a wake flow function with two terms: one indicates the effect of mean concentration; the other expresses the effect of concentration gradient. Umeyama and Gerritsen (1992)and Zhou and Ni (1995) suggested a Taylor series to express the wake flow function. Nevertheless the log-wake law can improve the accuracy of the velocity profiles in sediment-laden flows .But the effects of sediment suspension on κ and $\prod$ are still debatable.

2.2.3 Application of power law in sediment-laden flows

The power law formula is also applicable to a region between viscous sub-layer and the location of maximum velocity. It is generally given in the form of:

$$\frac{U}{U_{\max}} = \left(\frac{y}{h}\right)^{\frac{1}{N}} \tag{2.9}$$

The depth-averaged velocity obtained from the above equation can be written as:

$$\overline{U} = U_{\max}\frac{N}{N+1} \tag{2.10}$$

Assuming the above equation is applicable to the whole depth, and then the calculated depth-averaged velocity is:

$$\overline{U} = U_{\max} - \frac{U_*}{K} \tag{2.11}$$

From equations (2.10) and (2.11), the expression of velocity profile power N is given by:

$$N = K\frac{\overline{U}}{U_*} \tag{2.12}$$

In the study of the power law, Schlichting (1979) and Hinze(1975) using the pipe flow data collected by Nikuradse and Laufer, found the power law is better than the logarithmic law. Chen (1984) found the power law exponent N decreases as sediment concentration increases. This is due to the formation of high concentration layer near the channel bed, which reduces the amount of momentum exchange. As a result the velocity profile becomes non-uniform and N decreases accordingly. As sediment concentration increases, the layer will get thicker and the amount of momentum exchange will become uniform, hence N will approach a constant value. Karim and Kennedy (1987), using the relationship between κ and N and the κ equation derived by them, obtained another equation for N. In addition, the study of power law was also reported by Chien and Wan (1983) and Woo, Julien and Richardson (1988). Therefore, power law is still developing and more investigations will be needed to represent the perfect velocity profile.

2.3 Concentration Profiles in Sediment-laden flows

Sediment transport in turbulent flows is of fundamental importance in many disciplines. Since about 1935, much progress has been made in the mechanics of suspension. In 1934, from the work of von Karman and Rouse, it has been generally believed that in sediment suspension a turbulence related sediment transfer mechanism exists.

Most existing analytical and mathematical models for concentration profile of sediment-laden flows are based on the governing equations (Xie and Wei 1987; Zhang and Xie 1993).

$$\frac{\partial C}{\partial t} + u\frac{\partial C}{\partial x} = \frac{\partial}{\partial x}\left(D\frac{\partial C}{\partial x}\right) \tag{2.13}$$

in which **C** is the sediment volumetric concentration; the first term on the left-hand side is the concentration change with time; **u** is the convective velocity of sediment; the second term on the left-hand side is the transport by convention; **D** is the (constant) turbulent eddy viscosity; and the right-hand side is the transport by turbulent.

Examples of this kind of model are the widely accepted Rouse formula $\frac{C}{C_a} = \left(\frac{h-y}{y} \frac{a}{h-a} \right)^z$ for suspended sediment concentration distribution and the well-known logarithmic velocity profile developed initially.

In other words, for flow in an open channel the differential equation for sediment suspension can be written in a number of forms (Brush, 1962, Apmann and Rumer, 1967). The simplest form which described by (O'Brien, 1933) was

$$\varepsilon_s \frac{dC}{dy} + \omega C = 0 \tag{2.14}$$

where ε_s is the sediment transfer coefficient, C is the concentration at a point at distance y above the stream bed, and ω is the fall velocity of sediment particle. The first term of this equation represents the upward sediment transport by diffusion and the second term the downward transport by gravity. ε_s is often estimated as $\beta \upsilon_t$ where β is a proportionality coefficient and υ_t is the diffusion coefficient for momentum transfer that can be obtained by Boussinesq hypothesis and a mean velocity profile, i.e.

$$\upsilon_t = \frac{\tau}{\rho} \left(\frac{du}{dy} \right)^{-1} = u_*^2 \frac{\tau}{\tau_0} \left(\frac{du}{dy} \right)^{-1} \tag{2.15}$$

where ρ = fluid density, du/dy = velocity gradient along the y-axis, u_* = shear velocity, and τ and τ_0 = shear stress at y and y = 0, respectively. Therefore, solution of (2.14) gives

$$\frac{C}{C_a} = \exp\left[-\frac{\omega}{\beta u_*} \int_a^y \left(\frac{\tau}{\tau_0} \right)^{-1} \frac{du}{dy} dy \right] \tag{2.16}$$

where C_a = C at y = a. Eq.(2.16) shows that different mathematical models of the distribution of sediment concentration may be derived by using different models of the velocity and shear stress distributions.

We can see a classic example of a possible model that may be derived from (2.16) is the well-known Rouse equation:

$$\frac{C}{C_a} = \left(\frac{h-y}{y} \frac{a}{h-a} \right)^z \tag{2.17}$$

where C_a = C at y = a ; h = water depth and $z = \frac{\omega}{\beta \kappa u_*}$

in which κ = von Karman's constant. In deriving equation (2.17), the velocity distribution was represented by the Prandtl-von Karman logarithmic equation:

$$u = \frac{u_*}{\kappa} \ln \frac{y}{y_0} \tag{2.18}$$

which is valid near the bed but inaccurate near the water surface when the maximum velocity occurs below the surface. The shear distribution used in deriving (2.17) was

$$\frac{\tau}{\tau_0} = 1 - \frac{y}{h} \tag{2.19}$$

Equation (2.17) is invalid at or near the channel bed and, also, often inaccurate near the water surface, thus diminishing its usefulness in determining the mean (depth-averaged) sediment concentration. Estimation of depth-averaged velocity by Prandtl-von Karman velocity distribution equation, which is invalid near the bed, may not cause a large error since the velocity near the bed is small, but estimation of depth-averaged sediment concentration by (2.17), which is invalid near the bed, will cause a large error since the

sediment concentration at the channel bed is maximum and has a great effect on the mean sediment concentration.

From the detailed literature, we can see that in deriving an equation to describe the variation of suspended sediment concentration over the depth of flow in a river, it is necessary to specify how the sediment transfer coefficient ε_s varies with distance from the bed. This coefficient is analogous to the momentum transfer coefficient υ_t that appears in the theory of the diffusion of momentum [Hinze,1959; Schubaver and Tchen, 1961] .Therefore, the proportionality coefficient β that relates ε_s and υ_t was important.

2.4 Summary

All investigations of sediment-laden flows are to study the effects of sediment suspension on the model parameters in the log law, the log-wake law or the power law. However, a literature review shows that any of the log law, the log-wake law and the power law is not the best functional form of the velocity profile model in pipes and open-channels. Consequently, the developed concentration models incorporating the above velocity distribution equations could not also give a good estimation of the sediment concentration of the desired flow. So, further study of modified log-wake law which gives better solution for both velocity and concentration profiles will be described in the next chapters.

Chapter 3

Detail of Experimental data used

The data of the velocity and concentration profiles that was chosen for modeling was extracted from the research paper written by Neil L. Coleman (1986). This chapter discusses the experimental set up, method and procedures used by the original researcher to conduct the experiments. This chapter also discusses the difficulties encountered by the researcher in the experiment.

3.1 Experimental setup

The experiments were performed in a recirculating flume with a rectangular Plexiglas channel 356 mm wide and 15 m long, with slope adjustment capability for maintaining uniform flow. Velocity profiles were measured at a vertical location on the flume channel centerline 12 m downstream from the entrance. The velocity measuring instrument was a 10 mm diameter Pitot-static tube with a conical tip and a dynamic pressure tip opening 3.2 mm in diameter. An inclined manometer was used for withdrawing isokinetic samples of the sediment-water mixture for determining local suspended sediment concentration. For this purpose, the Pitot-static tube could be isolated from the manometer by appropriate valves and connected to a vacuum pump, sample receptacle, and regulating valve for controlling the sampling velocity. Flow uniformity was monitored by two point gauges. One gauge was located in the plane of the tip of the Pitot-static tube, while the other was located 6 m upstream. Secondary flow was minimized by a bank of tubular flow straighteners installed at the extreme upstream end of the flume channel. Three type of sands were used in the experiments as shown in Table 3.1.

Table 3.1 Experimental sands

Sand	D_{max} mm	D_{min} mm	D mm
1	0.088	0.125	0.105
2	0.177	0.250	0.210
3	0.350	0.500	0.420

3.2 Experimental Procedure

Prior to experiments, the flume was pre-calibrated for determining the channel bottom shear velocity at the base of the velocity profile. Preston tube measurements were made on the centerline of the channel bottom in conjunction with energy gradient measurements. A series of calibration curves was then plotted for calculating shear velocity from

$$u_* = \left[g y_t \left(S_e - S_w \right) \right]^{\frac{1}{2}}$$

where g is gravitation , y_t is total depth, S_e is energy gradient, and S_w is that part of the energy gradient associated with head losses due to the channel walls and that part of the channel bottom not immediately along the centerline. The calibration curves were graphs of S_w against y_t with discharge as a parameter.

The experimental procedure was to establish a uniform flow at constant discharge, depth, and energy gradient, to establish the clear water velocity profile by local velocity measurement at standard elevations, and then to monitor changes in the velocity profiles

resulting from systematic increases in suspended sediment concentration while holding other flow conditions constant. Velocity and concentration profiles were established by averaging two replications of each local measurement. After establishing the clear-water profiles, sand was added in 0.91 kg increments, with another set of measurements being made after each addition. Each increment of sand was injected time equal to at least five flume recirculation periods. An additional 30 min of mixing time were then allowed, following which discharge, depth and energy gradient were checked and the replicated velocity and concentration measurements were made. Before the measurements, the flow was inspected from below through the Plexiglas flume bottom to ensure that no sand was being deposited. Experiments were continued until a highly concentrated continuously moving sheet of sand was observed on the flume bottom and were discontinued immediately upon the appearance of deposition. In this way the whole range of concentration up to capacity transport could be covered with no stationary sand bed in the flume, while the virtual origin of the velocity profile remained at the flume channel bottom. Any changes observed in the velocity profiles could be attributed to increases in suspended sediment concentration alone and not to other factors such as changes in channel roughness. The experiments were repeated with three sands, each sized down to a single square root of two size class, the nominal diameters of 0.105, 0.210 and 0.420 mm, as described in Table 3.1, respectively. The discharge was held at 0.064 m^3/s, while the flow depth was held to an average of 169 mm with a standard deviation of 1.69 mm. Energy gradients were constant at 0.002 for all runs except for the last three runs with 0.420 mm sand; for these runs the energy gradient was 0.0022. Table 3.2 is a summary of experimental conditions for the 40 runs and Table 3.3 (see Appendix B) is a compendium

of the local velocities and concentrations at the respective standard measurement elevations.

Using the experimental data, the dimensionless flow depth was plotted against the dimensionless velocity of the flow in the next Chapter.

Table3.2 Experimental conditions

Run Number	Diameter D (mm)	Concentration Cm	Concentration C(delta)	flow depth h (mm)	channel slope S	Temperature T (Celcius)	delta (mm)	u_max (m/s)
1	0.105	0	0	172	0.002	21.1	133	1.054
2	0.105	3.05E-04	9.20E-05	171	0.002	24.6	126	1.045
3	0.105	5.80E-04	1.58E-04	172	0.002	25	127	1.043
4	0.105	8.70E-04	1.88E-04	171	0.002	25.3	129	1.046
5	0.105	1.12E-03	2.80E-04	171	0.002	23.9	129	1.046
6	0.105	1.45E-03	3.72E-04	170	0.002	24	127	1.052
7	0.105	1.68E-03	4.40E-04	171	0.002	22.7	128	1.053
8	0.105	1.86E-03	4.10E-04	173	0.002	23.3	133	1.044
9	0.105	2.50E-03	3.75E-04	172	0.002	24.4	132	1.051
10	0.105	2.79E-03	3.80E-04	171	0.002	23.9	131	1.063
11	0.105	3.08E-03	6.00E-04	169	0.002	24.2	132	1.081
12	0.105	3.40E-03	6.40E-04	173	0.002	24.7	137	1.049
13	0.105	3.58E-03	8.20E-04	171	0.002	22.7	127	1.065
14	0.105	4.02E-03	7.80E-04	171	0.002	22.7	131	1.065
15	0.105	4.15E-03	8.80E-04	171	0.002	22.9	128	1.075
16	0.105	4.40E-03	8.00E-04	171	0.002	23	128	1.073
17	0.105	4.70E-03	5.95E-04	171	0.002	23.8	140	1.065

18	0.105	4.82E-03	6.25E-04	172	0.002	22.8	129	1.053
19	0.105	4.80E-03	5.90E-04	170	0.002	23.4	129	1.072
20	0.105	5.03E-03	6.60E-04	170	0.002	23.9	129	1.07
21	0.21	0.00E+00	0.00E+00	169	0.002	23.8	126	1.048
22	0.21	2.45E-04	6.50E-05	170	0.002	23.8	127	1.027
23	0.21	5.60E-04	1.17E-04	170	0.002	23.8	125	1.047
24	0.21	8.15E-04	1.59E-04	169	0.002	23.8	127	1.05
25	0.21	1.21E-03	2.98E-04	167	0.002	23.9	125	1.069
26	0.21	1.43E-03	3.00E-04	171	0.002	19.5	130	1.045
27	0.21	1.89E-03	2.85E-04	168	0.002	23	127	1.069
28	0.21	2.00E-03	3.32E-04	170	0.002	22.9	129	1.063
29	0.21	1.79E-03	2.98E-04	168	0.002	23.3	130	1.083
30	0.42	2.49E-03	2.73E-04	168	0.002	23.7	131	1.092
31	0.42	2.68E-03	4.40E-04	172	0.002	23.9	133	1.06
32	0.42	0.00E+00	0.00E+00	173	0.002	21.7	129	1.025
33	0.42	6.50E-05	1.75E-05	174	0.002	22.5	131	1.036
34	0.42	1.03E-04	2.41E-05	172	0.002	23.3	127	1.044
35	0.42	1.77E-04	4.15E-05	172	0.002	23	131	1.055
36	0.42	2.67E-04	6.20E-05	171	0.002	23.6	130	1.082
37	0.42	3.65E-04	8.00E-05	167	0.002	21.7	130	1.081
38	0.42	4.55E-04	1.06E-04	167	0.0022	22.1	131	1.114
39	0.42	5.10E-04	1.12E-04	171	0.0022	22.3	132	1.096
40	0.42	5.45E-04	1.15E-04	171	0.0022	22.9	132	1.101

3.3 Experimental difficulties faced

In the original experiment, there were a lot of difficulties faced by the researcher. These difficulties could cause inaccuracies in the results obtained and affect the comparison between the theoretical equation and the experimental data. The difficulties faced are as follows:

1. The measurements of the velocity and concentration of the sediment near the channel bed was difficult as the instruments used were bulky. Thus the velocity and concentration data near the bed were inaccurate and cannot be used for analysis.
2. The viscosity of the mixture and the flow were significantly changed by the presence of large concentration of sediments.
3. Since extremely high velocities were required to keep large amounts of coarse sediment in suspension, supercritical flow was used. This caused a small difference between the bed slope and the water surface to result in the energy slope being considerably different from the bed and water surface slopes.
4. Inaccuracies in the concentration profiles were obtained for runs with low concentration of sediment.

Chapter 4

Method of Analysis and Discussions for Velocity Profile

To represent the data of the flows by a better solution instead of using Standard log-wake law, modified log-wake law could be used, developed by Guo (2002), by only changing the von Karman constant. The modified log-wake law has been constructed from a theoretical analysis, asymptotic matching and empirical deduction. Section 4.1 presents the application of modified log-wake law in sediment laden flow and shows how the model parameters are determined. Section 4.2 explains the methods and procedures involved in programming and analysis. Section 4.3 interprets the results obtained using the analytical methods in previous introduction. And Section 4.4 touches on the findings of this study and makes a discussion. Finally, the last Section 4.5 gives the summary of this chapter.

4.1 Application of modified log-wake law in sediment laden flow

The modified log- wake law model, developed for clear water by Guo (2002), could be further written for sediment-laden flow as,

$$\frac{u_{\max}-u}{u_*}=-\frac{1}{\kappa}\left(\ln\xi-\frac{1}{25}\frac{u_{\max}}{u_{*b}}\frac{u_{*w}}{u_{*b}}\cos^2\frac{\pi\xi}{2}+\frac{1-\xi^3}{3}\right) \qquad (4.1)$$

in which,

u_{max} = maximum velocity in the flow direction

u = time-averaged velocity in the downstream direction

u_* = shear velocity in two-dimensional boundary layers

u_{*b} = average bed shear velocity

u_{*w} = average sidewall shear velocity

ξ = normalized distance z relative to the boundary layer thickness δ

δ = boundary layer thickness at the channel centerline and

κ = von Karman constant.

In this equation (4.1), only the von Karman constant κ varies with sediment concentration. The least square method could be used for determining this value of κ. Thus the application of this equation could be proved to determine the velocity profile in the sediment laden flow as follow:

Case 1: For fine sediment (diameter = 0.105 mm)

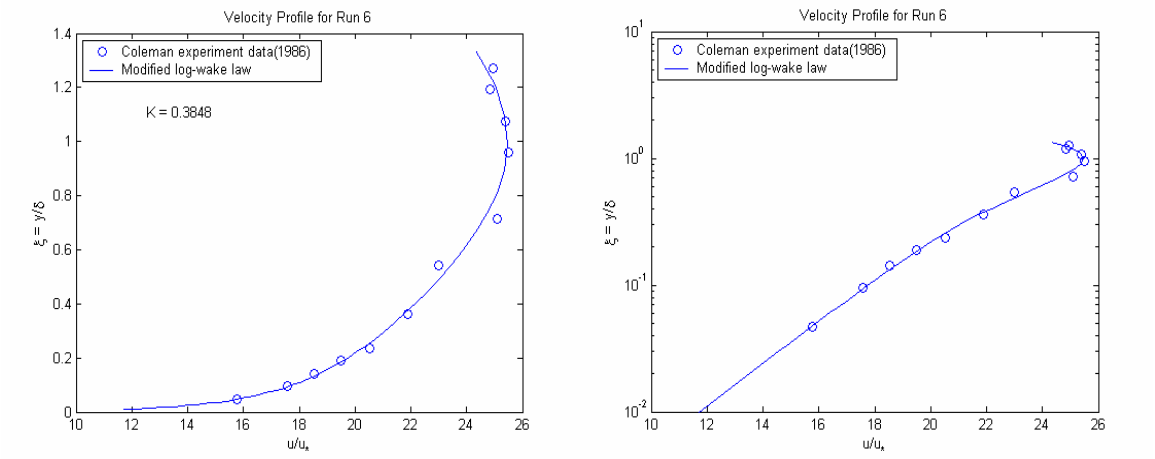

Case 2: For medium sediment (diameter = 0.210 mm)

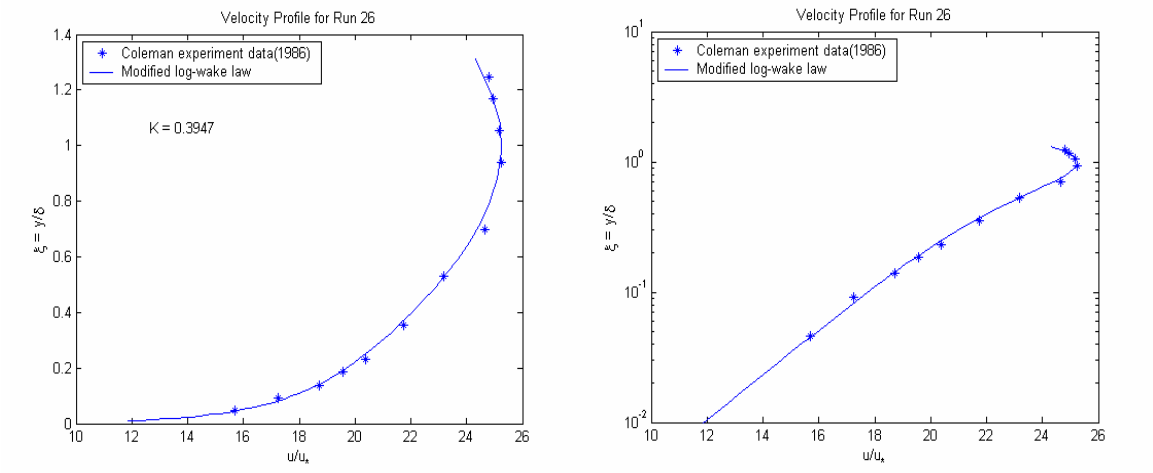

Case 3: For coarse sediment (diameter = 0.420 mm)

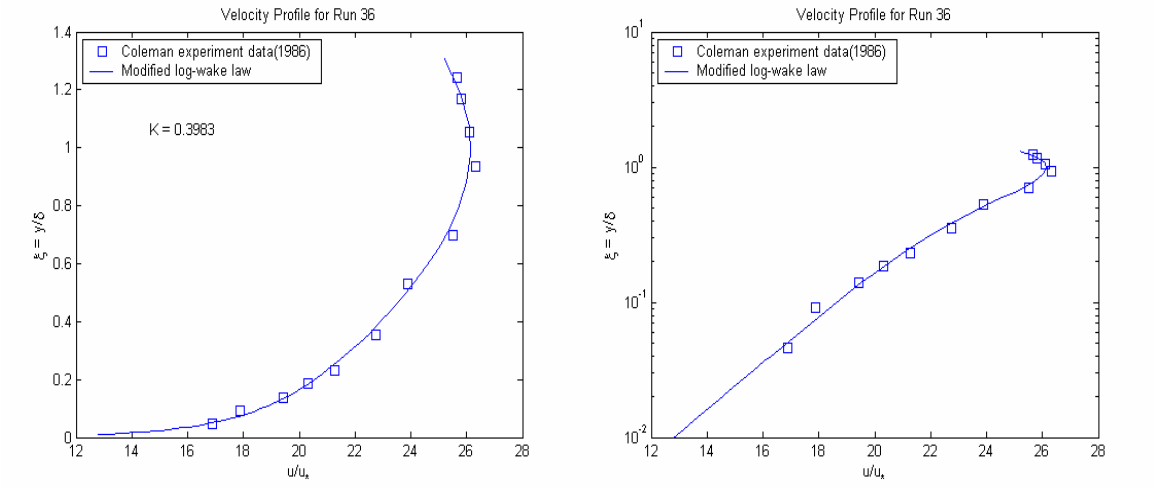

Fig (4.1) Comparison of modified log-wake law with Coleman's experimental data(1986) for sediment –laden flow

From these plots, it could be seen that the modified log-wake law could represent the data very well. In addition, the rest figures for all runs were appended at the end of this thesis (in Appendix B).

4.2 Methods and Procedures involved in programming

A simple Matlab program was used to plot out the experimental data. This simple Matlab program optimized the data so that the theoretical modified log-wake curve fitted the orientation of the data.

To perform the optimization, an intrinsic function of the Matlab was used. In Matlab version 6.5, the function is known as lsqcurvefit. It performs least square non-linear approximation between the data points and the theoretical modified log-wake equation (4.1). The method of least square performs the optimization by minimizing the sum of the squares of the deviation between the actual experimental data points and the data points generated by modified log-wake equation (4.1). There is only one parameter, von Karman constant, κ in the modified log- wake law to optimize for velocity profile. This sample program is appended at the end of this thesis (Appendix A).

4.3 Method of Analysis

To have a general idea of how the velocity profiles of the sediment-laden flow varied with different concentrations of sediment, plots of the various velocity profiles of different sediment-laden flow runs were made. In all plots, both the X and Y axis of the graph had dimensionless parameters i.e., plotting of the dimensionless depth ($\xi = \frac{y}{\delta}$) against the dimensionless velocity (u/u*) of the flow was made. This type of graph was made to show the effect that the change in vertical distance from the bed surface has on the velocity.

After the parameter was obtained from the data, a relation between the gross flow Richardson number = $\left[R_i = \frac{g\delta(\rho_0 - \rho_\delta)}{\rho u_*^2} \right]$, a weighted measure of overall suspension concentration, and the parameter κ used in the modified log-wake law equation (4.1) had to be made to determine how the parameter κ changed with different sediment concentration. The sediment concentration used was in the form of volumetric sediment concentration. This was because the volumetric sediment concentration has no dimensions. Hence, a dimensionless value would give an individual better idea of how the parameter κ value varied with the sediment concentration without being tied to the absolute value of the sediment concentration. Throughout the calculation, the density of sediment was taken as 2650kg/m^3. Then, the graph of the variation of von Karma constant κ versus volumetric sediment concentration was established as follows:

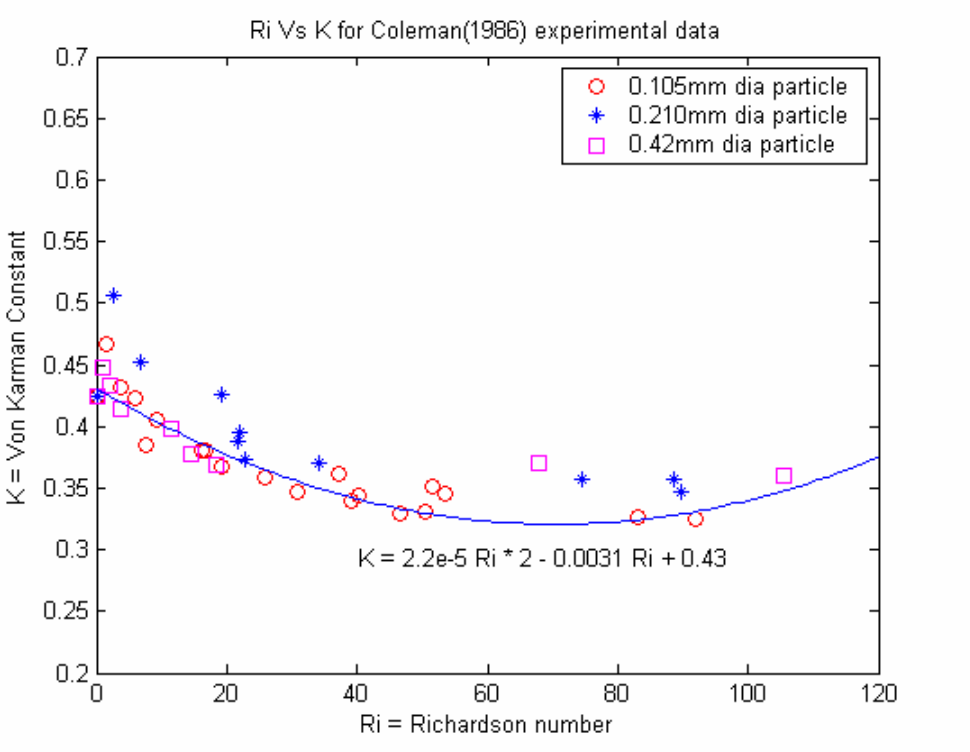

Fig (4.2) Establishing of relationship between Richardson number (concentration gradient) and von Karman constant κ

4.4 Effect of suspended load on the velocity distribution

4.4.1 Results

The von Karman constant, the main parameter for velocity distribution, for clear water κ_0 was nearly constant as described by early researchers. While, that for sediment laden flow (κ) followed a trend of decreasing with increasing sediment concentration. This trend in von Karman constant to decrease as concentration of suspended sediment increases is consistent with earlier findings of Vanoni,1946; Brooks,1954; Einstein and Ning Chien,1955. Moreover, the results show that the density gradient (the Richardson

number Ri) has a significant effect on the von Karman constant κ. Thus, a linear relation between κ and Ri has been fitted to the data as

$$\kappa = 2.2\text{e-}5\ \mathrm{Ri}^2 - 0.0031\ Ri + 0.43$$

$$\frac{\kappa}{\kappa_0} = 0.00005\ \mathrm{Ri}^2 - 0.0072\ Ri + 1$$

in which κ_0 is the von Karman constant 0.43 for clear water flows. From these results, it suggests that the effect of suspended sediment in a flow is to reduce the value of von Karman constant below its value for clear water.

4.4.2 Comparison

For comparison purposes, several vertical velocity profiles of Coleman's log-wake law and Modified log-wake law were plotted together. The reason for doing so was that the modified log-wake law could be better than the Coleman's log-wake law in practically.

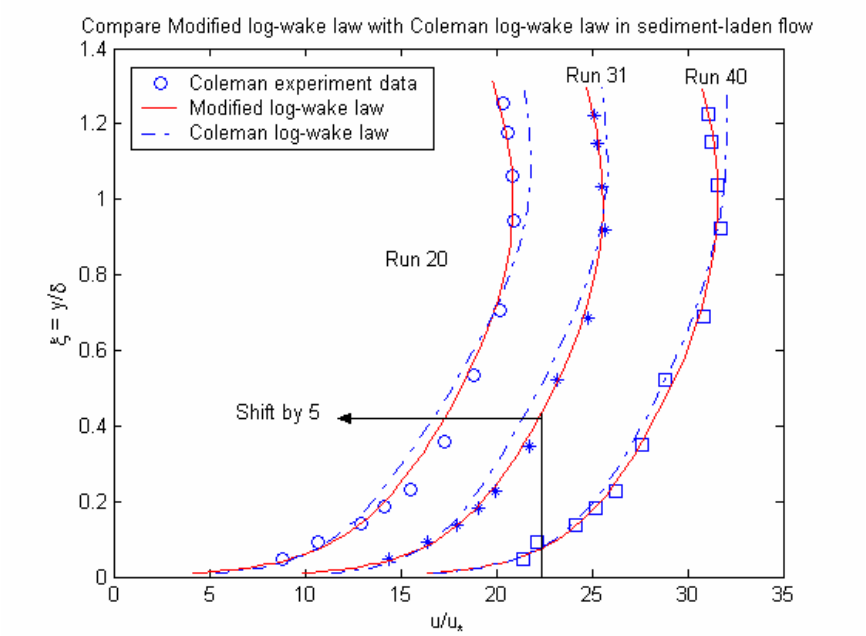

Fig (4.3) Compare Modified log-wake law with Coleman log-wake law in sediment-laden flow

4.4.3 Discussion

Using Coleman's experimental data as a model, it could be seen in fig (4.2) that the rate of variation of the von Karman constant κ was different for each of the three different sizes of sediment. It showed that the coarser sediment although reducing κ had less effect than the finer sediment.

Moreover, the existence of suspended sediment particles could be seen to have the effect of decreasing the gradient of the velocity profile in inner flow region and increasing in outer flow region (as shown in Fig 4.4 - Fig 4.6).

Next, from the following equation by Boussinesq

$$\tau = \rho \upsilon_t \frac{du}{dy} \tag{4.3}$$

it is obviously seen that velocity gradient (du/dy) also has the relation with shear stress (τ) and the coefficient of momentum exchange (υ_t).

Therefore, we could draw a conclusion that the increase in sediment concentration reduces not only the turbulence transfer coefficient in inner region but also the resistance of the flow in outer region. This phenomenon could be observed in the following Figs.

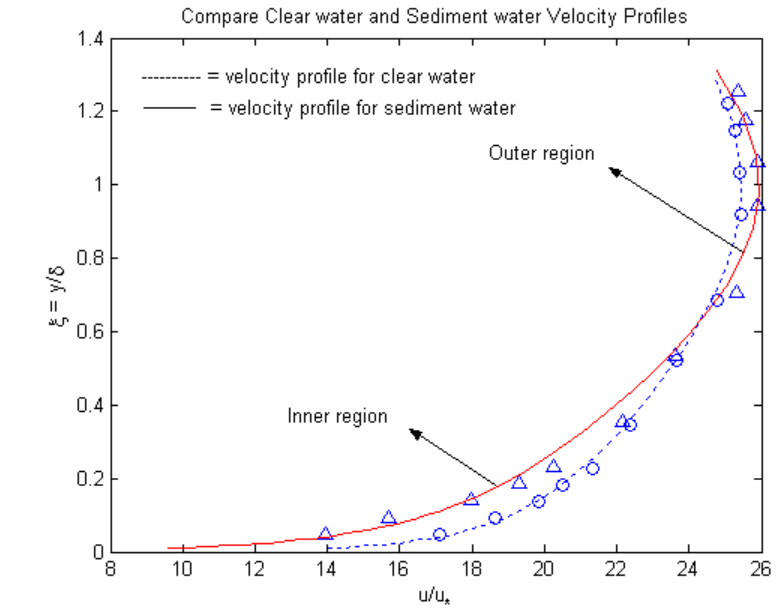

Fig (4.4) Comparison of Clear-water velocity profile with Sediment water velocity profile from the experimental series of 0.105 mm sand (runs 1 and 19, respectively).

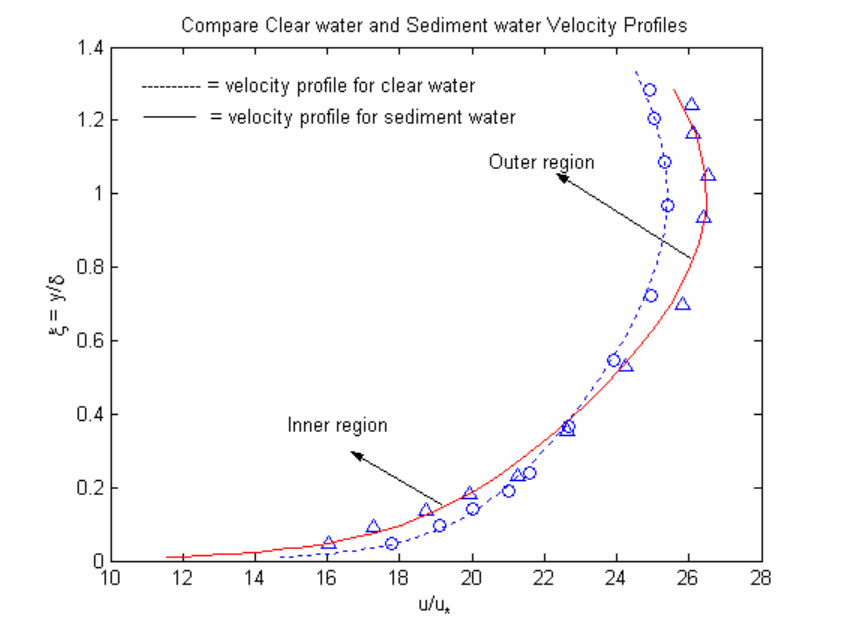

Fig (4.5) Comparison of Clear-water velocity profile with Sediment water velocity profile from the experimental series of 0.210 mm sand (runs 21 and 30, respectively).

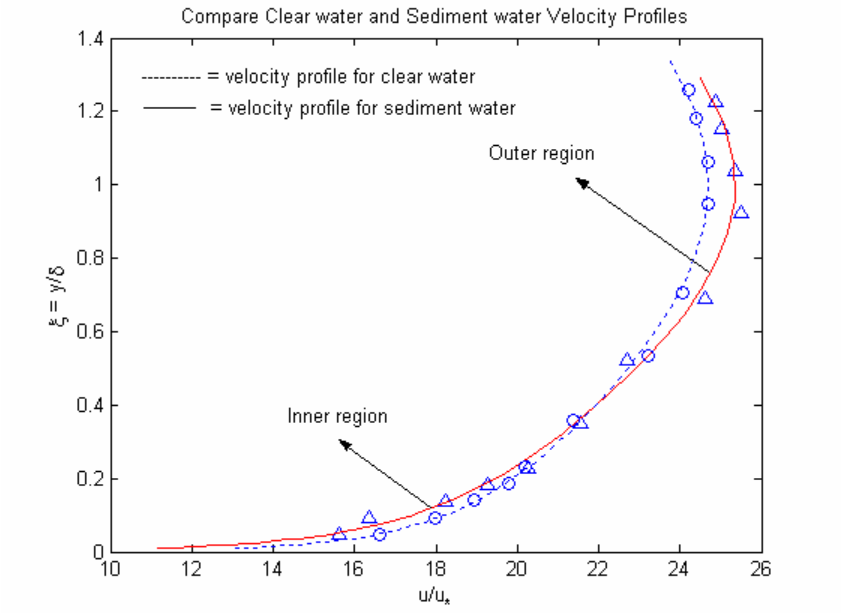

Fig (4.6) Comparison of Clear-water velocity profile with Sediment water velocity profile from the experimental series of 0.420 mm sand (runs 32 and 40, respectively).

4.5 Summary

The effect of sediment concentration on velocity profile of modified log-wake law was investigated. The changing of model parameter was analyzed and then tested with the available measured data (conducted by Coleman 1996). The results are satisfactory for various sediment concentration flow cases. Therefore, this chapter can be summarized as follows:

1. The existence of suspended sediment particles in the flow affects velocity profiles significantly.
2. The velocity profile of sediment laden flow in open channel could be described by using the modified log-wake law in which only von Karman constant κ was changed.
3. The effect of suspended sediment could be regarded as a factor that makes the value of von Karman constant κ of sediment water lower than that of clear water.
4. The decreases in the velocity gradient and the turbulent shear stress in inner region of the flow are probably caused by the increase in sediment suspension.

Chapter 5

Method of Analysis and Discussions for Concentration Profile

The purpose of this chapter is to provide the method of analysis for the distribution of suspended sediment concentration profile. A theoretical equation for the distribution of suspended sediment concentration profile is obtained from the incorporation of the modified log-wake law equation into the differential equation of sediment suspension. The finalized theoretical equation is then compared with the measurements of flows with various sediment concentrations.

5.1 Method of Analysis

5.1.1 Theoretical background for Concentration equation

Modern theories of suspended load transportation are based upon the developments in the mechanics of turbulent fluid flows.

Consider a two-dimensional turbulent flow in the x direction with a velocity u(y), where y is normal to x. Then according to Renolds, the shear parallel to x on a plane normal to y may be expressed by

$$\tau = -\rho \overline{u' v'} \tag{5.1}$$

where ρ is the mass density of the fluid and u' and v' are the turbulent velocity fluctuations in the x and y directions respectively. The bar denotes mean value.

Moreover, Boussinesq introduced an expression for the shear of the form,

$$\tau = \rho \upsilon_t \frac{du}{dy} \tag{5.2}$$

where the quantity $\rho \upsilon_t$ is analogous to the coefficient of viscosity in the expression for viscous shear. u is the mean velocity in the x direction. The quantity υ_t has the dimension of a kinematics viscosity and varies from point to point.

Then, equation (5.2) may be written in the following form,

$$\tau = \upsilon_t \frac{d}{dy}(\rho u) \tag{5.3}$$

in which, the term $\frac{d}{dy}(\rho u)$ is the momentum gradient in the y direction. Since the shear stress is equal to the momentum transferred through unit area in unit time, the quantity υ_t is a coefficient expressing the exchange of fluid between neighboring filaments. Thus, this quantity is called the coefficient of turbulent (or momentum) exchange.

For steady condition of particle suspension, such as occurs in suspended-sediment transportation, the turbulent transfer of particles in the upward direction is balanced by the settling of the particles due to the force of gravity,i.e.,

$$-\varepsilon_s \frac{dC}{dy} = \omega C \tag{5.4}$$

in which ω is the settling velocity of the particles. Then the differential equation for suspended sediment becomes like that,

$$\omega C + \varepsilon_s \frac{dC}{dy} = 0 \tag{5.5}$$

By integrating the equation (5.5), we get the following solution,

$$\ln \frac{C}{C_a} = -\omega \int_a^y \frac{dy}{\varepsilon_s} \tag{5.6}$$

where C_a is the concentration at an arbitrary reference level y = a.

In the early investigation, the experimental sediment-distribution measurements were compared with the theoretical distribution which assumes that the coefficient for the turbulent transfer of suspended sediment ε_s is the same as the coefficient for the turbulent transfer of momentum υ_t.

However, the measured sediment distributions have the same form as the theoretical distribution but do not agree quantitatively with them, thus showing, the invalidity of the assumption that the transfer coefficient for sediment ε_s was equal to that for momentum υ_t.

Therefore, ε_s is often estimated as $\beta\upsilon_t$ in which β is a proportionality coefficient. Such a relation is furnished by the momentum transfer theory, equation (5.2), which yields the expression for the coefficient of turbulent exchanges υ_t as follows,

$$\frac{\varepsilon_s}{\beta} = \upsilon_t = \frac{\tau}{\rho \frac{du}{dy}} \qquad \text{or}$$

$$\varepsilon_s = \beta\upsilon_t = \beta \frac{\tau}{\rho \frac{du}{dy}} \tag{5.7}$$

Then, by substituting equation (5.7) into equation (5.6), we get the following concentration equation:

$$\ln\frac{C}{C_a} = -\frac{\rho\omega}{\beta}\int_a^y \frac{\frac{du}{dy}}{\tau}dy \tag{5.8}$$

In a uniform open-channel flow, one has known that the shear stress is linearly distributed along the vertical direction of the channel, i.e.,

$$\tau = \tau_0 \frac{h-y}{h} \qquad \text{or}$$

By substituting $\xi = \frac{y}{h}$, it becomes

$$\tau = \tau_0(1-\xi) \tag{5.9}$$

Then, introducing equation (5.9) into equation (5.8) results the following relation,

$$\ln\frac{C}{C_a} = -\frac{\rho\omega}{\beta\tau_0}\int_a^y \frac{\frac{du}{dy}}{1-\xi}dy \tag{5.10}$$

where τ_0 is the shear stress at the bottom and can be calculated from $\tau_0 = \rho u_*^2$, the coordinate y will be normalized by the thickness h in wide channel, i.e., $\xi = \frac{y}{h}$. But for narrow channel, the maximum velocity occurs below the free surface, thus the normalized distance becomes $\xi = \frac{y}{\delta}$ in which δ = the distance from the channel bed to the place of maximum velocity occurs.

By substituting $\tau_0 = \rho u_*^2$ and $\xi = \frac{y}{\delta}$ for narrow open channel, we can get the following equation:

$$\ln\frac{C}{C_a} = -\frac{\rho\omega}{\beta\rho u_*^2}\int_a^y \frac{\frac{du}{\delta d\xi}}{1-\xi}\delta d\xi \tag{5.11}$$

Rearranging the above equation (5.11), it becomes

$$\ln\frac{C}{C_a} = -\frac{\omega}{\beta u_*}\int_a^y \frac{\frac{1}{u_*}\frac{du}{d\xi}}{1-\xi} d\xi \tag{5.12}$$

By using $\frac{1}{u_*}\frac{du}{d\xi}$, which comes from the velocity defect form of the modified log wake equation (4.1), the distribution of sediment concentration can be calculated from the equation (5.12) for different sediment fractions.

5.1.2 Incorporation of modified log-wake law into concentration model

To establish a general concentration profile equation of the sediment-laden flow, we have to start from the velocity defect form of the modified log-wake law presented in previous chapter, i.e.,

$$\frac{u_{\max}-u}{u_*} = -\frac{1}{\kappa}\left(\ln\xi - \frac{1}{25}\frac{u_{\max}}{u_{*b}}\frac{u_{*w}}{u_{*b}}\cos^2\frac{\pi\xi}{2} + \frac{1-\xi^3}{3}\right) \tag{5.13}$$

Then, to facilitate for differentiating and integrating, we substitute a polynomial version i.e., $[\cos^2\frac{\pi\xi}{2} \approx 1-3\xi^2+2\xi^3]$ in the place of cosine-square version in equation (5.13). Therefore, the resultant equivalent version becomes in the following form,

$$\frac{u_{\max}-u}{u_*} = -\frac{1}{\kappa}\left(\ln\xi - \frac{1}{25}\frac{u_{\max}}{u_{*b}}\frac{u_{*w}}{u_{*b}}(1-3\xi^2+2\xi^3) + \frac{1-\xi^3}{3}\right) \tag{5.14}$$

But, before substituting we have examined the equivalent case as shown in figure (5.1).

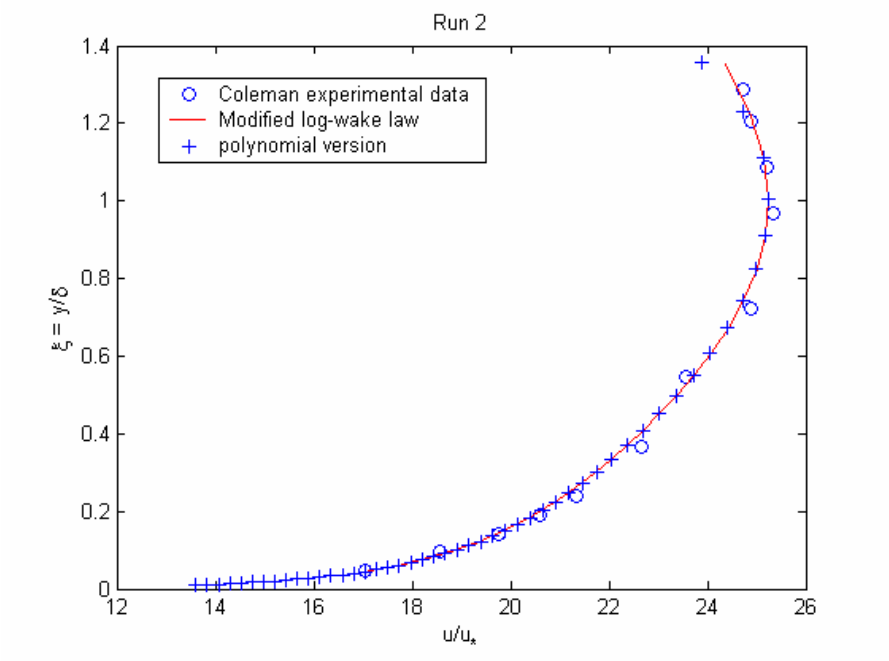

Fig (5.1) Comparison of the cosine-square version with the polynomial version of the modified log-wake law

After checking completely, we differentiate equation (5.14) with respect to ξ and then the result becomes

$$\frac{1}{u_{*b}}\frac{du}{d\xi}=\frac{1}{\kappa}\left(\frac{1}{\xi}-\frac{1}{25}\frac{u_{\max}}{u_{*b}}\frac{u_{*w}}{u_{*b}}\left(-6\xi+6\xi^2\right)-\xi^2\right) \tag{5.15}$$

5.1.3 Establishment of Concentration equation

Introducing equation (5.15) into equation (5.12) gives the following equation,

$$\ln\frac{C}{C_a}=-\frac{\omega}{\beta u_*\kappa}\int_{\xi_a}^{\xi}\left(\frac{\frac{1}{\xi}-\frac{1}{25}\frac{u_{\max}}{u_{*b}}\frac{u_{*w}}{u_{*b}}\left(-6\xi+6\xi^2\right)-\xi^2}{1-\xi}\right)d\xi$$

$$\ln\frac{C}{C_a} = -\frac{\omega}{\beta u_* \kappa}\int_{\xi_a}^{\xi}\left\{\frac{1}{\xi(1-\xi)} - \frac{6}{25}\frac{u_{\max}}{u_{*b}}\frac{u_{*w}}{u_{*b}}\left(-\frac{\xi}{1-\xi}+\frac{\xi^2}{1-\xi}\right)-\frac{\xi^2}{1-\xi}\right\}d\xi$$

Integrating the above equation, we obtain

$$\ln\frac{C}{C_a} =$$

$$-\frac{\omega}{\beta u_* \kappa}\left[\ln\frac{\xi}{1-\xi} - \frac{6}{25}\frac{u_{\max}}{u_{*b}}\frac{u_{*w}}{u_{*b}}\left((\ln(1-\xi)+\xi)+(-\ln(1-\xi)-\xi-\frac{\xi^2}{2})\right)-\left(-\ln(1-\xi)-\xi-\frac{\xi^2}{2}\right)\right]_{\xi_a}^{\xi}$$

$$= -\frac{\omega}{\beta u_* \kappa}\left\{\ln\frac{\xi(1-\xi_a)}{(1-\xi)\xi_a} - \frac{6}{25}\frac{u_{\max}}{u_{*b}}\frac{u_{*w}}{u_{*b}}\left(-\frac{\xi^2}{2}+\frac{\xi_a^2}{2}\right)-\ln\frac{1-\xi_a}{1-\xi}+\frac{\xi^2}{2}-\frac{\xi_a^2}{2}+\xi-\xi_a\right\}$$

$$= -\frac{\omega}{\beta u_* \kappa}\left\{\ln\frac{\xi}{\xi_a} - \frac{6}{25}\frac{u_{\max}}{u_{*b}}\frac{u_{*w}}{u_{*b}}\left(-\frac{\xi^2}{2}+\frac{\xi_a^2}{2}\right)+\frac{\xi^2}{2}-\frac{\xi_a^2}{2}+\xi-\xi_a\right\}$$

$$= -\frac{\omega}{\beta u_* \kappa}\left\{\ln\frac{\xi}{\xi_a} + (\frac{3}{25}\frac{u_{\max}}{u_{*b}}\frac{u_{*w}}{u_{*b}}+\frac{1}{2})(\xi^2-\xi_a^2)+\xi-\xi_a\right\} \qquad (5.16)$$

Finally the structure of equation (5.16) can be generalized as follow:

$$\ln\frac{C}{C_a} = -\frac{\omega}{\beta u_* \kappa}\left\{\ln\frac{\xi}{\xi_a} + \alpha(\xi^2-\xi_a^2)+(\xi-\xi_a)\right\} \qquad (5.17)$$

Where α is sidewalls coefficient; ω = settling velocity of sediment; β = proportionality coefficient; and κ = von Karman coefficient.

By using this equation (5.17) it is possible to plot the curves of relative sediment distribution as shown in figure (5.2).

Case 1: For fine sediment (diameter = 0.105 mm)

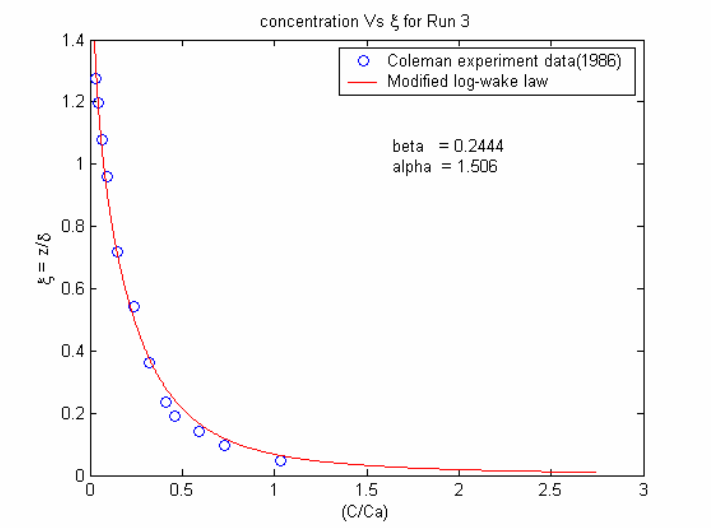

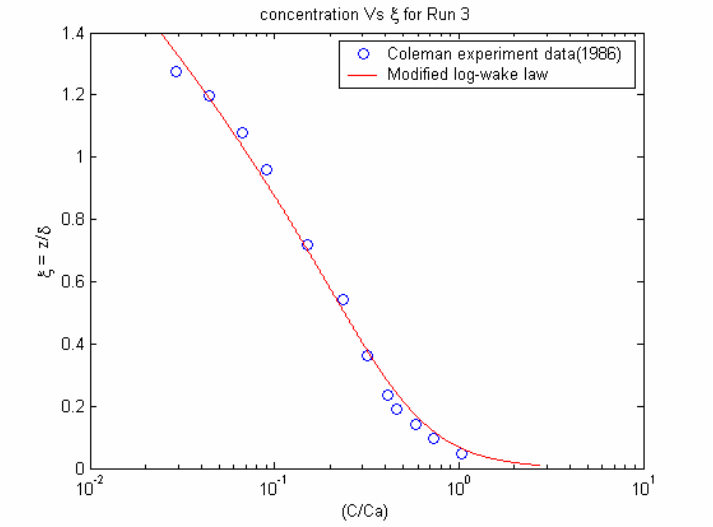

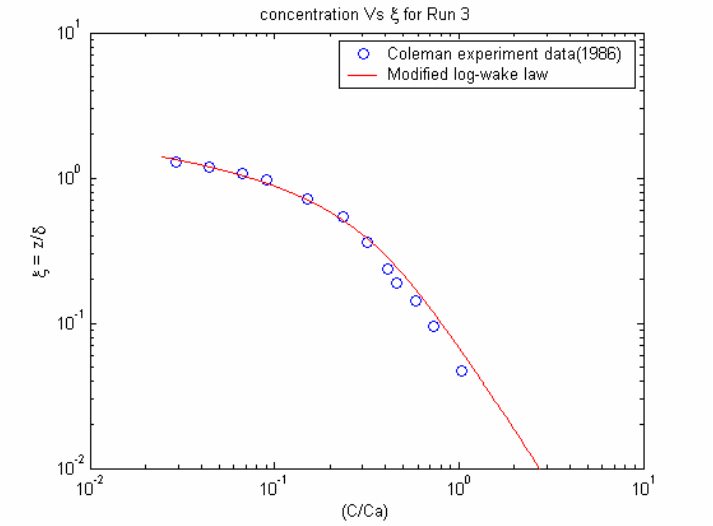

Case 2: For medium sediment (diameter = 0.210 mm)

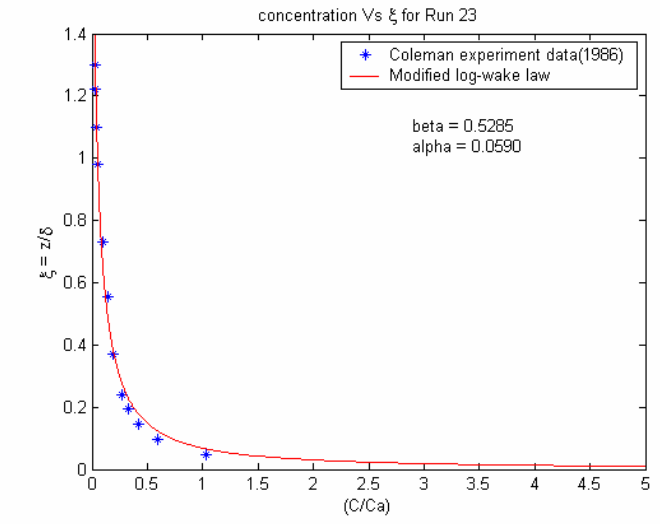

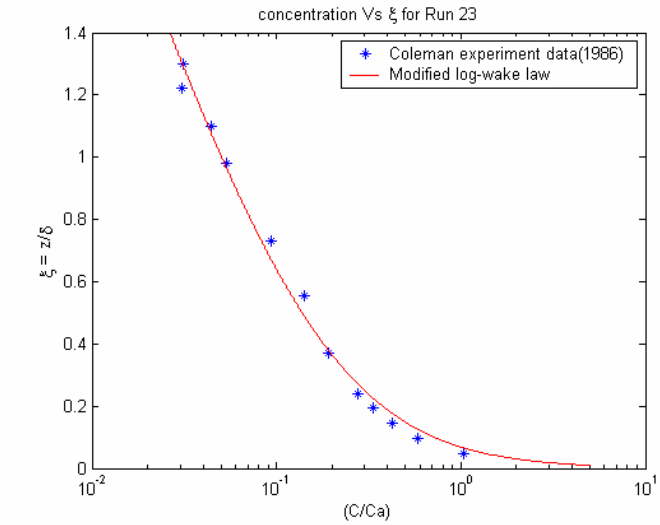

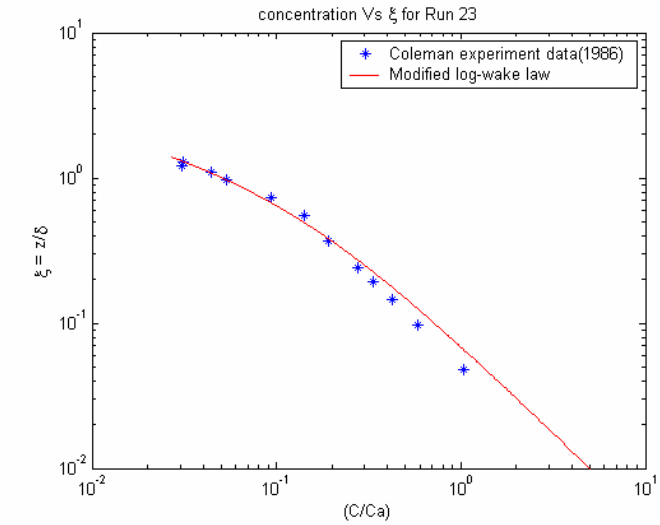

Case 3: For coarse sediment (diameter = 0.420 mm)

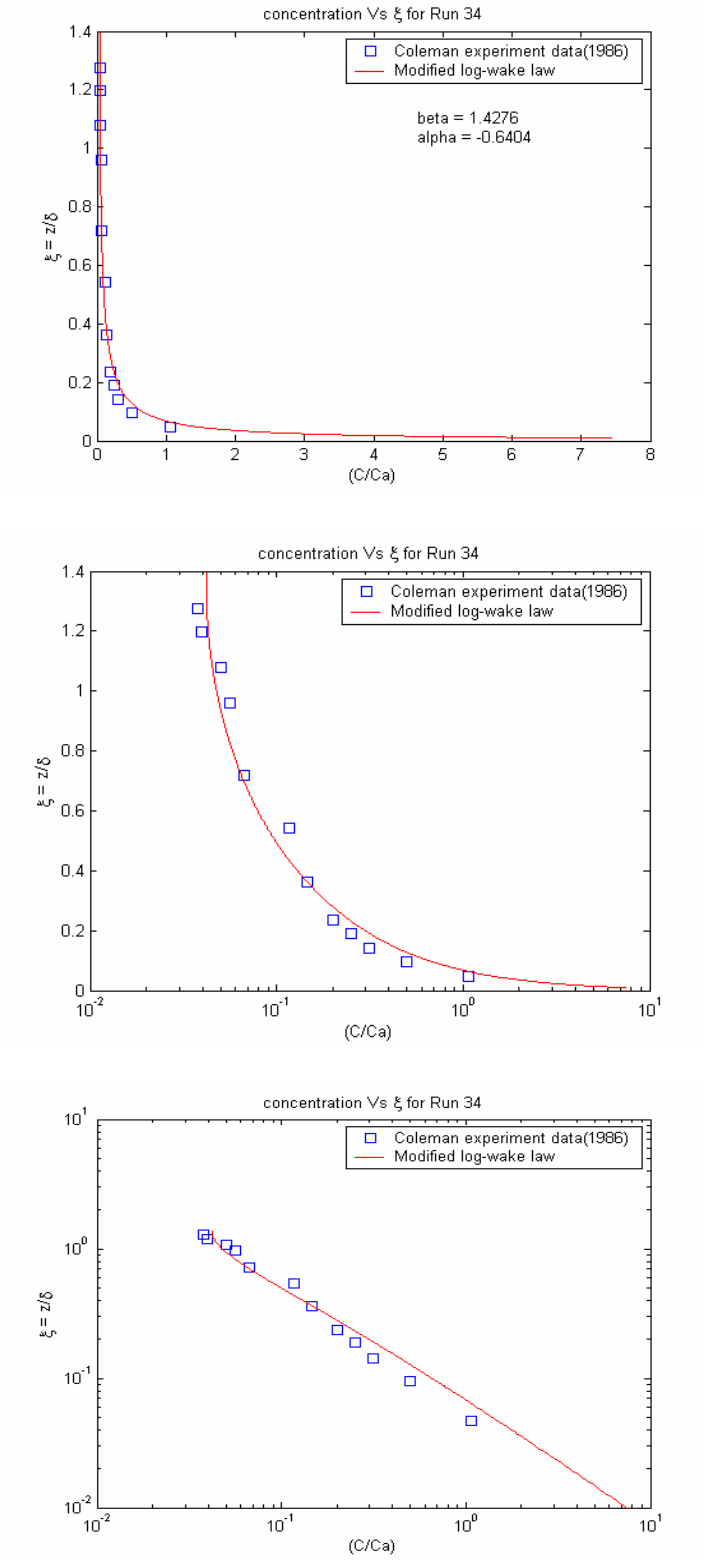

Fig (5.2) Plot of concentration Vs dimensionless water depth.

In all plots, both the X and Y axis of the graph had dimensionless parameters. The graphs on the above pages show briefly how the concentration profiles vary with distance from the bed for different types of sediment used. The testing results for the other runs were appended in Appendix D. From the above graphs, we could see that our presented concentration profile model was structurally applicable in the prediction of concentration profile of sediment.

5.1.4 Finding parameters in concentration equation

In our finalized concentration equation (5.17), we have only two parameters β and α to optimize. These parameters can be obtained using the Matlab program (shown in Appendix A). Hence, the Matlab program optimized these parameters so that the theoretical curve fitted the orientation of the experimental data. However κ value is substituted from the previous optimization result of the velocity profile.

Then, to investigate a value for the settling velocity, we apply the following mathematical equation- 5.18, which relates the settling velocity to the sediment fluid properties.

$$\frac{\omega d}{\upsilon} = \frac{d_*^3}{24 + \frac{\sqrt{3}}{2} d_*^{3/2}} \tag{5.18}$$

in which ω = settling velocity; d = sediment particle diameter; υ = kinematics viscosity of fluid; and

$$d_* = \left(\frac{(\rho_s - \rho)g}{\rho \upsilon^2} \right)^{\frac{1}{3}} d \tag{5.19}$$

where ρ_s = density of the sediment (ie., sand = 2650 kg/m^3) ; ρ = density of water (1000 kg/m^3) .

But, in flow with suspended sediment, treatment of the sediment-water mixture as a single fluid requires an expression for the kinematics mixture viscosity (Graf,1971; Coleman,1981). So we apply the following equation.

$$\upsilon = \frac{\mu_w(1 + 2.5 + 6.25C_{avg}^2 + 15.62C_{avg}^3)}{\rho_m} \tag{5.20}$$

where $\rho_m = \rho_w + (\rho_s - \rho_w)C_{avg}$

$\mu_w = \mu_0 e^{y1}$ = dynamic viscosity of water at a given temperature degree Celsius

in which μ_0 = dynamic viscosity of water at zero degree Celsius = 0.001792 and

$$y_1 = a + b\left(\frac{T_0}{T_k}\right) + c\left(\frac{T_0}{T_k}\right)^2 \tag{5.21}$$

in which

T_k = given temperature in Kelvin; T_0 = 273.16;

and the constants a = -1.94; b = -4.8; c = 6.74.

5.1.5 Comparison of present model with classical Rouse's equation

It is shown in Fig (5.3) that the difference between the present model and the Rouse's equation is not so much. But the Rouse's equation (seen in previous chapter) gives over estimation of flow concentration in some place. Thus, the present model could describe the sediment laden flow much better than the Rouse's equation that was commonly used in this field.

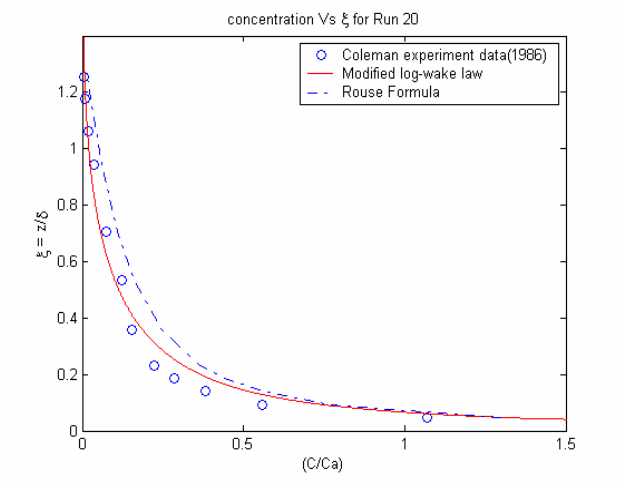

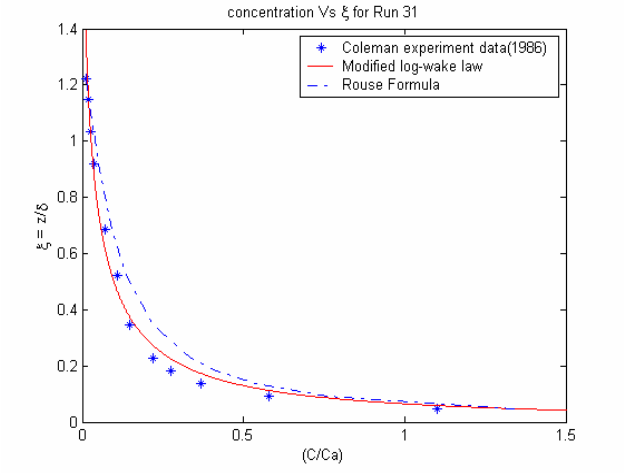

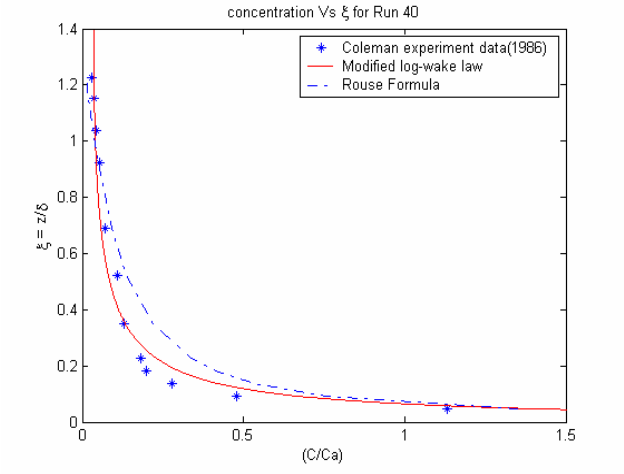

Fig (5.3) Comparison of present concentration model with Rouse's equation

5.2 Establishing relationship between parameters and Concentration gradient

In theoretical concentration profile equation (5.17), there were three parameters (κ, β, α). But we kept κ as a known value that was optimized from the velocity profile. Therefore, the optimization of parameters was done on the two parameters (β, α).

After the parameters were obtained from the data, a relation between sediment concentration gradient and the parameters were made.

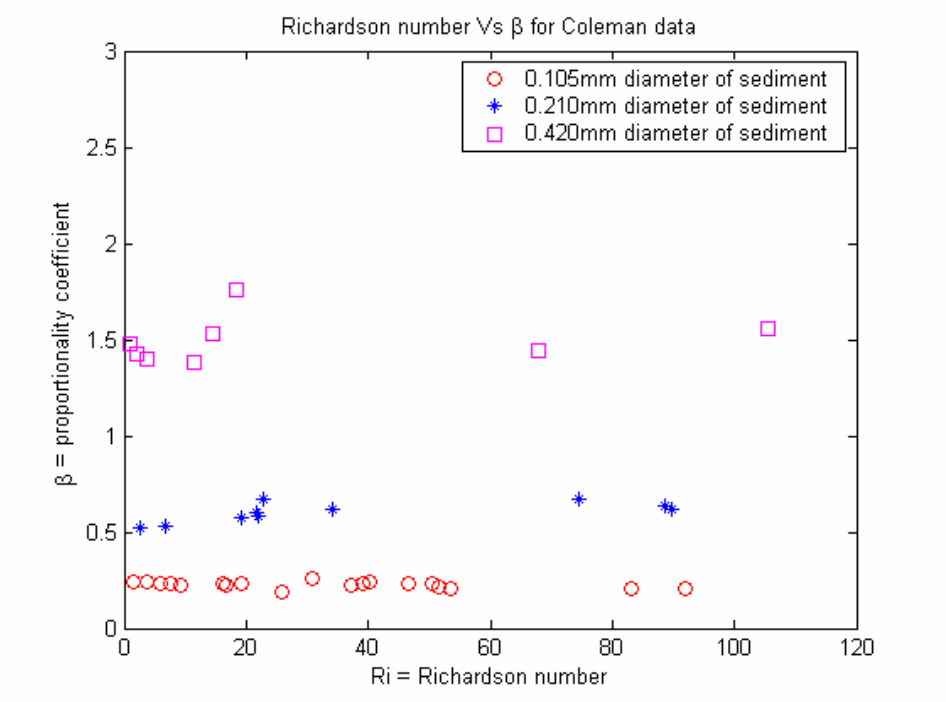

Fig (5.4) Checking of beta coefficient with sediment concentration gradient

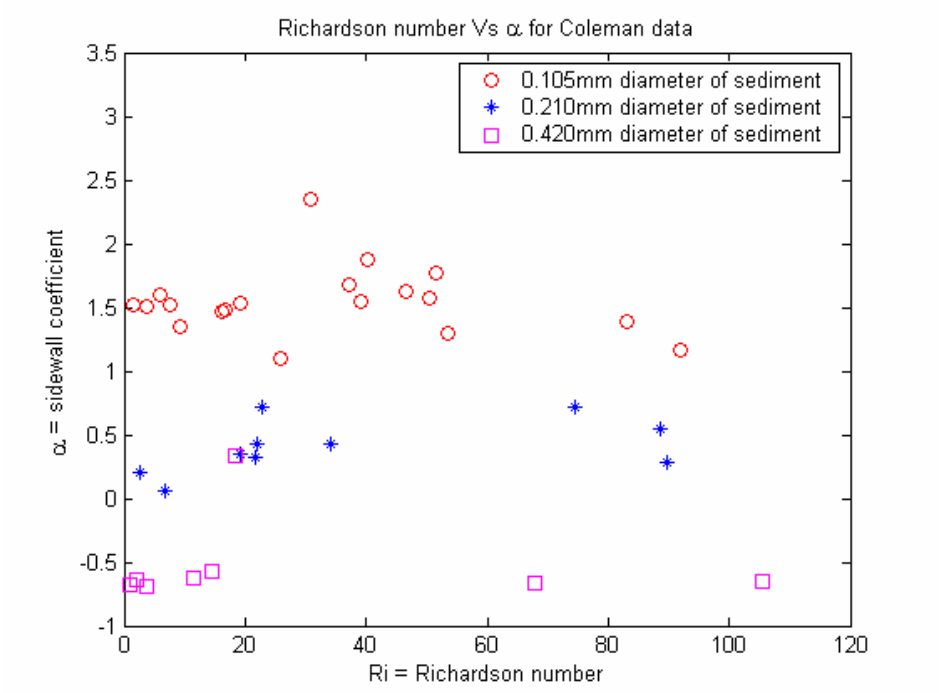

Fig (5.5) Checking of alpha coefficient with sediment concentration gradient

From these graphs, one could see that β and α did not change with sediment concentration gradient. These parameters only changed with the sizes of sediment particles. So we can try to establish a relationship between the values of β to that of the diameter size of the sediment.

From the β values obtained,

β ~ 0.3 for 0.105 mm diameter of sediment (fine) particle

β ~ 0.65 for 0.210 mm diameter of sediment (medium) particle

β ~ 1.5 for 0.420 mm diameter of sediment (coarse) particle

That means for the fine and medium sizes of sediment, the sediment transfer coefficient ε_s is smaller than the momentum transfer coefficient υ_t, while the opposite is true for the coarse sediment.

5.3 Establishing relationship between parameters and settling velocity

From another point of view, we could examine the effect of settling velocity of sediment particles on both parameters β and α . These results were shown in the following figures.

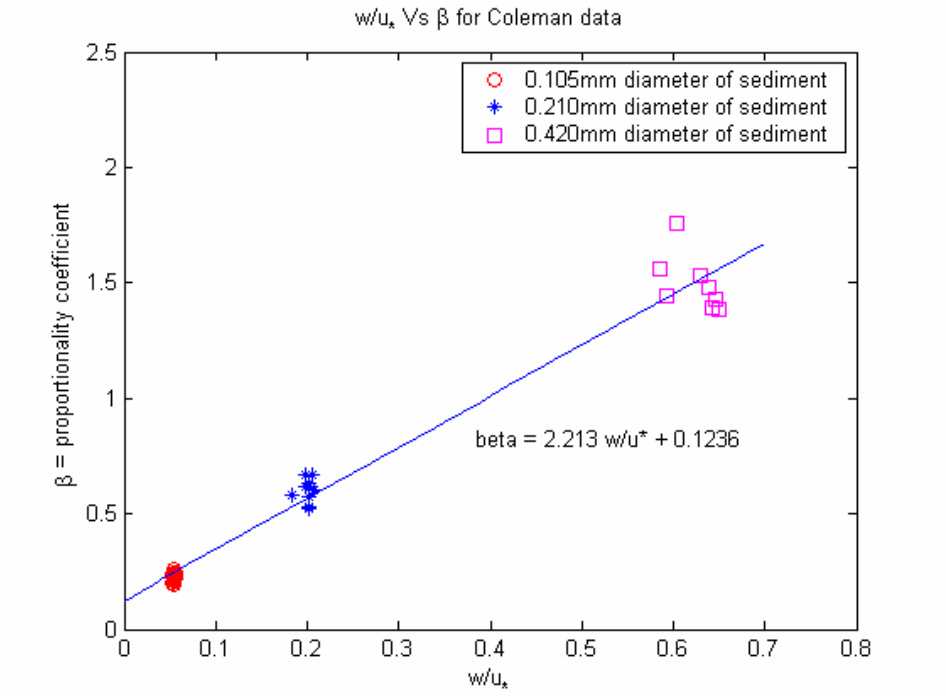

Fig (5.6) Checking of beta coefficient with settling velocity of suspended sediment.

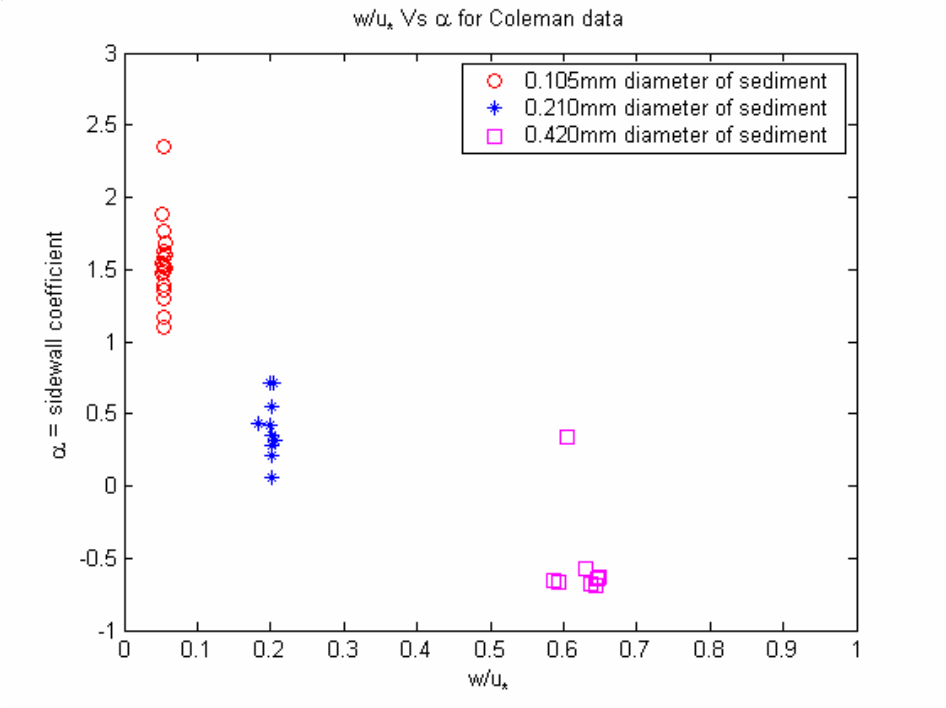

Fig (5.7) Checking of alpha coefficient with settling velocity of suspended sediment.

From the above figure (5.6), one can deduce that β varies directly with fall velocity for a constant flow condition as defined by u*. Moreover, its value will become larger for larger particles, other things being equal and we can propose the functional relationship between β and w/u* as follow:

β = 2.213 w/u* + 0.1236.

However, for the case of α parameter, a correlation between coefficient α and w/u* is unclear. We can only say that α becomes smaller for larger particles and the physical relationship between them require further studies.

5.4 Summary

This chapter presented the mathematical model for the concentration profile that can completely describe the distribution of the sediment concentration from the channel bed to the water surface. In this model, we incorporate velocity distribution equation that corresponds to modified log-wake law with the model. The main results of this chapter are as follow.

The distribution of the relative concentration of suspended load is in the form of the derived distribution equation (5.17) which consists of two parameters: the proportionality coefficient (β) for sediment transfer mechanism and the sidewalls coefficient (α) for secondary current. These two parameters need to be used in this model because in theoretical consideration, the analysis of turbulence events cannot be substituted for the analysis of sediment events. Thus, these parameters become important for sediment dynamics.

Moreover, the changes of the proportionality coefficient (β) with various sediment particles sizes shows that the value of β is about 0.3 for smaller particle size and otherwise, the value of β will increase to some what. But it is invariant with sediment concentration gradient. In addition, it is observed that the β<1 value is true for the sediment size up to medium size particles (i.e., about 0.2 mm ~ 0.3mm diameter). This suggestion agrees with the results of Graf and Cellino (2002) who conducted their experiment with the sand particles of 0.135mm and 0.230mm diameter. But they overlooked for coarse particle. Thus, from our results point of view, β > 1 value could be possible for coarse particle sediments.

Chapter 6

Conclusions

Application of modified log-wake law in sediment-laden flow is presented and tested with experimental data. The following conclusions are obtained:

1. The general equation for velocity profile in sediment-laden flow is

$$\frac{u_{\max}-u}{u_*}=-\frac{1}{\kappa}\left(\ln\xi-\frac{1}{25}\frac{u_{\max}}{u_{*b}}\frac{u_{*w}}{u_{*b}}\cos^2\frac{\pi\xi}{2}+\frac{1-\xi^3}{3}\right)$$

2. By only changing von Karman constant, the velocity profile of modified log-wake law compares very well with Coleman's (1986) experimental data in smooth rectangular channels as shown in figs (4.1).
3. The analysis of the application of modified log-wake law in sediment-laden flow indicates that the von Karman coefficient is dependent upon the amount of suspended sediment in an open channel flow and it decreases with increasing sediment concentration in the flows as shown in fig (4.2).
4. The Karman coefficient is a function of the gross flow Richardson number (concentration gradient) in fig (4.2).
5. The modified log-wake law can provide a better velocity gradient for turbulent mixing studies and give the corresponding concentration profile.
6. The general structure of the concentration profile is:

$$\ln\frac{C}{C_a}=-\frac{\omega}{\beta u_*\kappa}\left\{\ln\frac{\xi}{\xi_a}+\alpha(\xi^2-\xi_a^2)+(\xi-\xi_a)\right\}$$

7. The concentration profile has three parameters: (i) the von Karman constant carried from the velocity profile model; (ii) the proportionality coefficient (β) for sediment transfer mechanism (iii) the sidewalls coefficient (α).
8. The proportionality coefficient (β) is directly proportional to the size of the sediment and the settling velocity. But (β) is independent of the sediment concentration.
9. The secondary current effect coefficient (α) is independent of the properties of the sediment and that of the sediment concentration.

References:

Cardoso, A.H., Graf, W.H. and Gust, G.(1989). “Uniform flow in smooth open-channel.” J.Hydr.Res., IAHR, 27(5),603-616.

Chiu,C.L. and Chiou, J.D.(1987). “Structure of 3-D flow in rectangular open-channels.” J.Hydr.Res., IAHR, 112(11), 1050-1068.

Chiu,C.L. and Lin, G.F.(1983). “Computation of 3-D flow and shear in open channels.” J.Hydr.Eng., ASCE, 109(11), 1424-1440.

Chiu,C.L. and Tung, N.C. (2002). “Maximum velocity and regularities in open-channels.” J. Hydr.Eng., ASCE, 128(4), 390-398.

Coles,D.E.(1956).”The law of the wake in the turbulent boundary layer.” *J.Fluid Mech.*,1,191-226.

Coleman,N.L.(1981) .”Velocity profiles with suspended sediment.” *J.Hydr.Res.,19(3),211-229.*

Coleman, N.L.(1986). “Effects of suspended sediment on the open-channel distribution.” *Water Resources Research, AGU,22(10), 1377-1384.* 03.

Einstein, H.A. and Chien, N.(1955) . “Effects of heavy sediment concentration near the bed on velocity and sediment distribution.” U.S. Army Corps of Engineers, Missouri River Division Rep. No.8.

Elata, C. and Ippen, A.T.(1961). “The dynamics of open channel flow with suspensions of neutrally buoyant particles.” Technical Report No.45, Hydrodynamics Lab, MIT.

Guo,J.(1998).”Turbulent velocity profiless in clear water and sediment-laden flows.” *PhD dissertation,Colorado State University, Fort Collins, CO.*

Guo,J. and Julien,P.Y.(2001a).” Turbulent velocity profiles in sediment-laden flows.” *J.Hydr.Res.*, IAHR, 39(1),11-23.

Guo,J. and Julien,P.Y.(2001b). “ Modified log-wake law for turbulent flows in smooth pipes.” *J.Hudr.Res.*,IAHR(in review).

Guo, J. and Julien, P.Y.(2002). “Boundary shear stress in smooth rectangular open-channels.” J.Hydr.Engrg., ASCE(in review)

Hinze, J.O.(1975) . *Turbulence*.2nd Ed.,McGraw-Hill,790p.

Hu, C.H. and Hui, Y.J.(1995). Mechanical and Statistical Laws in Open-Channel Flows. China Science Press, Beijing, China (in Chinese), 343p.

Itakura, T. and T. Kishi, 1980, Open channel flow with suspended sediments, J.of the Hydr. Div.,ASCE, No. HY8, pp. 1325-1343.

Keulegan, G. H. (1938). “Laws of turbulent flow in open-channels.” J .Research., Nat. Bureau of Standards, 21(6) , 707-741.

Kirkgoz,S. (1989) . “Turbulent velocity profiles for smooth and rough open-channel flow.” *J.Hydr. Engrg.,* ASCE, 115(11) , 1543-1561.

Kironoto, B.A. and Graf, W.H.(1994). “Turbulence characteristics in rough uniform open-channel flow.” *Proc. Instn Civ. Engrs Wat. Marit. & Energy,* 106(12),333-344.

Knight, D.W., Demetriou J.D. and Mohammed, E.H.(1984). “Boundary shear in smooth rectangular channels.” J.Hydr.Eng., ASCE, 110(4) , 405-422.

Laufer,J.(1954).The structure of turbulence in fully developed pipe flow. Report 1174, National Advisory Committee for Aeronautics, Washington,D.C.

Lyn, D.A.(1986). Turbulence and Turbulent Transport in Sediment-Laden Open-Channel Flows. W.M. Keck Laboratory of Hydraulics and Water Resources, California Institute of Technology, Pasadena, CA.

Lyn, D.A.(1988) . “A similarity approach to turbulent sediment-laden flows in open-channels.” J.Fluid Mechanics, 193,1-26.

Lyn,D.A.(2000).”Regression Residuals and mean profioes in uniform open-channels flows.” J.Hydr.Engrg.,ASCE,126(1),24-32.

Lyn,D.A.(2001).”Regression Residuals and mean profiles in uniform open-channel flows.”Closure,J.Hydr.Engrg.,ASCE,127(8),705.

Muste,M.(2001). “ Regression Residuals and mean profiles in uniform open-channel flows.” *J.Hydr.engrg*.,ASCE,127(8),703-705.

Naot, D. and Rodi, W.(1982). “Calculation of secondary currents in channel flow. J.Hydr. Div., ASCE, 108(8), 948-968.

Neil L. Coleman “Effects Of Suspended Sediment On The Open-Channel Velocity Distribution” [1986] Paper number 5W4091, American Geophysical Union

Nezu, I. And Rodi,W(1986). “Open-channel flow measurements with a Laser Doppler Anemometer.” *J.Hydr. Engrg*., ASCE,112(5),335-355.

Schlichting, H.(1979).*Boundary-layer Theory*. McGraw-Hill,817p.

Tominaga, A. and Nezu, I (1992) . “Velocity profiles in steep open-channel flows.” *J.Hydr. Engrg.,* ASCE, 118(1),73-90.

Vanoni, V.A. and Nomicos,G.N.(1960). “Resistance properties in sediment-laden streams.” Trans., ASCE, 125, Paper No.3055, 1140-1175.

Vanoni, V.A.(1975). Sedimentation engineering. ASCE, New York, N.Y., Chapter I I.

Wang, Z. and Plate, E.J.(1996).”A preliminary study on the turbulence structure of flows of non-Newtonian fluid.” *J.Hydr.Res*. IAHR, 34(3), 345-361.

White,F.M(1991). Viscous fluid flow.McGraw-Hill,614p.

APPENDIX A SAMPLE MATLAB PROGRAM

Velocity Profile Program

```
[filename, filepath]=uigetfile('*.*', 'Open data file');

if isequal(filename,0), disp ('File not found'); return; end

Data = load([filepath, '\', filename], '-ascii');


z = Data(:,1);                          % (mm) distance from the channel bed

u = Data(:,2);                          % (m/s) velocity data at a given distance from the channel bed

Data2 = [0.1326   1.054     172

0.1259    1.045     171

0.127     1.043     172

0.1288    1.046     171

0.1286    1.046     171

0.1273    1.052     170

0.1281    1.053     171

0.1329    1.044     173

0.1322    1.051     172

0.1312    1.063     171

0.1316    1.081     169

0.1374    1.049     173

0.1274    1.065     171

0.1309    1.065     171

0.1282    1.075     171

0.1276    1.073     171

0.1402    1.065     171

0.1291    1.053     172

0.1292    1.072     170

0.1291    1.07      170
```

```
0.1261   1.048    169
0.1272   1.027    170
0.1246   1.047    170
0.1274   1.05     169
0.1249   1.069    167
0.1301   1.045    171
0.1274   1.069    168
0.1291   1.063    170
0.1301   1.083    168
0.1306   1.092    168
0.1325   1.06     172
0.1288   1.025    173
0.1308   1.036    174
0.127    1.044    172
0.1306   1.055    172
0.1302   1.082    171
0.1296   1.081    167
0.1305   1.114    167
0.1315   1.096    171
0.1321   1.101    171];

h = Data2(21,3);                        %  (mm)  flow depth
b = 356;                                % (mm) channel width
S = 0.002;                              % slope of channel bed
umax = Data2(21,2);                     % (m/s) maximum velocity of sediment-laden flow
delta = Data2(21,1).*1e3;               % (mm) distance from the channel bed to the point of maximum velocity
tau_b = (4./pi.*atan(exp(-pi.*h./b)) + pi./4.*h./b.*exp(-h./b));          % non-dimension bed shear stress
u_starb = sqrt(tau_b.*9.81.*h./1000.*S);                                  %  shear velocity at the bed
```

```
tau_w = b./2./h.*(1 - tau_b);                    % non-dimension wall shear stress
u_starw = sqrt(tau_w.*9.81.*h./1000.*S);         % shear velocity at the wall
x = z./delta;                                    % non-dimension normalized depth
y = (umax - u)./u_starb;
U = u./u_starb;
figure(1)
plot(U,x,'o'), hold on
figure(2)
semilogy(U,x,'o'), hold on
fun=inline(['(-sqrt(3).*exp(1)./2.*Pi.*(log(x)-
(',num2str(umax),'./(25.*',num2str(u_starb),').*cos(pi.*x./2).^2)+ (1 - x.^3)./3))'],'Pi','x');
Pi = lsqcurvefit(fun,[0.1], x, y)
x1 = logspace(-2, log10(h./delta), 50);
y1 = umax./u_starb + (sqrt(3).*exp(1)./2).*Pi.*(log(x1)-(umax./(25.*u_starb).*cos(pi.*x1./2).^2)+ (1 -
x1.^3)./3)
figure(1)
plot(y1,x1),  hold off
ylabel('{\xi} = y/{\delta}');
xlabel('u/u_*');
title('Velocity Profile for Run 23');
legend('Coleman experiment data(1986)','Modified log-wake law,2');
figure(2)
semilogy(y1,x1),  hold off
ylabel('{\xi} = y/{\delta}');
xlabel('u/u_*');
title('Velocity Profile for Run 23');
legend('Coleman experiment data(1986)','Modified log-wake law,2');
```

Concentration Profile Program

```
[filename, filepath]=uigetfile('*.*', 'Open data file');

if isequal(filename,0), disp ('File not found'); return; end

Data = load([filepath, '\', filename], '-ascii');

z = Data(:,1);                                  % (mm) depth of water level from the channel bed

C = Data(:,2);  % (m3/m3) given experimental concentration at a various level of depth from channel bed


Data2 = [0.000245       0.000065        0.00213 0.00095 127.2   0.0414  0.21    0.002   170
        0.5057  1.027   23.8
0.000560        0.000117        0.00570 0.00204 124.6   0.0414  0.21    0.002   170     0.4522
        1.047   23.8
0.000815        0.000159        0.01580 0.00321 127.4   0.0414  0.21    0.002   169     0.4256
        1.050   23.8
0.001210        0.000298        0.01750 0.00463 124.9   0.0414  0.21    0.002   167     0.3876
        1.069   23.9
0.001430        0.000300        0.01780 0.00508 130.1   0.0414  0.21    0.002   171     0.3947
        1.045   19.5
0.001890        0.000285        0.01900 0.00633 127.4   0.0414  0.21    0.002   168     0.3733
        1.069   23.0
0.002000        0.000332        0.02780 0.00759 129.1   0.0414  0.21    0.002   170     0.3704
        1.063   22.9
0.001790        0.000298        0.05700 0.00884 130.1   0.0414  0.21    0.002   168     0.3566
        1.083   23.3
0.002490        0.000273        0.07100 0.0102  130.6   0.0414  0.21    0.002   168     0.3572
        1.092   23.7
0.002680        0.000440        0.07100 0.0109  132.5   0.0414  0.21    0.002   172     0.3462
        1.060   23.9
];
```

```
h = Data2(2,9)  ;                    % (mm)  depth of water level
b = 356;                             % (mm) channel width
S = Data2(2,8);                      % channel bed slope
umax = Data2(2,11);                  % (m/s) maximum velocity
delta = Data2(2,5);                  % (mm) the location of maximum vertical velocity occurs

tau_b = (4./pi.*atan(exp(-pi.*h./b)) + pi./4.*h./b.*exp(-h./b));   % non-dimension
u_starb = sqrt(tau_b.*9.81.*h./1000.*S);                          % shear velocity at channel bed
tau_w = b./2./h.*(1 - tau_b);                                     % non-dimension
u_starw = sqrt(tau_w.*9.81.*h./1000.*S);                          %  velocity due to channel wall
ro_s = 2650 ;                                                     % density of sediment
ro_w = 1000 ;                                                     % density of water
C_avg = Data2(2,1) ;                                              % average concentration of sediment-water mixture
T = Data2(2,12) ;                                                 % given temperature in celcius
T_k = 273.16 + T;                                                 % change given T in celcius to T in Kelvin
a =  -1.94 ;                                                      % fixed coefficient in formula for finding dynamic viscosity of water
b = -4.8 ;
c = 6.74 ;
T_0 = 273.16;                                                     % Temperature in Kelvin at zero degrees Celsius
mu_0 = 0.001792 ;                                                 % dynamic viscosity of water at zero degree celcius
y1 = a + b *(T_0/T_k) + c *(T_0/T_k)^2;
mu_w = mu_0 .* exp(y1);                                           % dynamic viscosity of water at a given temperature in Kelvin
nu = (mu_w*(1 + 2.5 + 6.25 *(C_avg^2) + 15.62 *(C_avg^3)))/(1000 + 1650 *C_avg);   % kinematic viscosity of sediment
g = 9.81;                                                         % gravitational accelaration
d =Data2(2,7)./1000;                                              % diameter of sediment  (m)
d_star = (((ro_s - ro_w)*g/(ro_w * nu^2)) ^ (1/3)) * d            % d_*
w = (nu/d)* (d_star^3)/(24 + (sqrt(3)/2)*(d_star^1.5))            % settling velocity of sediment by Guo
```

```
x = z./delta;                                   % (kazad) normalized depth of water level (non dimension)
x_0 = 0.05.*h ./delta;                          %(kazad _ 0)
Ca = Data2(2,4);                                % concentration at y = 12 mm
K =  Data2(2,10) ;                              % corresponding von Karman constant
y =log(C./Ca);
fun = inline([' (-',num2str(w),'./(',num2str(u_starb.*K),'.*Pi(1))) .*(log (x./',num2str(x_0),') + Pi(2).*(x.^2 -
(',num2str(x_0),').^2) + (x - ',num2str(x_0),'))'],'Pi','x');

Pi = lsqcurvefit(fun,[1.0 0.1], x, y);
x1 = 0.01:0.001:1.4;
B =  (-w./(u_starb.*K.*Pi(1))).*(log (x1./x_0) + Pi(2).*(-x_0.^2 + x1.^2) +(x1 - x_0));

D = exp(B) ;
A =C./Ca;

figure(1)
plot(A,x,'*'),hold on
plot(D,x1,'r-'),hold off
ylabel('{\xi} = z/{\delta}'  );
xlabel('(C/Ca)');
title('concentration Vs {\xi} for Run 23');
legend('Coleman experiment data(1986)','Modified log-wake law');

figure(2)
semilogx(A,x,'*'),hold on
semilogx(D,x1,'r-'),hold off
ylabel('{\xi} = z/{\delta}'  );
xlabel('(C/Ca)');
title('concentration Vs {\xi} for Run 23');
```

```
legend('Coleman experiment data(1986)','Modified log-wake law');

figure(3)

loglog(A,x,'*'),hold on

semilogx(D,x1,'r-'),hold off

ylabel('{\xi} = z/{\delta}'  );

xlabel('(C/Ca)');

title('concentration Vs {\xi} for Run 23');

legend('Coleman experiment data(1986)','Modified log-wake law');
```

APPENDIX B
VELOCITY AND CONCENTRATION EXPERIMENTAL DATA

Run Number	Velocity and Concentration	y , mm											
		6	12	18	24	30	46	69	91	122	137	152	162
1	u(m/s)	0.709	0.773	0.823	0.849	0.884	0.927	0.981	1.026	1.054	1.053	1.048	1.039
	C(1e-4)	0	0	0	0	0	0	0	0	0	0	0	0
2	u(m/s)	0.705	0.768	0.817	0.852	0.883	0.938	0.975	1.03	1.049	1.043	1.03	1.023
	C(1e-4)	8.5	6.4	5.2	4.2	3.7	2.8	2.4	1.4	0.81	0.65	0.5	0.3
3	u(m/s)	0.68	0.738	0.795	0.836	0.87	0.922	0.963	1.025	1.048	1.039	1.028	1.02
	C(1e-4)	17	12	9.7	7.6	6.8	5.3	3.9	2.5	1.5	1.1	0.73	0.48
4	u(m/s)	0.665	0.74	0.802	0.829	0.863	0.922	0.965	1.023	1.049	1.048	1.033	1.024
	C(1e-4)	28	19	15	12	10	7.5	5.9	3.7	2.2	1.4	1	0.56
5	u(m/s)	0.662	0.717	0.788	0.814	0.852	0.911	0.968	1.028	1.038	1.047	1.03	1.027
	C(1e-4)	40	26	19	16	14	11	7.8	5	2.8	2	1.3	0.86
6	u(m/s)	0.652	0.727	0.766	0.805	0.848	0.905	0.951	1.037	1.054	1.049	1.026	1.031
	C(1e-4)	51	32	24	20	17	12	9.6	6.2	3.4	2.3	1.4	0.77
7	u(m/s)	0.639	0.709	0.77	0.804	0.849	0.924	0.962	1.03	1.061	1.051	1.04	1.027
	C(1e-4)	62	40	32	25	21	15	12	7.6	4.3	3	1.8	1.1
8	u(m/s)	0.63	0.696	0.751	0.8	0.831	0.902	0.958	1.012	1.044	1.046	1.033	1.028
	C(1e-4)	77	49	36	30	24	17	14	8.6	5	3.4	2	1.2
9	u(m/s)	0.621	0.683	0.751	0.804	0.842	0.897	0.945	1.028	1.048	1.05	1.04	1.032
	C(1e-4)	90	60	42	34	27	19	15	9.6	5.4	3.5	1.9	1.2
10	u(m/s)	0.619	0.688	0.759	0.808	0.841	0.912	0.976	1.033	1.061	1.062	1.05	1.045
	C(1e-4)	110	66	49	39	32	21	17	11	5.5	3.4	2	1
11	u(m/s)	0.625	0.688	0.761	0.812	0.855	0.929	0.989	1.05	1.085	1.077	1.07	1.063
	C(1e-4)	120	78	54	41	35	24	18	12	5.9	3.2	1.8	0.7
12	u(m/s)	0.598	0.669	0.731	0.796	0.83	0.912	0.964	1.004	1.052	1.058	1.045	1.033
	C(1e-4)	130	82	56	44	36	25	19	12	7	4	2.3	1.3
13	u(m/s)	0.6	0.665	0.747	0.798	0.844	0.914	0.973	1.038	1.07	1.062	1.045	1.039
	C(1e-4)	140	90	63	49	40	28	21	14	7.4	4.4	2.4	1.3
14	u(m/s)	0.598	0.669	0.746	0.8	0.84	0.922	0.971	1.042	1.067	1.062	1.051	1.048
	C(1e-4)	150	98	68	52	44	30	23	14	8	4.6	2.4	1.2
15	u(m/s)	0.588	0.674	0.746	0.799	0.85	0.918	0.98	1.052	1.074	1.07	1.059	1.05
	C(1e-4)	170	100	71	54	44	31	24	16	8.2	4.5	2.3	1.3
16	u(m/s)	0.583	0.661	0.744	0.804	0.854	0.922	0.978	1.051	1.074	1.07	1.057	1.046
	C(1e-4)	180	110	74	56	47	32	25	16	7.9	4.6	2.2	1.2

17	u(m/s)	0.586	0.655	0.75	0.804	0.838	0.938	0.976	1.022	1.071	1.071	1.06	1.053
	C(1e-4)	190	110	64	58	4.7	31	24	15	7.6	4.7	2.1	1.4
18	u(m/s)	0.579	0.688	0.734	0.78	0.836	0.916	0.966	1.027	1.054	1.053	1.049	1.024
	C(1e-4)	190	110	74	56	46	32	24	15	8	5.2	2.5	1.3
19	u(m/s)	0.576	0.649	0.743	0.798	0.838	0.916	0.976	1.047	1.07	1.07	1.057	1.048
	C(1e-4)	210	120	77	59	48	32	25	16	8	4.4	2.2	1.6
20	u(m/s)	0.57	0.648	0.743	0.791	0.848	0.922	0.986	1.043	1.07	1.068	1.057	1.048
	C(1e-4)	230	120	82	61	48	33	26	16	7.6	4	2	1.1
21	u(m/s)	0.734	0.789	0.827	0.867	0.891	0.936	0.987	1.03	1.048	1.046	1.033	1.028
	C(1e-4)	0	0	0	0	0	0	0	0	0	0	0	0
22	u(m/s)	0.738	0.775	0.814	0.841	0.855	0.916	0.953	1.015	1.026	1.024	1.012	1.008
	C(1e-4)	9.8	6.3	4.2	3.3	3	2.1	1.6	1.1	0.64	0.5	0.42	0.32
23	u(m/s)	0.717	0.764	0.816	0.839	0.866	0.918	0.971	1.03	1.052	1.039	1.027	1.021
	C(1e-4)	21	12	8.6	6.8	5.8	3.9	2.9	1.9	1.1	0.9	0.63	0.64
24	u(m/s)	0.684	0.742	0.794	0.844	0.872	0.922	0.959	1.03	1.056	1.049	1.034	1.024
	C(1e-4)	34	18	13	11	8.6	6	4.5	2.7	1.6	1.2	0.89	0.63
25	u(m/s)	0.66	0.737	0.79	0.844	0.872	0.934	0.984	1.051	1.073	1.063	1.048	1.04
	C(1e-4)	48	26	18	13	11	7.6	5.9	3.6	2.2	1.5	1.1	0.68
26	u(m/s)	0.649	0.713	0.775	0.809	0.843	0.899	0.96	1.02	1.045	1.041	1.032	1.027
	C(1e-4)	54	32	22	18	14	9.7	7.8	4.8	2.8	2.1	1.5	1.1
27	u(m/s)	0.662	0.72	0.775	0.801	0.863	0.925	0.984	1.042	1.075	1.064	1.052	1.044
	C(1e-4)	66	40	26	21	17	12	8.9	5.3	2.8	2	1.4	0.88
28	u(m/s)	0.638	0.714	0.771	0.811	0.848	0.91	0.967	1.04	1.065	1.06	1.043	1.044
	C(1e-4)	80	48	31	23	19	13	9.8	5.9	3.3	2.3	1.7	1.2
29	u(m/s)	0.648	0.701	0.776	0.823	0.853	0.93	0.991	1.055	1.084	1.082	1.066	1.064
	C(1e-4)	95	52	34	26	21	17	11	6.4	3.4	2.6	1.6	0.98
30	u(m/s)	0.661	0.713	0.772	0.822	0.876	0.932	0.999	1.064	1.089	1.093	1.076	1.074
	C(1e-4)	110	57	39	28	24	16	12	7.1	3.7	2.7	1.8	1.1
31	u(m/s)	0.598	0.679	0.743	0.791	0.828	0.899	0.96	1.026	1.063	1.058	1.048	1.042
	C(1e-4)	120	63	40	30	24	16	12	7.1	3.7	2.7	1.8	1.1
32	u(m/s)	0.689	0.746	0.786	0.821	0.838	0.887	0.994	0.999	1.024	1.025	1.012	1.004
	C(1e-4)	0	0	0	0	0	0	0	0	0	0	0	0
33	u(m/s)	0.69	0.746	0.791	0.832	0.853	0.903	0.948	1.027	1.018	1.042	1.027	1.018
	C(1e-4)	2.7	1.4	8.6	0.66	0.57	0.43	0.34	0.23	0.19	0.16	0.14	0.12
34	u(m/s)	0.709	0.745	0.788	0.82	0.861	0.906	0.952	1.019	1.046	1.05	1.029	1.012
	C(1e-4)	5.1	2.4	1.5	1.2	0.97	0.7	0.56	0.32	0.27	0.24	0.19	0.18
35	u(m/s)	0.688	0.733	0.788	0.826	0.863	0.917	0.96	1.019	1.065	1.06	1.045	1.028
	C(1e-4)	9.3	4.1	2.2	1.7	1.5	1.1	0.86	0.56	0.42	0.34	0.31	0.25

36	u(m/s)	0.698	0.74	0.804	0.841	0.881	0.942	0.988	1.055	1.09	1.08	1.068	1.062
	C(1e-4)	17	6.8	3.8	3	2.3	1.7	1.2	0.88	0.61	0.48	0.4	0.32
37	u(m/s)	0.674	0.724	0.796	0.835	0.871	0.92	0.985	1.05	1.086	1.077	1.067	1.058
	C(1e-4)	19	7.8	4.7	3.6	2.9	2.2	1.7	1.1	0.8	0.63	0.54	0.43
38	u(m/s)	0.716	0.735	0.81	0.847	0.884	0.952	0.998	1.091	1.118	1.11	1.098	1.092
	C(1e-4)	22	11	6	4.6	4	2.7	2.2	1.4	0.96	0.79	0.64	0.55
39	u(m/s)	0.677	0.745	0.798	0.826	0.871	0.936	0.989	1.068	1.099	1.096	1.084	1.072
	C(1e-4)	27	11	6.2	4.9	4	3	2.3	1.6	1	8.8	0.8	0.64
40	u(m/s)	0.678	0.71	0.792	0.836	0.879	0.936	0.985	1.069	1.107	1.101	1.086	1.08
	C(1e-4)	26	11	6.4	4.6	4.2	3	2.5	1.6	1.2	0.97	0.8	0.69

APPENDIX C RESULTED VELOCITY PROFILE FIGURES

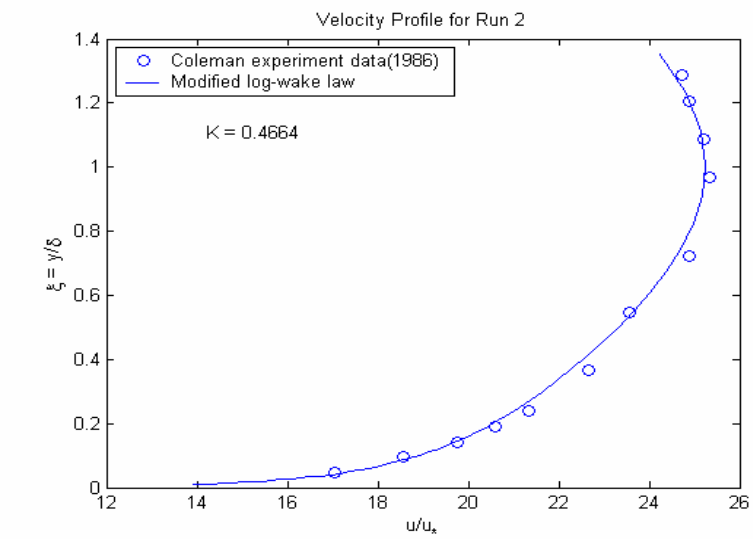

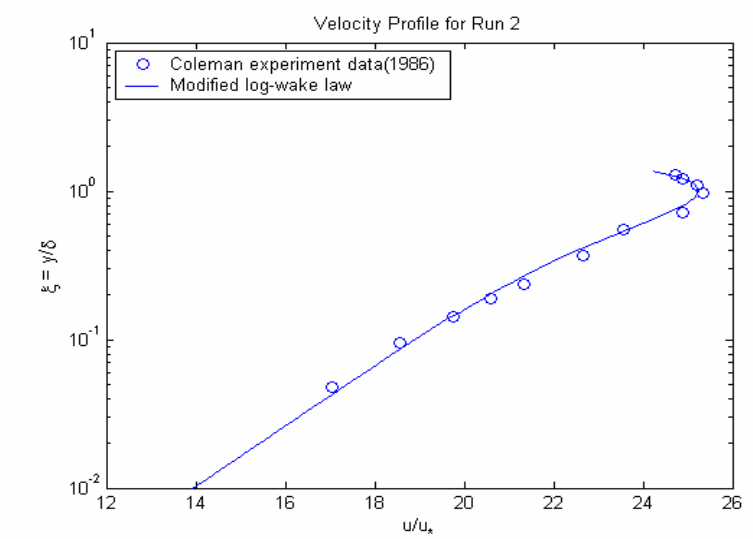

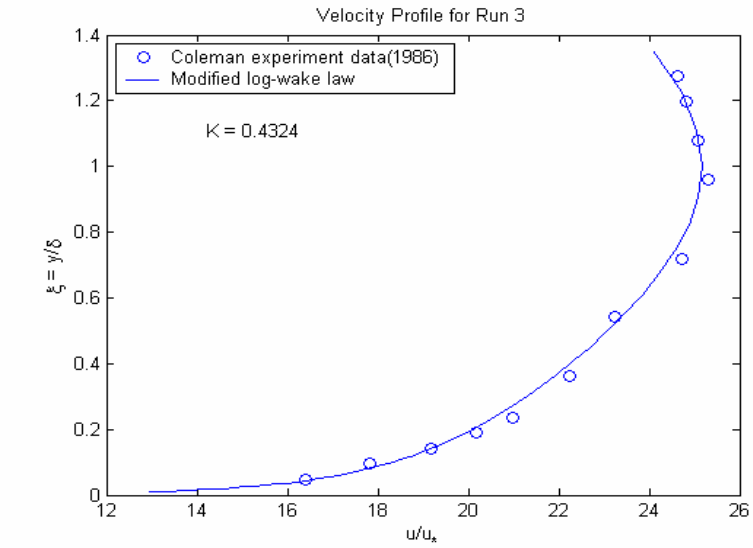

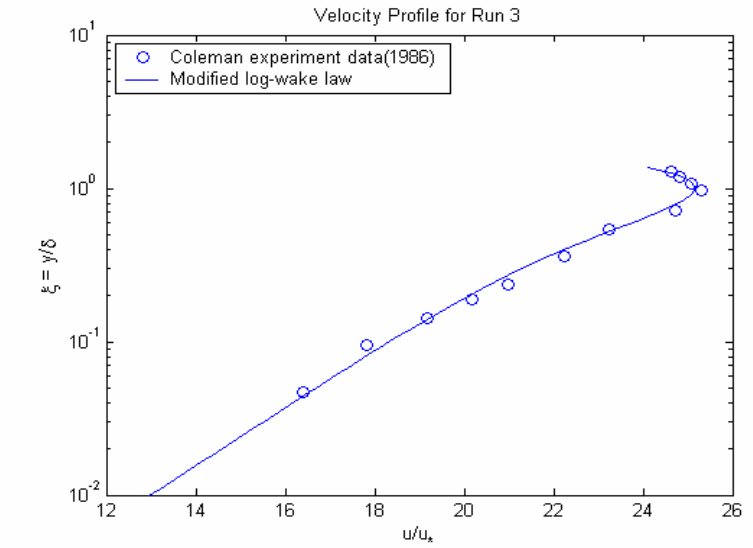

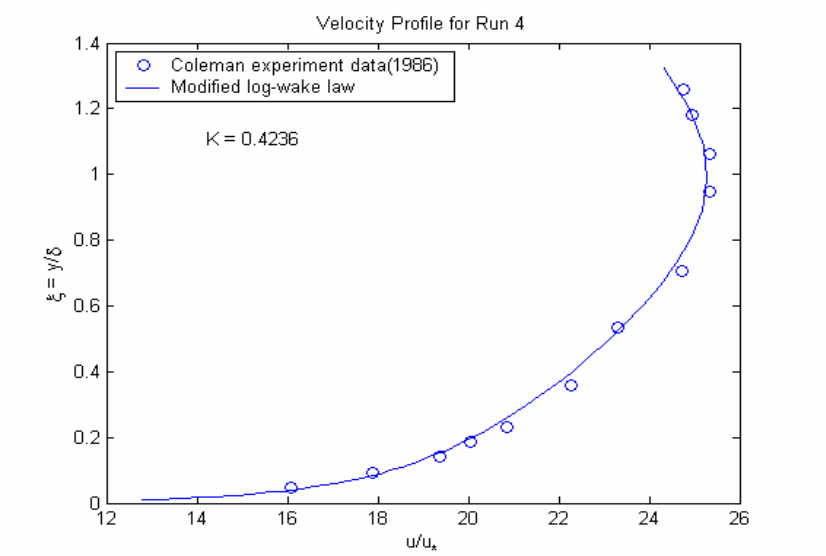
Velocity Profile for Run 4
Coleman experiment data(1986)
Modified log-wake law
K = 0.4236
ξ = y/δ
u/u*

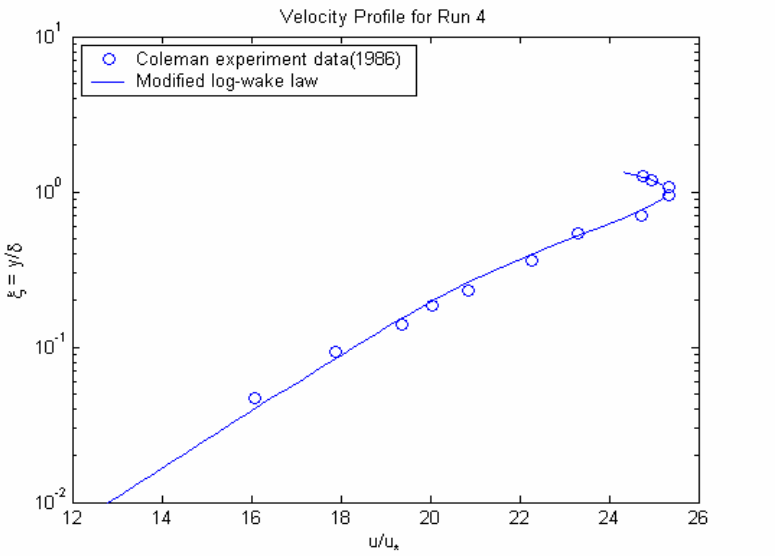
Velocity Profile for Run 4
Coleman experiment data(1986)
Modified log-wake law
ξ = y/δ
u/u*

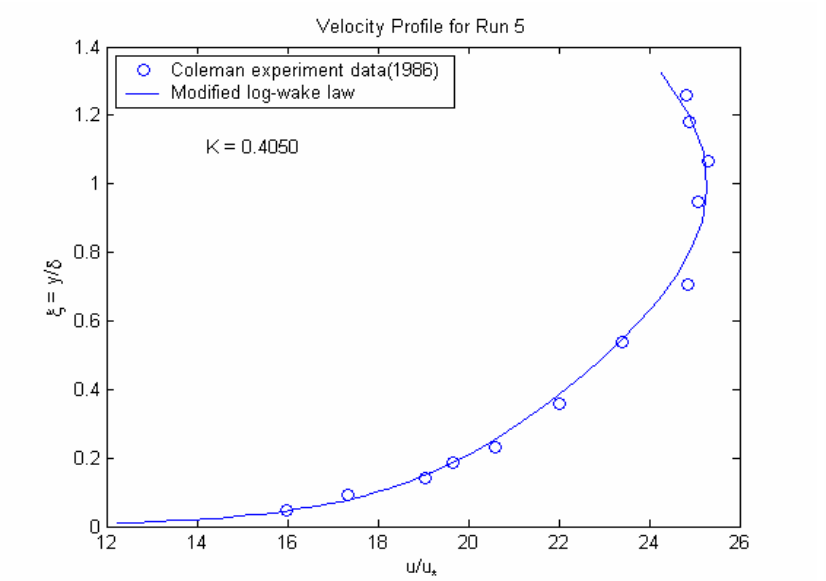
Velocity Profile for Run 5
Coleman experiment data(1986)
Modified log-wake law
K = 0.4050
ξ = y/δ
u/u*

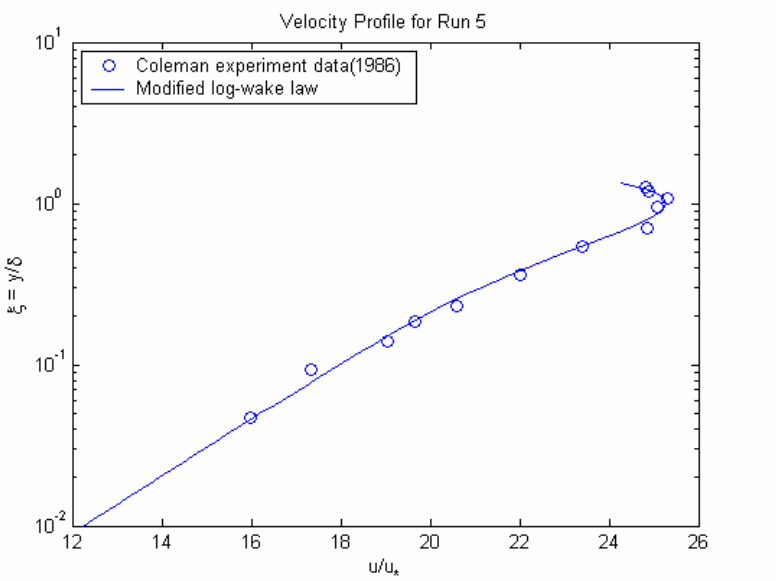
Velocity Profile for Run 5
Coleman experiment data(1986)
Modified log-wake law
ξ = y/δ
u/u*

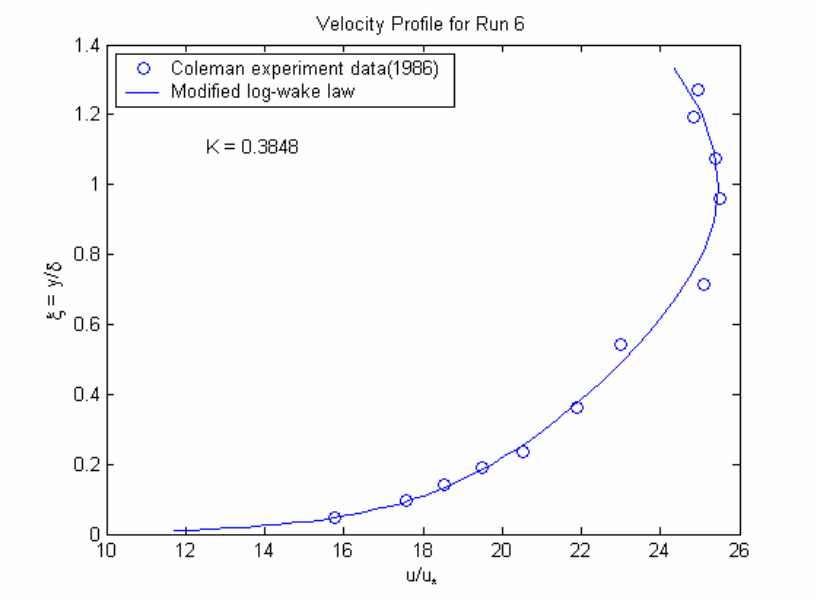
Velocity Profile for Run 6
Coleman experiment data(1986)
Modified log-wake law
K = 0.3848
ξ = y/δ
u/u*

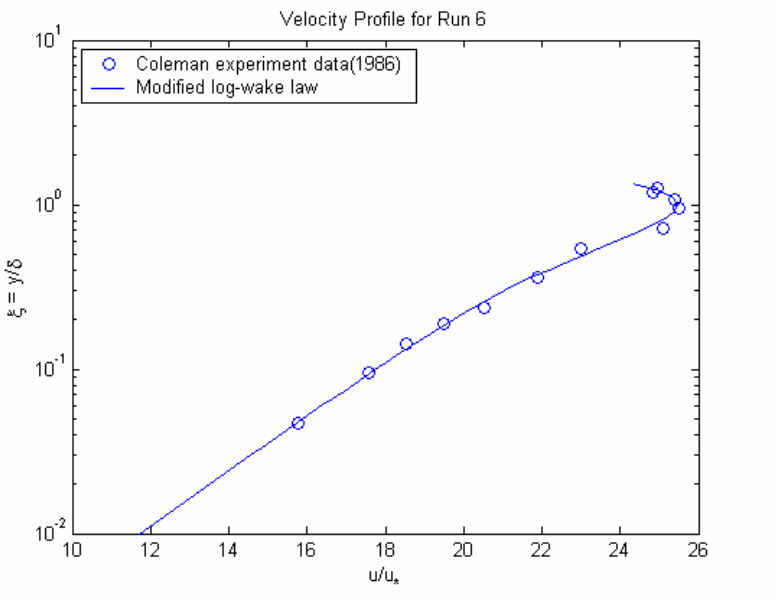
Velocity Profile for Run 6
Coleman experiment data(1986)
Modified log-wake law
ξ = y/δ
u/u*

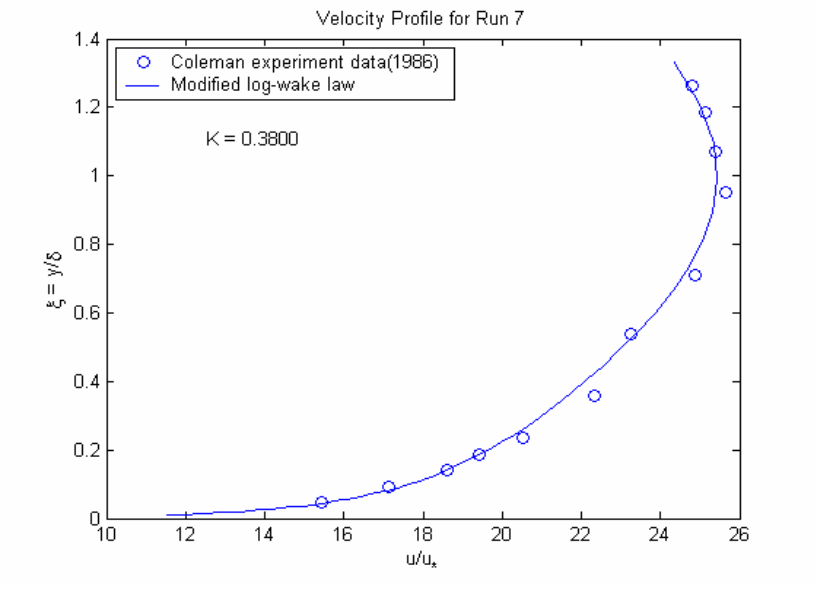
Velocity Profile for Run 7
Coleman experiment data(1986)
Modified log-wake law
K = 0.3800
ξ = y/δ
u/u*

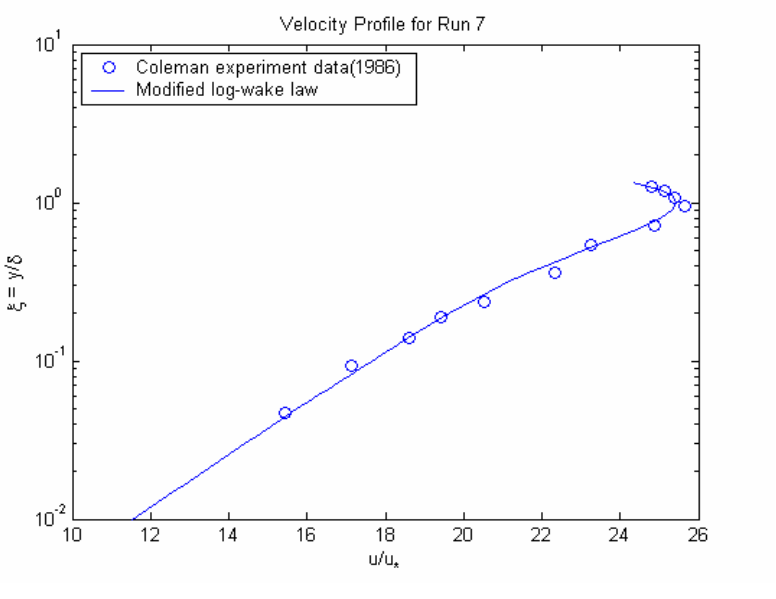
Velocity Profile for Run 7
Coleman experiment data(1986)
Modified log-wake law
ξ = y/δ
u/u*

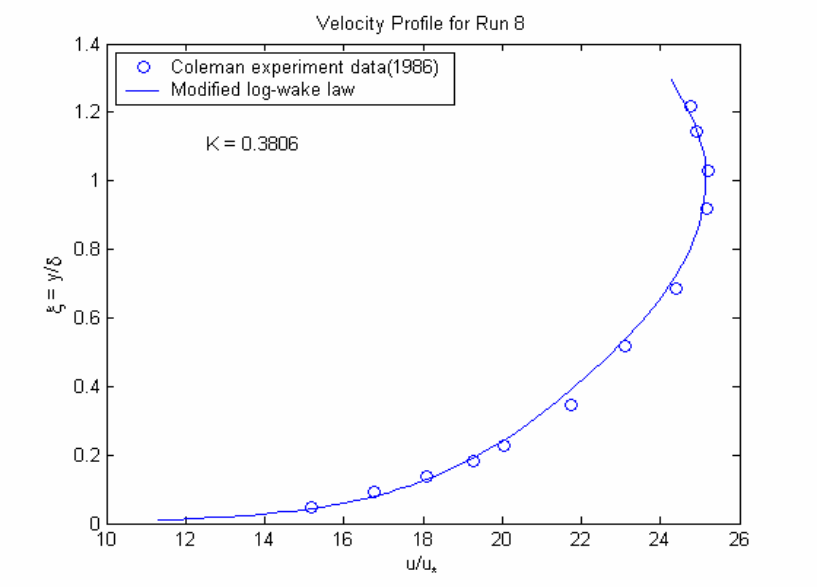
Velocity Profile for Run 8
Coleman experiment data(1986)
Modified log-wake law
K = 0.3806
ξ = y/δ
u/u*

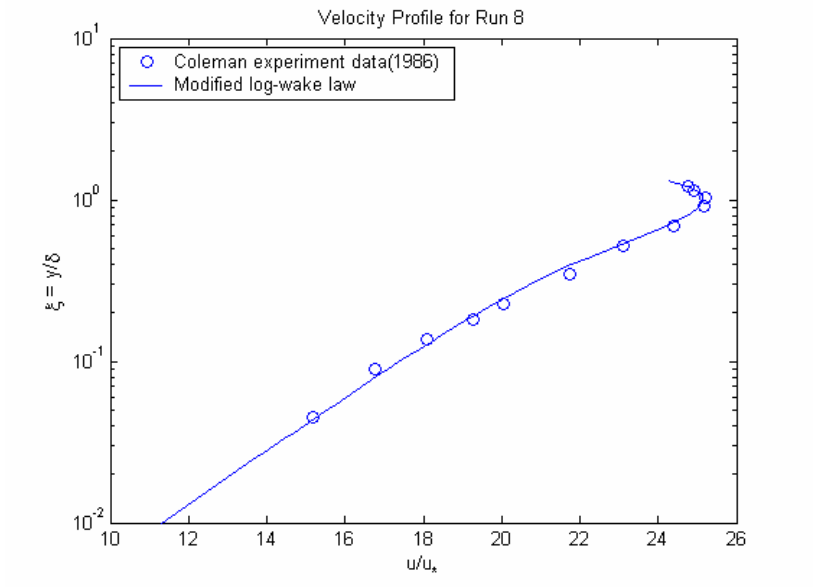
Velocity Profile for Run 8
Coleman experiment data(1986)
Modified log-wake law
ξ = y/δ
u/u*

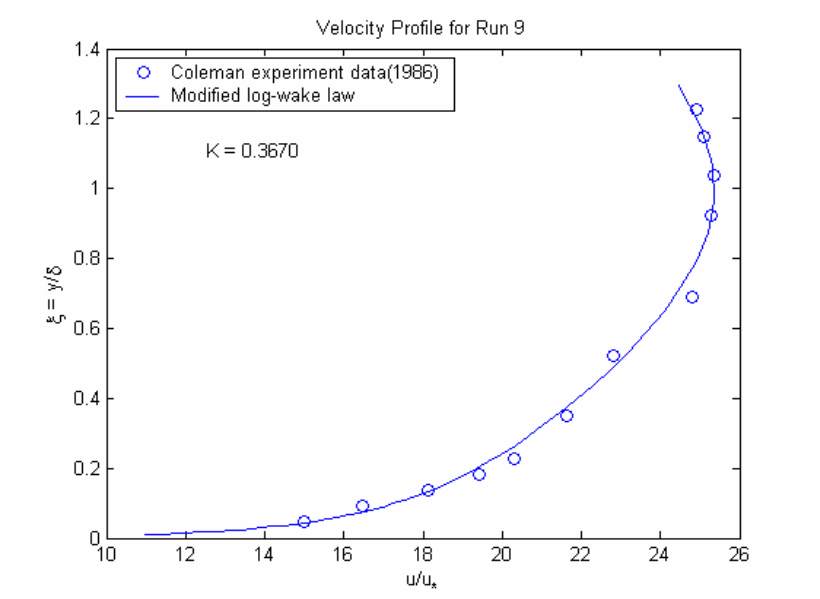
Velocity Profile for Run 9
Coleman experiment data(1986)
Modified log-wake law
K = 0.3670
ξ = y/δ
u/u*

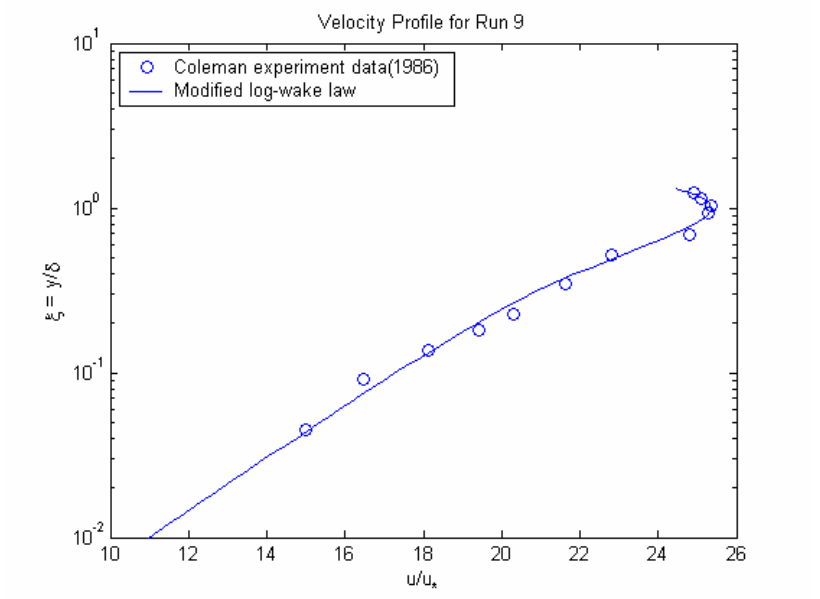
Velocity Profile for Run 9
Coleman experiment data(1986)
Modified log-wake law
ξ = y/δ
u/u*

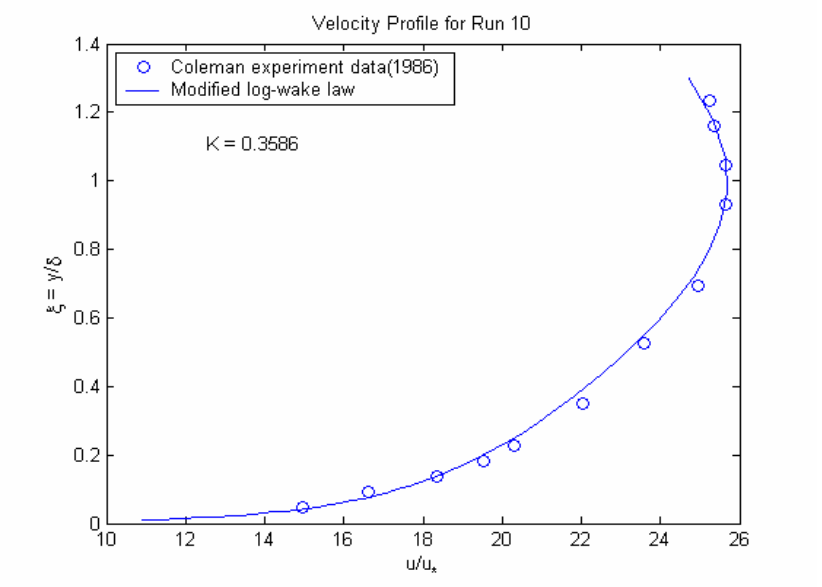
Velocity Profile for Run 10
Coleman experiment data(1986)
Modified log-wake law
K = 0.3586
ξ = y/δ
u/u*

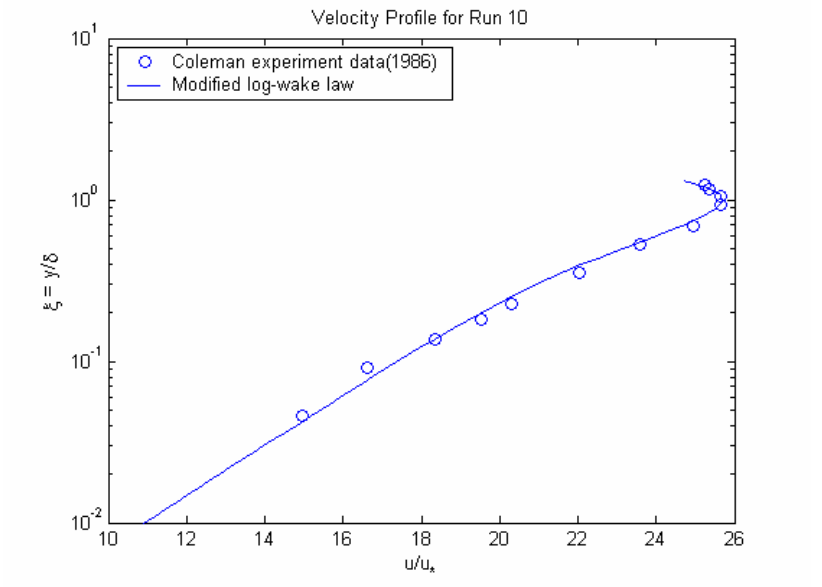
Velocity Profile for Run 10
Coleman experiment data(1986)
Modified log-wake law
ξ = y/δ
u/u*

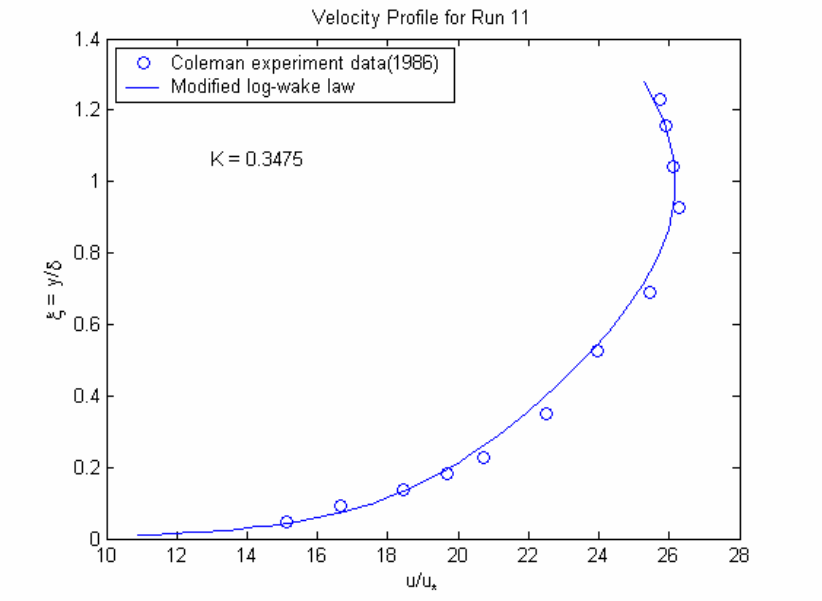
Velocity Profile for Run 11
Coleman experiment data(1986)
Modified log-wake law
K = 0.3475
ξ = y/δ
u/u*

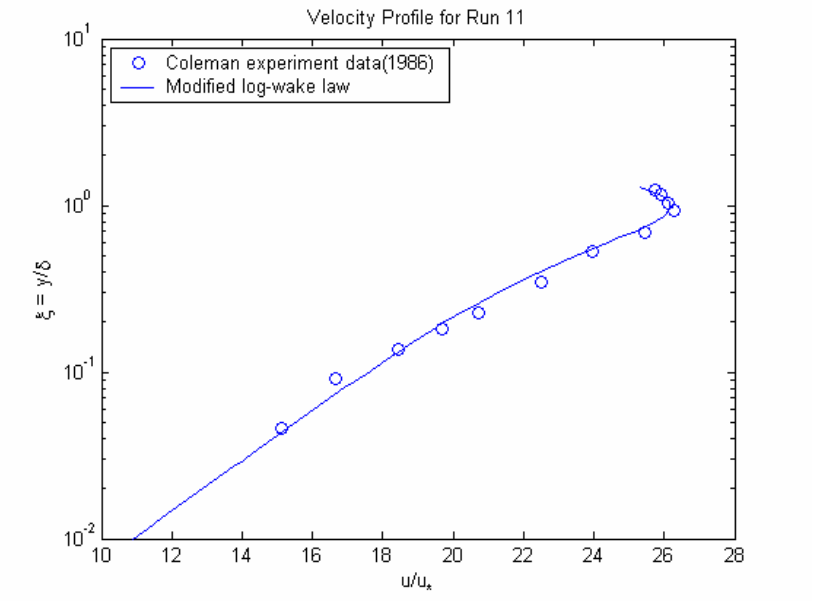
Velocity Profile for Run 11
Coleman experiment data(1986)
Modified log-wake law
ξ = y/δ
u/u*

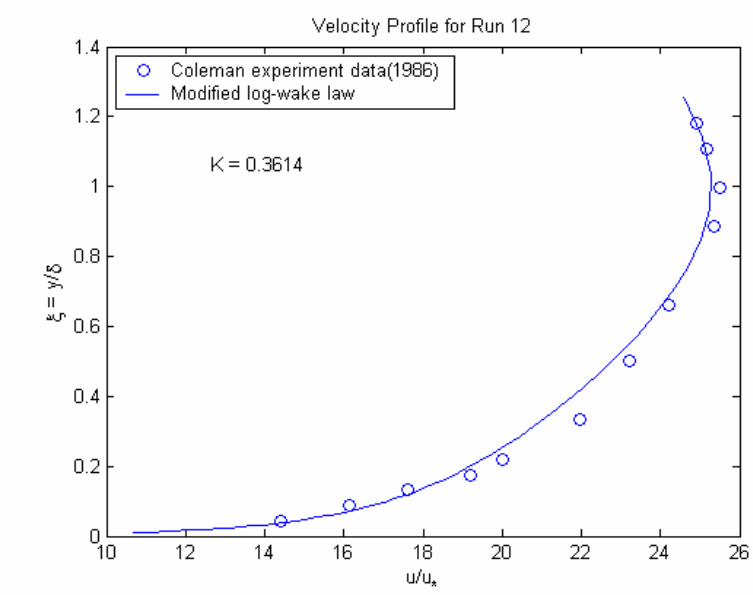
Velocity Profile for Run 12
Coleman experiment data(1986)
Modified log-wake law
K = 0.3614
ξ = y/δ
u/u*

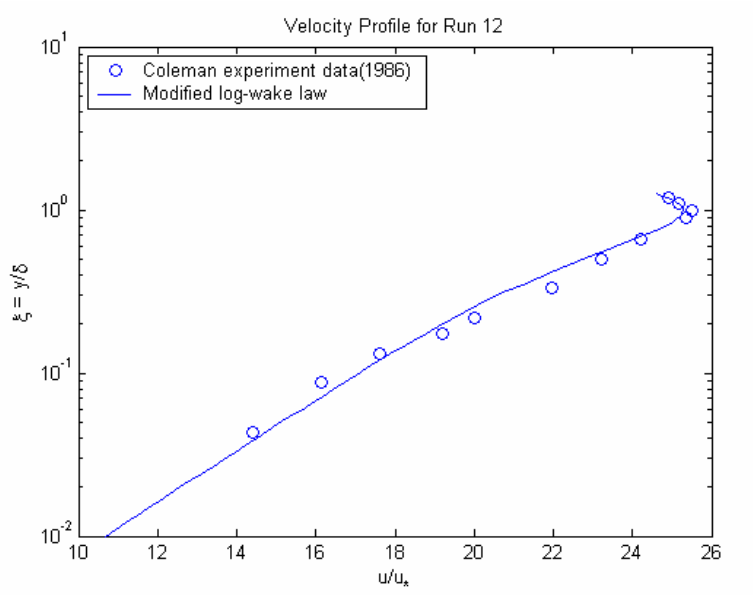
Velocity Profile for Run 12
Coleman experiment data(1986)
Modified log-wake law
ξ = y/δ
u/u*

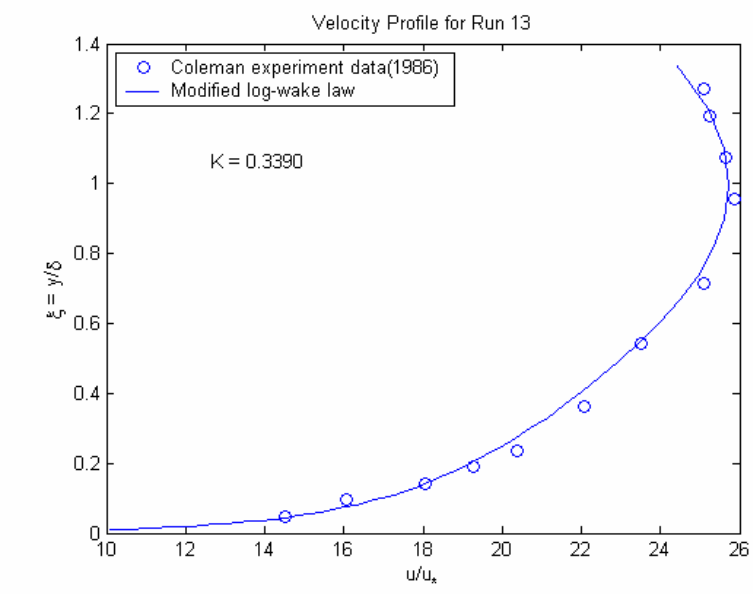
Velocity Profile for Run 13
Coleman experiment data(1986)
Modified log-wake law
K = 0.3390
ξ = y/δ
u/u*

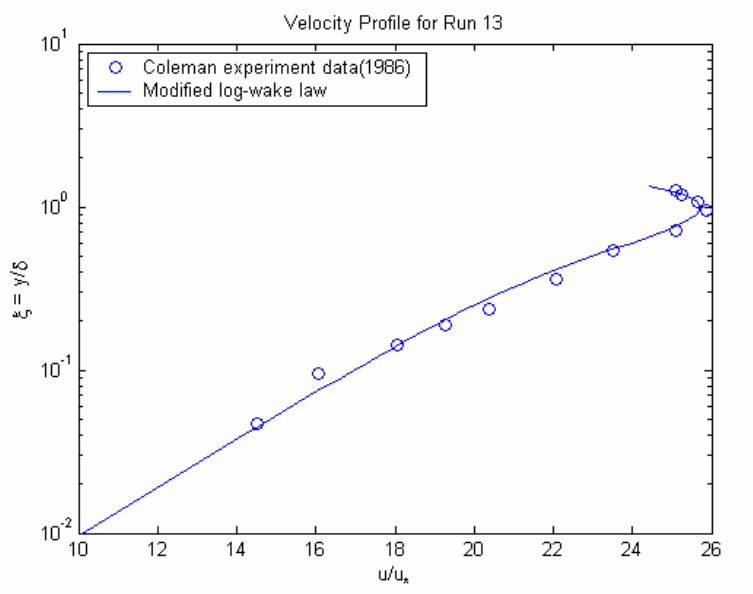
Velocity Profile for Run 13
Coleman experiment data(1986)
Modified log-wake law
ξ = y/δ
u/u*

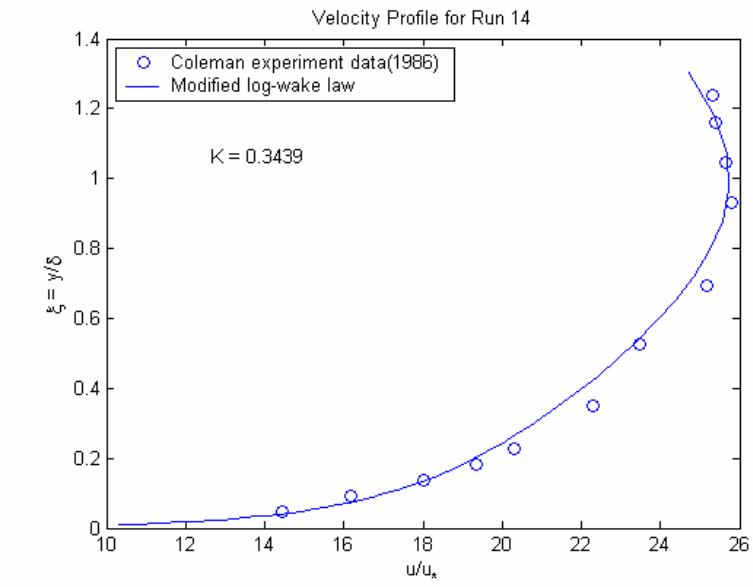
Velocity Profile for Run 14
Coleman experiment data(1986)
Modified log-wake law
K = 0.3439
ξ = y/δ
u/u*

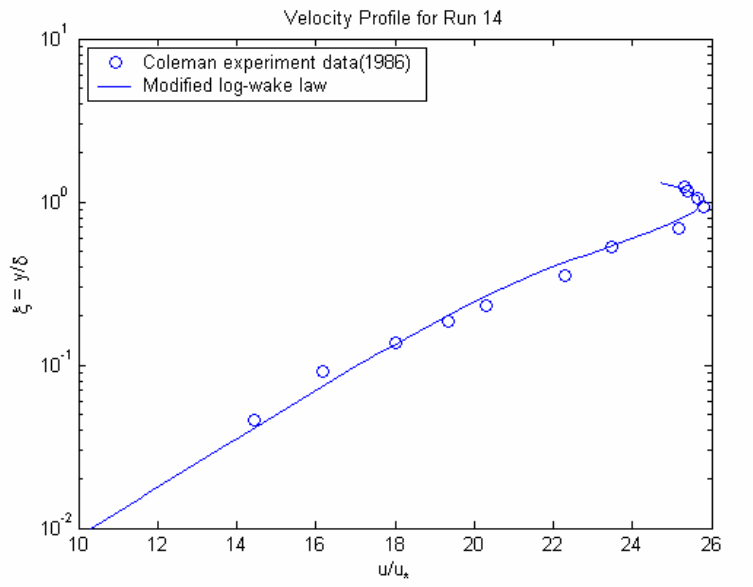
Velocity Profile for Run 14
Coleman experiment data(1986)
Modified log-wake law
ξ = y/δ
u/u*

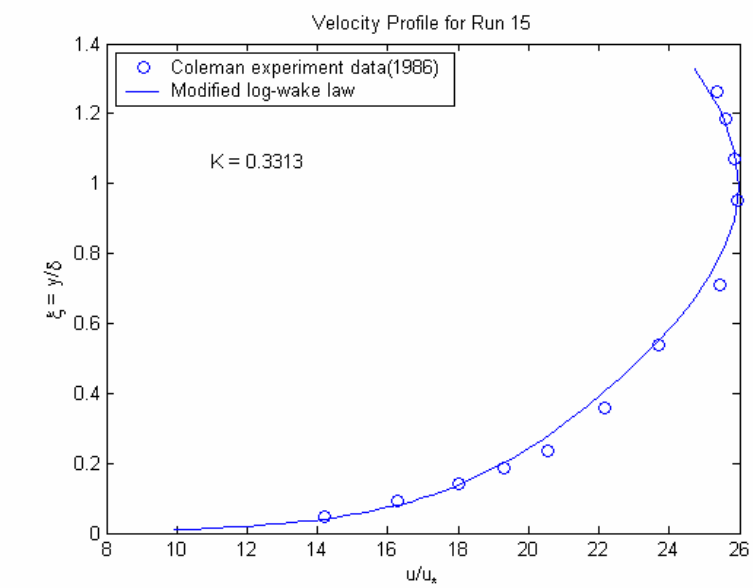
Velocity Profile for Run 15
Coleman experiment data(1986)
Modified log-wake law
K = 0.3313
ξ = y/δ
u/u*

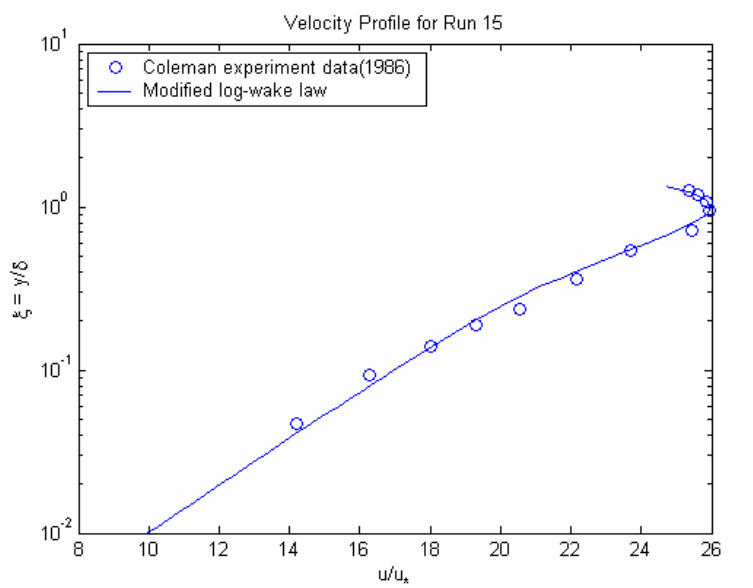
Velocity Profile for Run 15
Coleman experiment data(1986)
Modified log-wake law
ξ = y/δ
u/u*

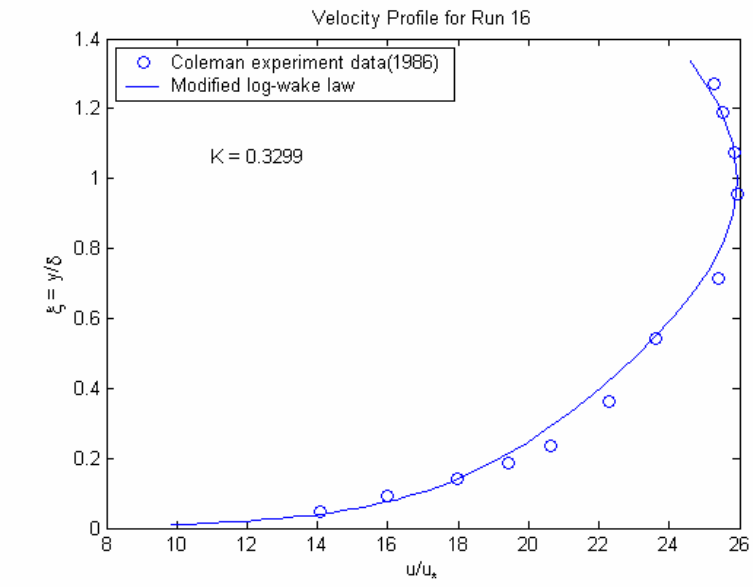
Velocity Profile for Run 16
Coleman experiment data(1986)
Modified log-wake law
K = 0.3299
ξ = y/δ
u/u*

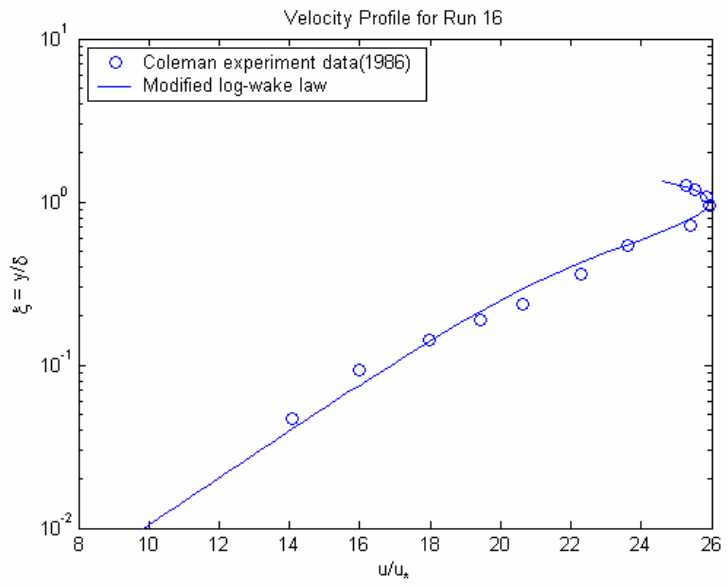
Velocity Profile for Run 16
Coleman experiment data(1986)
Modified log-wake law
ξ = y/δ
u/u*

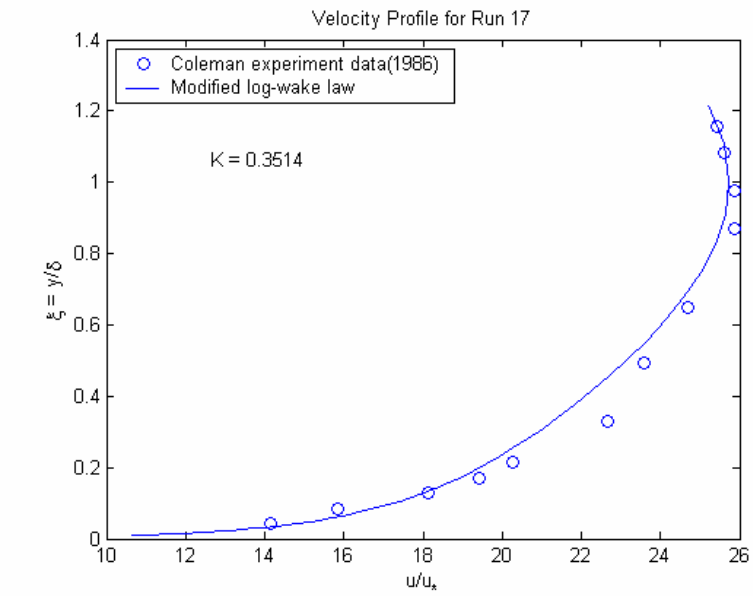
Velocity Profile for Run 17
Coleman experiment data(1986)
Modified log-wake law
K = 0.3514
ξ = y/δ
u/u*

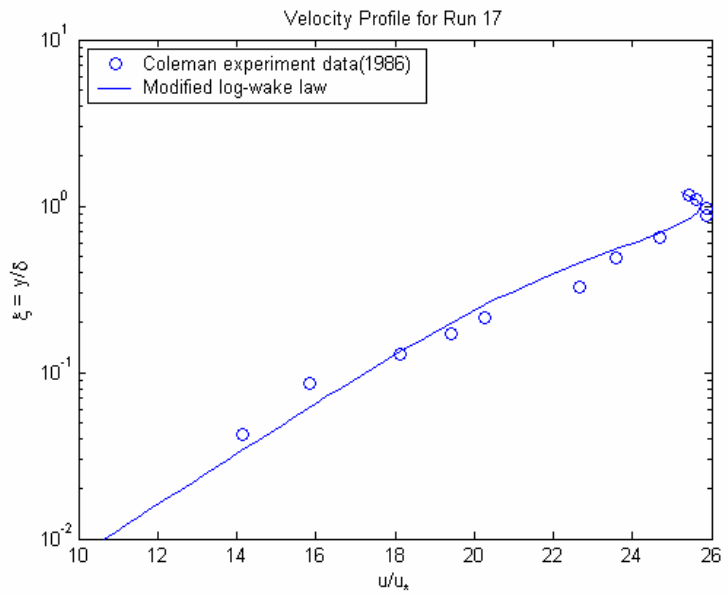
Velocity Profile for Run 17
Coleman experiment data(1986)
Modified log-wake law
ξ = y/δ
u/u*

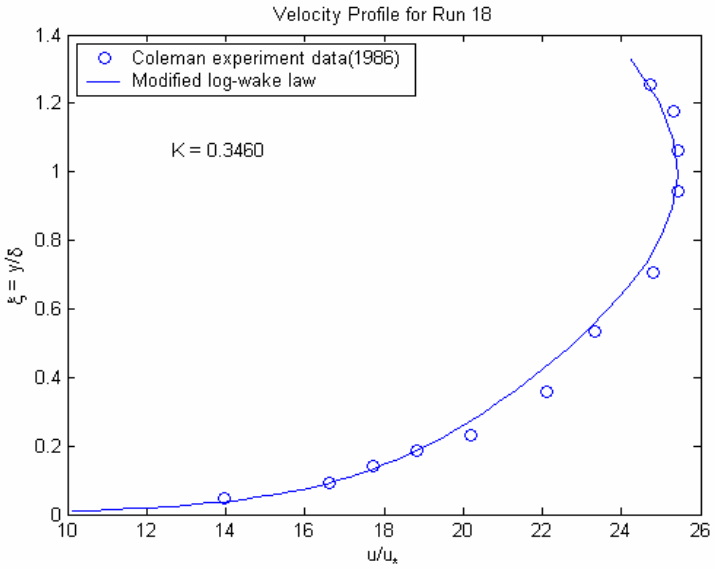
Velocity Profile for Run 18
Coleman experiment data(1986)
Modified log-wake law
K = 0.3460
ξ = y/δ
u/u*

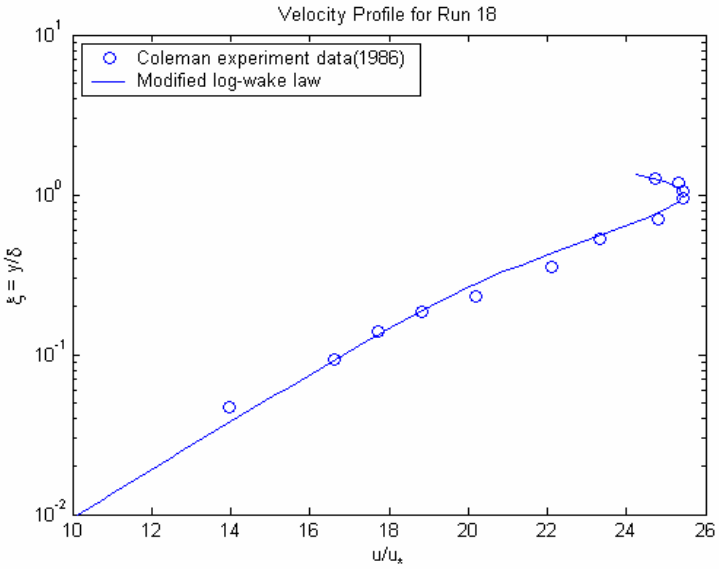
Velocity Profile for Run 18
Coleman experiment data(1986)
Modified log-wake law
ξ = y/δ
u/u*

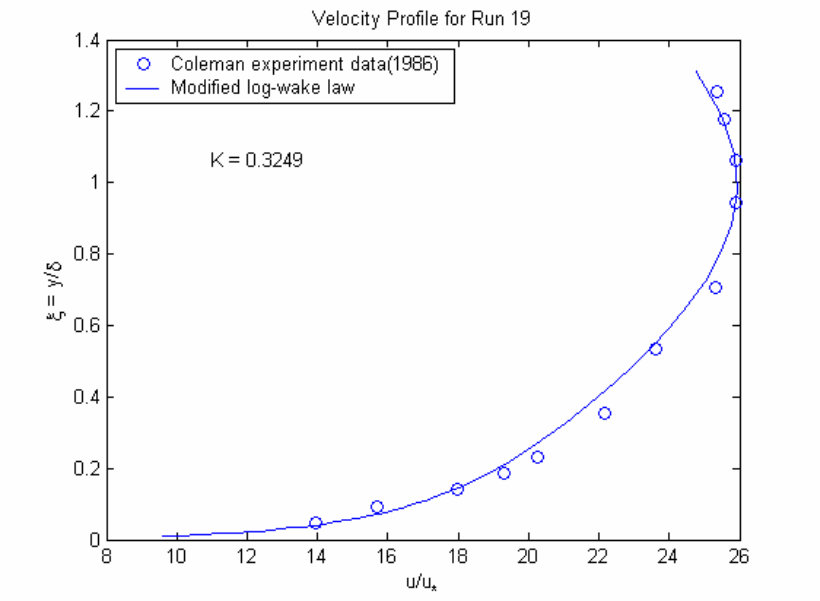
Velocity Profile for Run 19
Coleman experiment data(1986)
Modified log-wake law
K = 0.3249
ξ = y/δ
u/u*

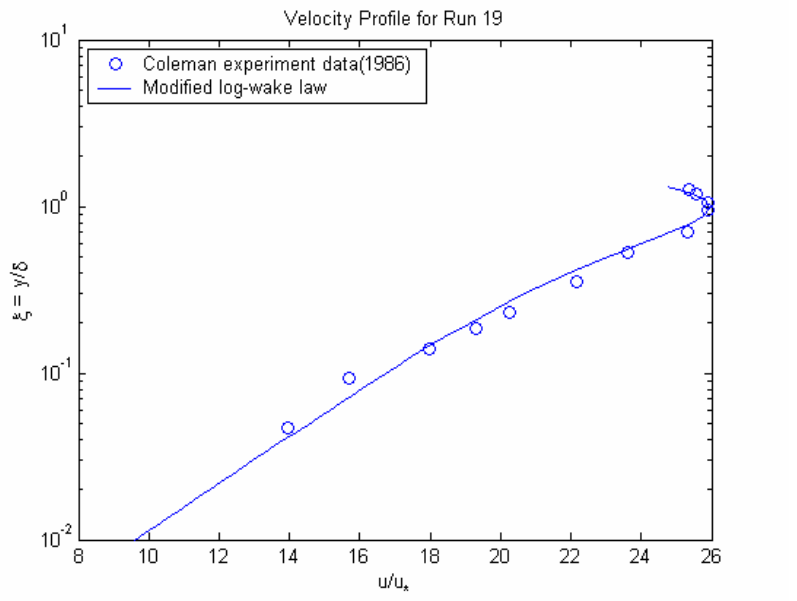
Velocity Profile for Run 19
Coleman experiment data(1986)
Modified log-wake law
ξ = y/δ
u/u*

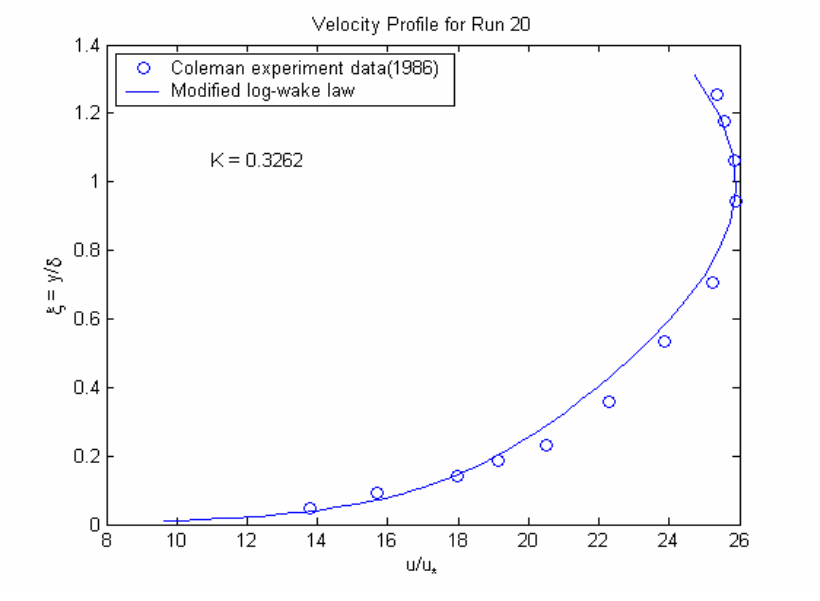
Velocity Profile for Run 20
Coleman experiment data(1986)
Modified log-wake law
K = 0.3262
ξ = y/δ
u/u*

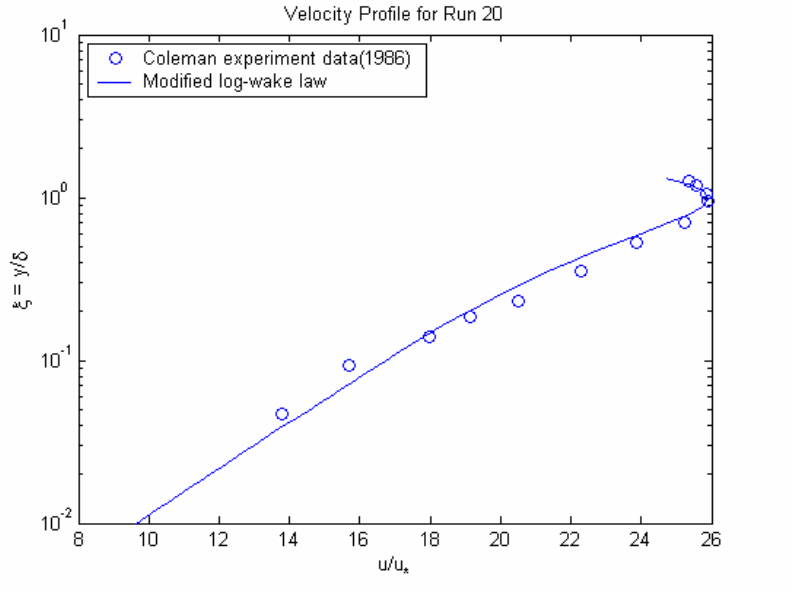
Velocity Profile for Run 20
Coleman experiment data(1986)
Modified log-wake law
ξ = y/δ
u/u*

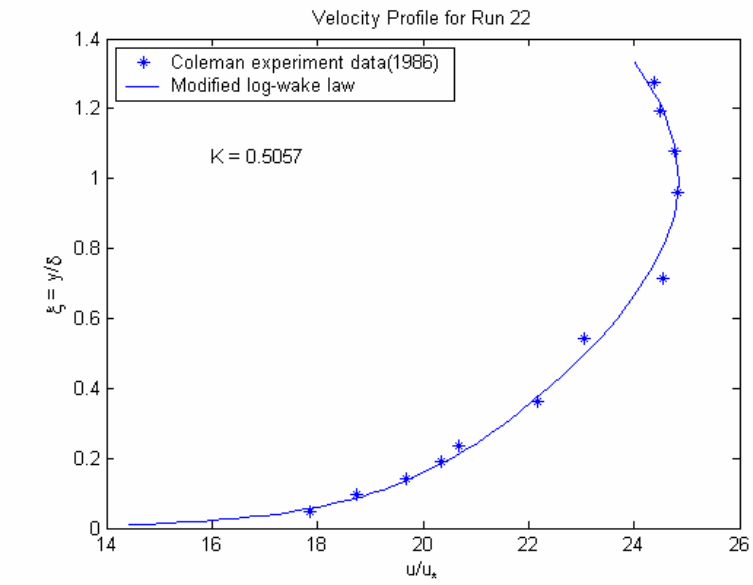
Velocity Profile for Run 22
Coleman experiment data(1986)
Modified log-wake law
K = 0.5057
ξ = y/δ
u/u*

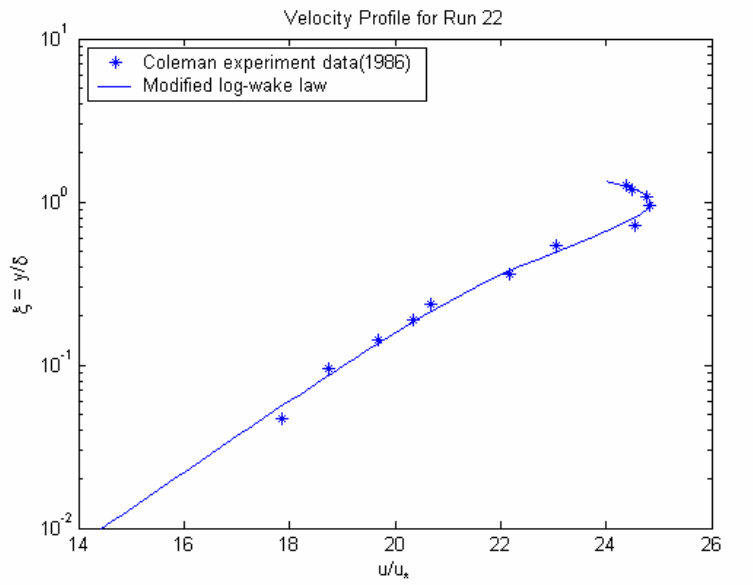
Velocity Profile for Run 22
Coleman experiment data(1986)
Modified log-wake law
ξ = y/δ
u/u*

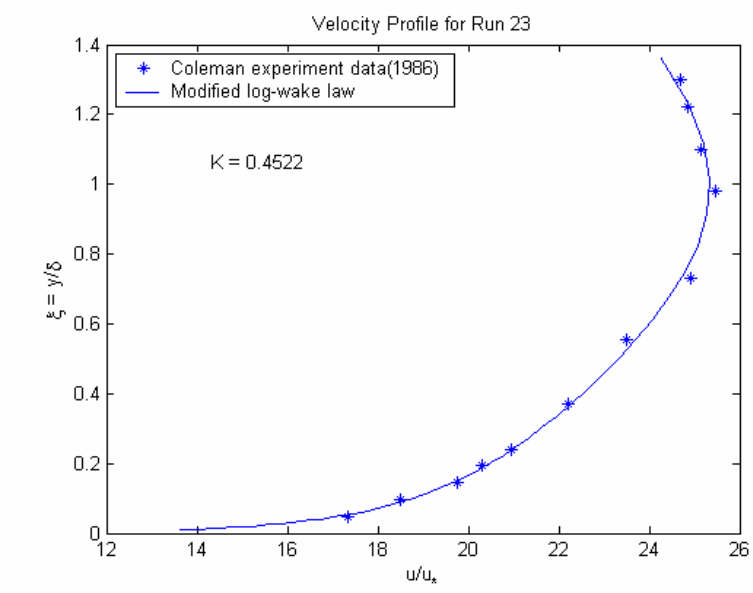
Velocity Profile for Run 23
Coleman experiment data(1986)
Modified log-wake law
K = 0.4522
ξ = y/δ
u/u*

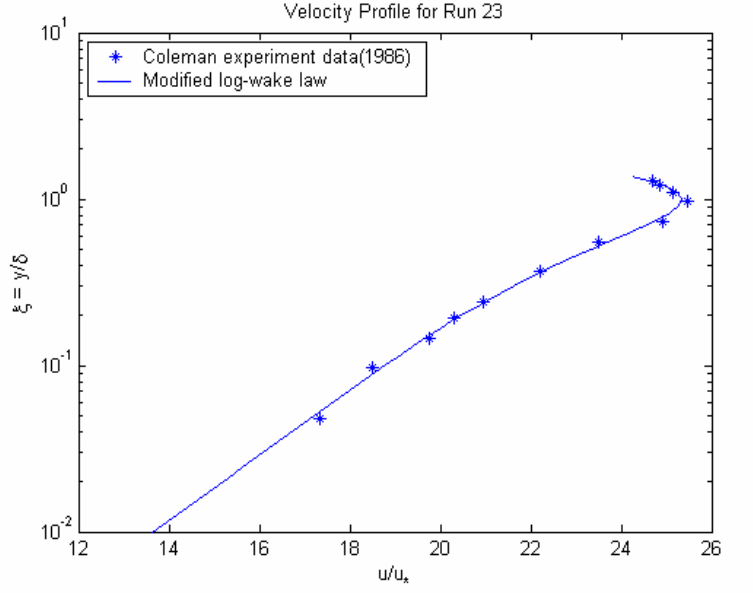
Velocity Profile for Run 23
Coleman experiment data(1986)
Modified log-wake law
ξ = y/δ
u/u*

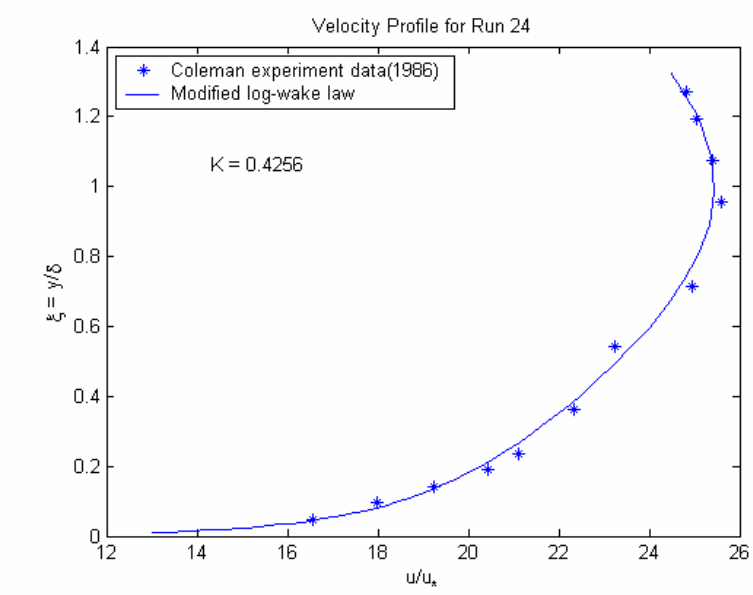
Velocity Profile for Run 24
Coleman experiment data(1986)
Modified log-wake law
K = 0.4256
ξ = y/δ
u/u*

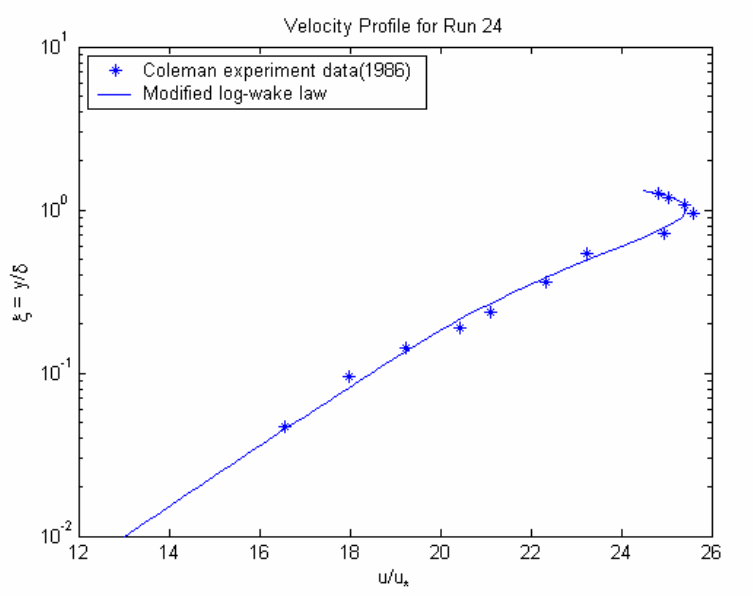
Velocity Profile for Run 24
Coleman experiment data(1986)
Modified log-wake law
ξ = y/δ
u/u*

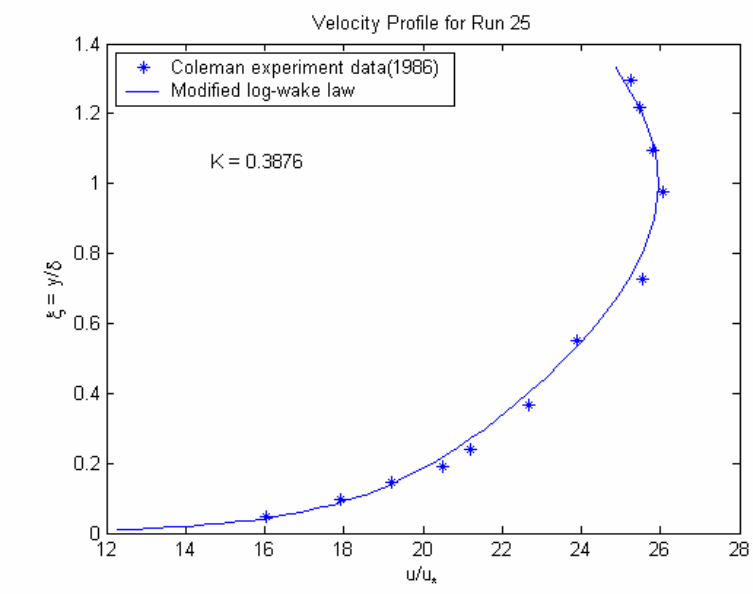
Velocity Profile for Run 25
Coleman experiment data(1986)
Modified log-wake law
K = 0.3876
ξ = y/δ
u/u*

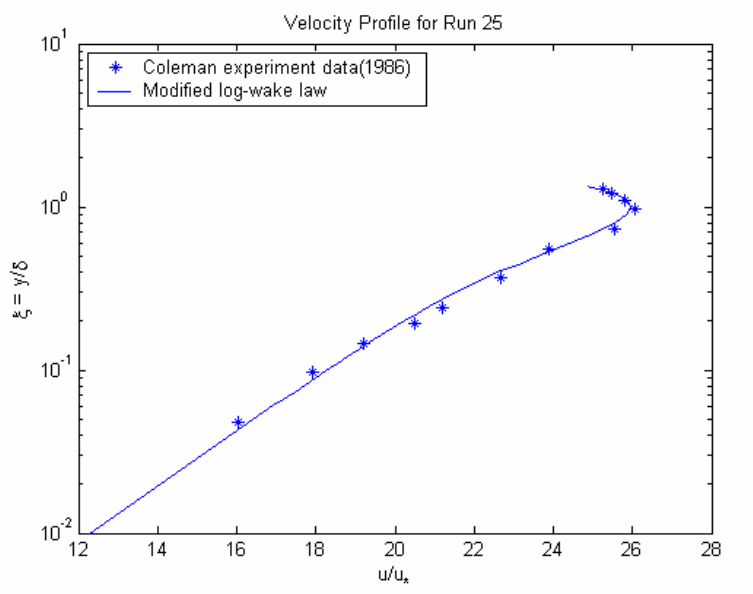
Velocity Profile for Run 25
Coleman experiment data(1986)
Modified log-wake law
ξ = y/δ
u/u*

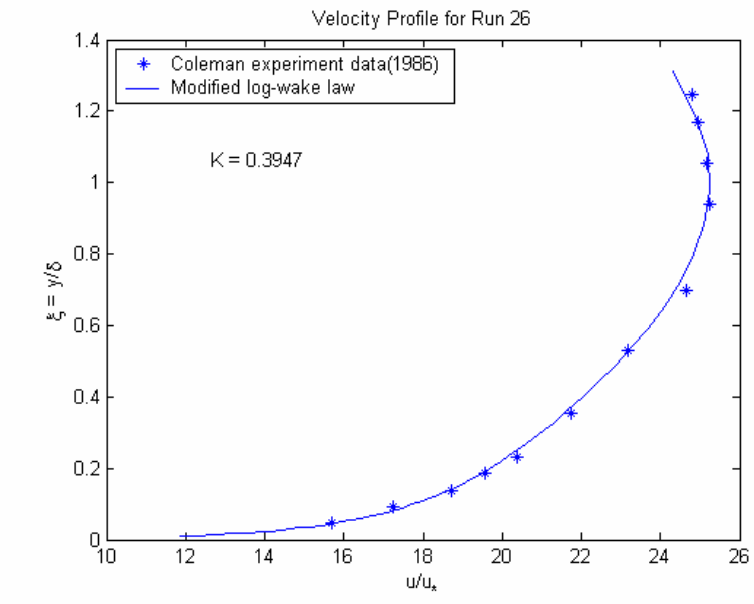
Velocity Profile for Run 26
Coleman experiment data(1986)
Modified log-wake law
K = 0.3947
ξ = y/δ
u/u*

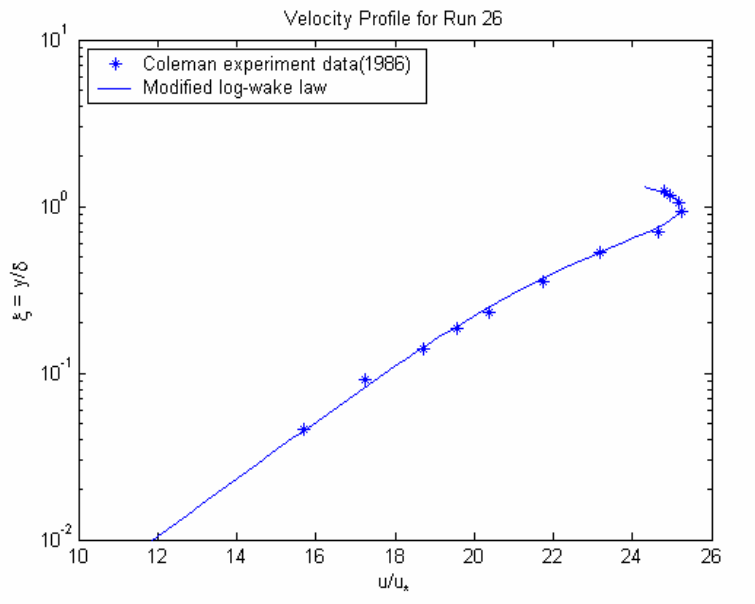
Velocity Profile for Run 26
Coleman experiment data(1986)
Modified log-wake law
ξ = y/δ
u/u*

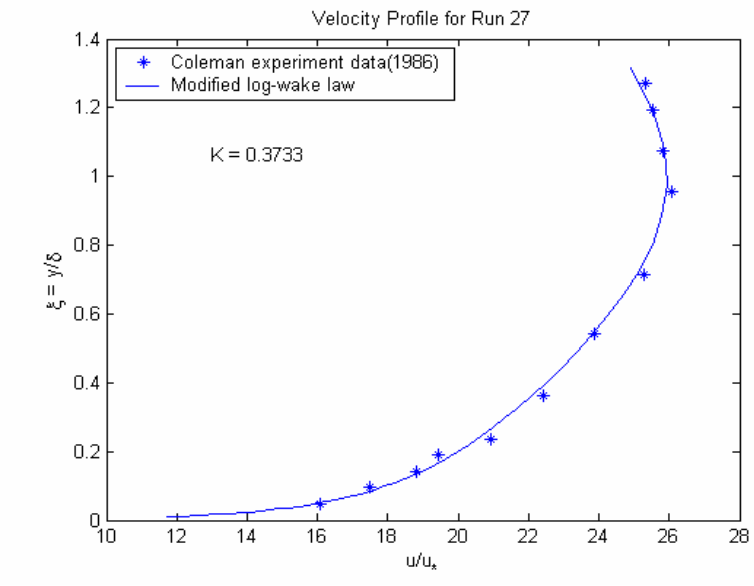
Velocity Profile for Run 27
Coleman experiment data(1986)
Modified log-wake law
K = 0.3733
ξ = y/δ
u/u*

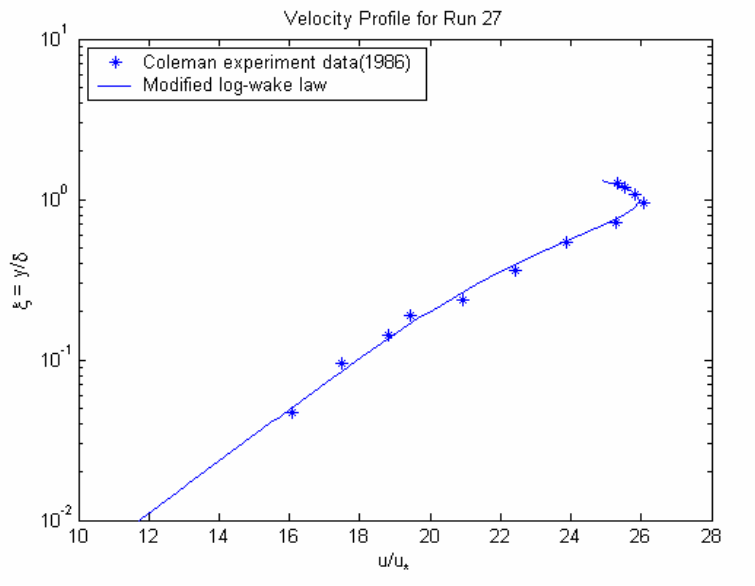
Velocity Profile for Run 27
Coleman experiment data(1986)
Modified log-wake law
ξ = y/δ
u/u*

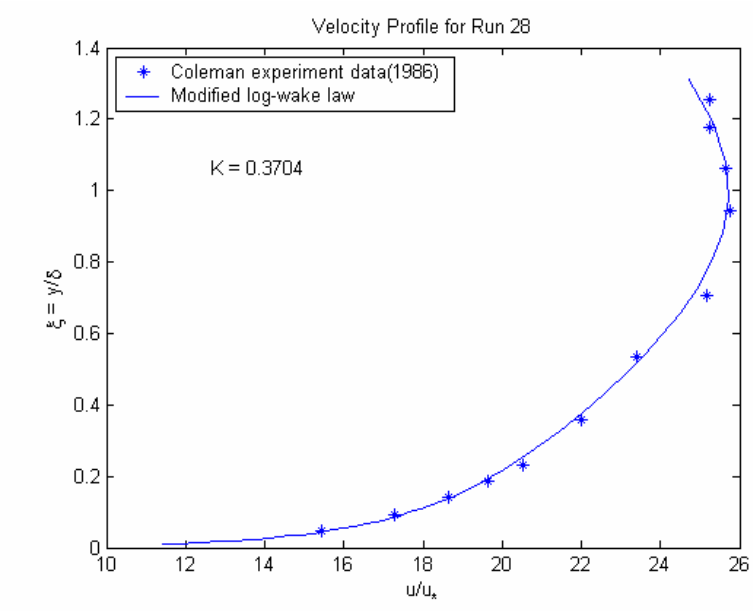
Velocity Profile for Run 28
Coleman experiment data(1986)
Modified log-wake law
K = 0.3704
ξ = y/δ
u/u*

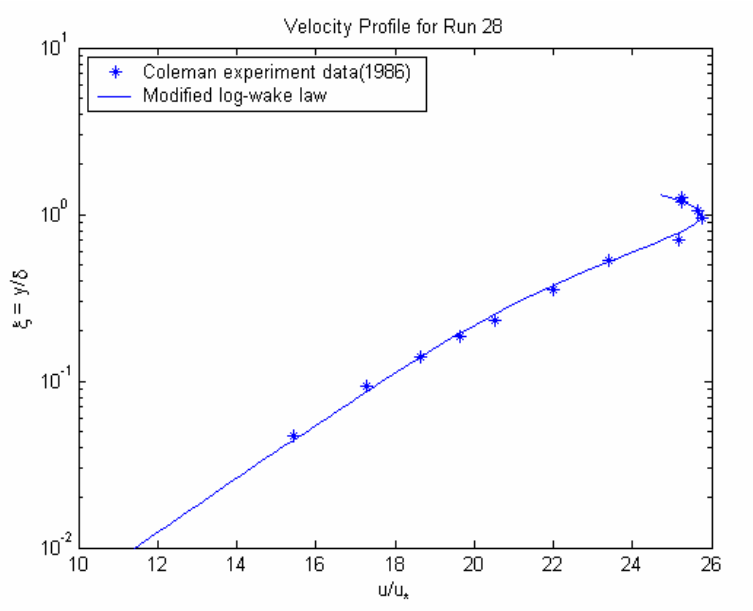
Velocity Profile for Run 28
Coleman experiment data(1986)
Modified log-wake law
ξ = y/δ
u/u*

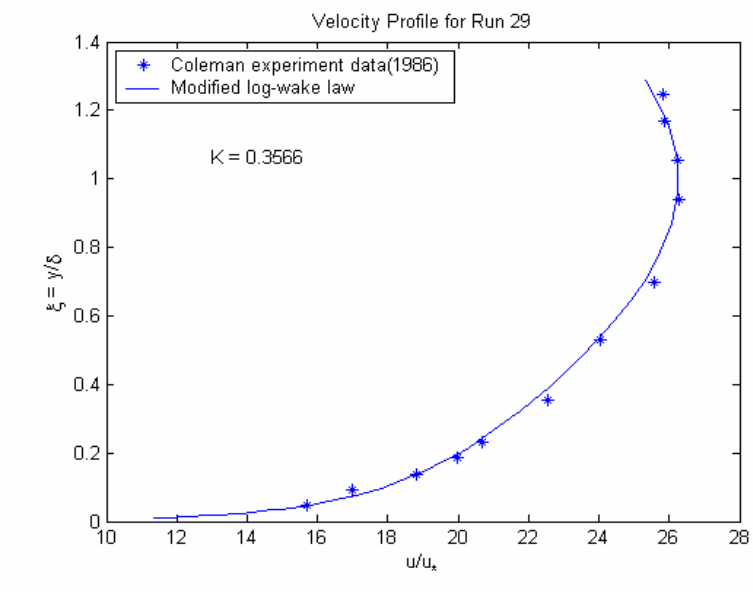
Velocity Profile for Run 29
Coleman experiment data(1986)
Modified log-wake law
K = 0.3566
ξ = y/δ
u/u*

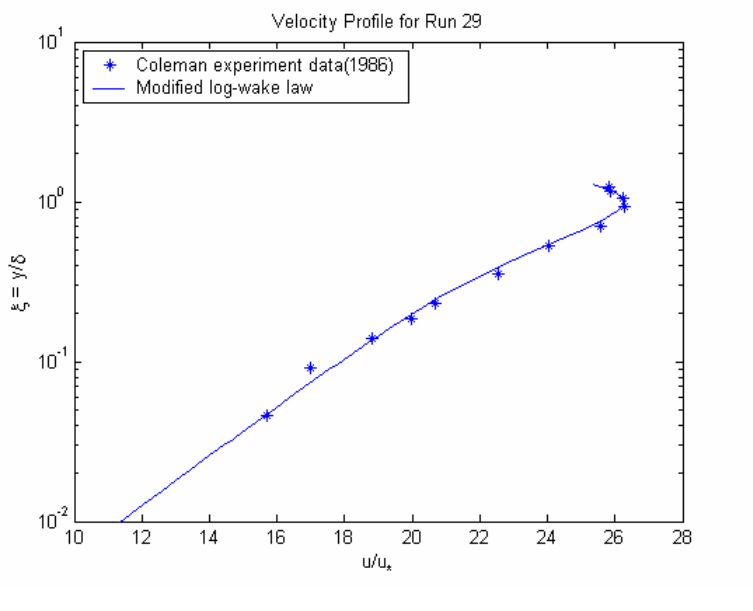
Velocity Profile for Run 29
Coleman experiment data(1986)
Modified log-wake law
ξ = y/δ
u/u*

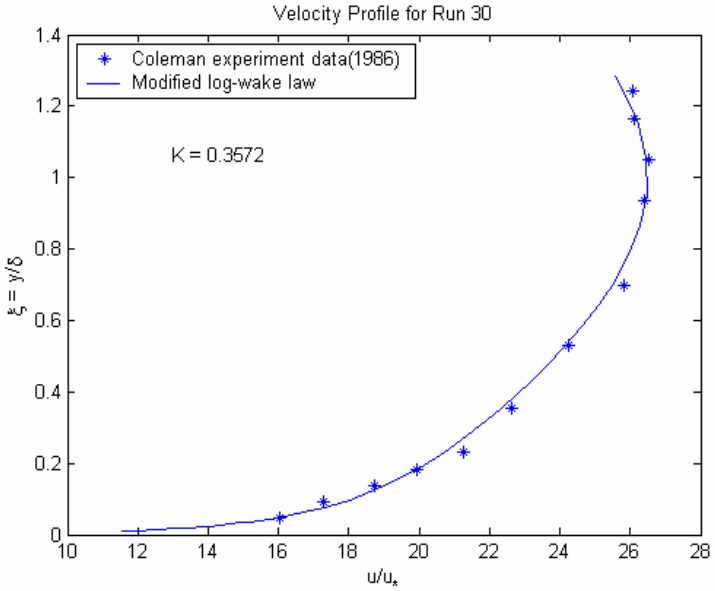
Velocity Profile for Run 30
Coleman experiment data(1986)
Modified log-wake law
K = 0.3572
ξ = y/δ
u/u*

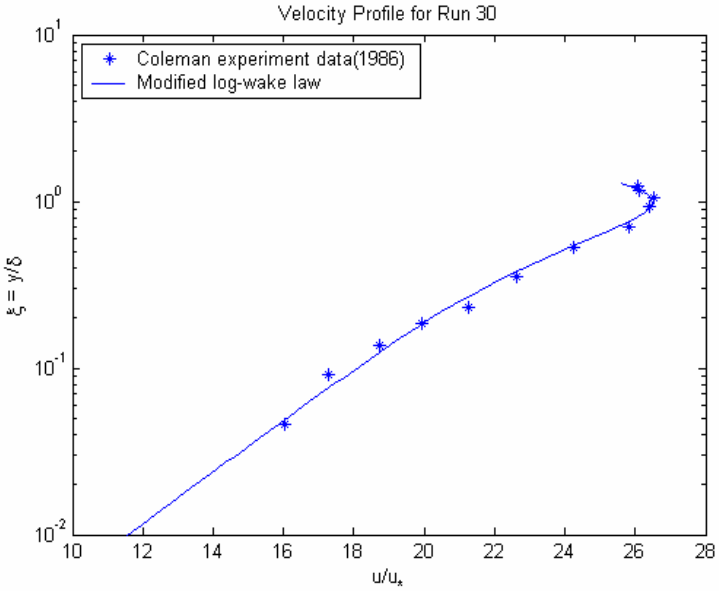
Velocity Profile for Run 30
Coleman experiment data(1986)
Modified log-wake law
ξ = y/δ
u/u*

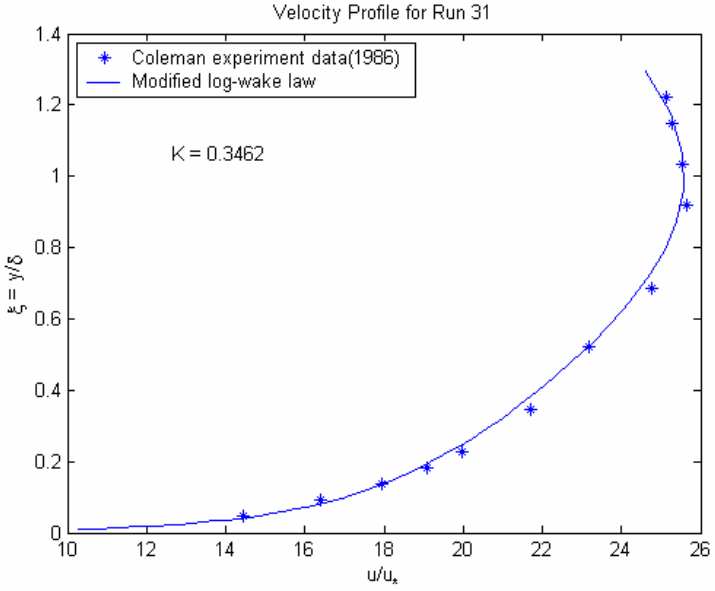
Velocity Profile for Run 31
Coleman experiment data(1986)
Modified log-wake law
K = 0.3462
ξ = y/δ
u/u*

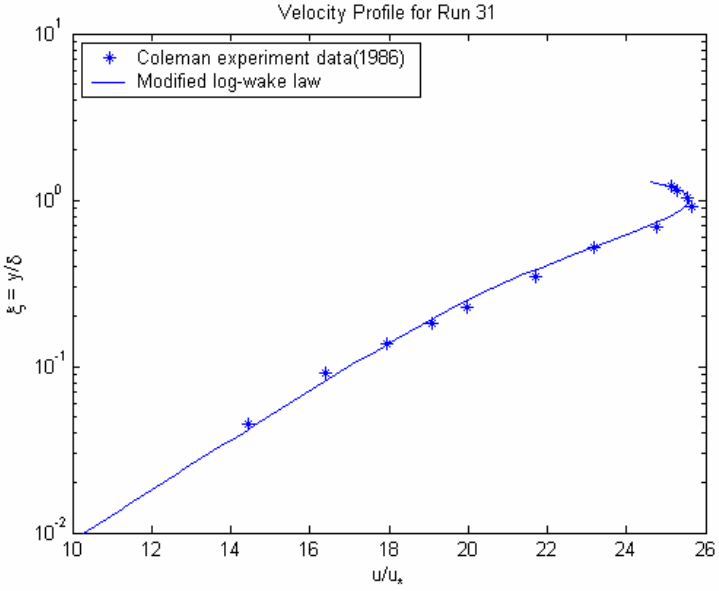
Velocity Profile for Run 31
Coleman experiment data(1986)
Modified log-wake law
ξ = y/δ
u/u*

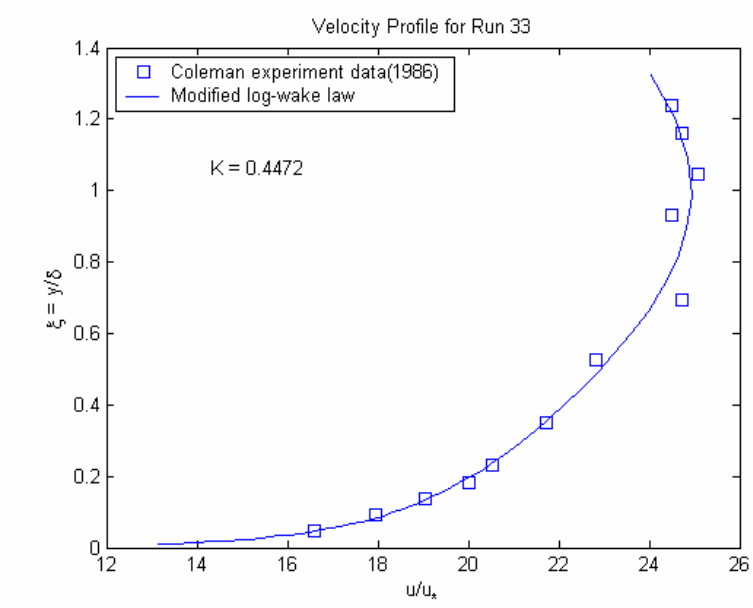
Velocity Profile for Run 33
Coleman experiment data(1986)
Modified log-wake law
K = 0.4472
ξ = y/δ
u/u*

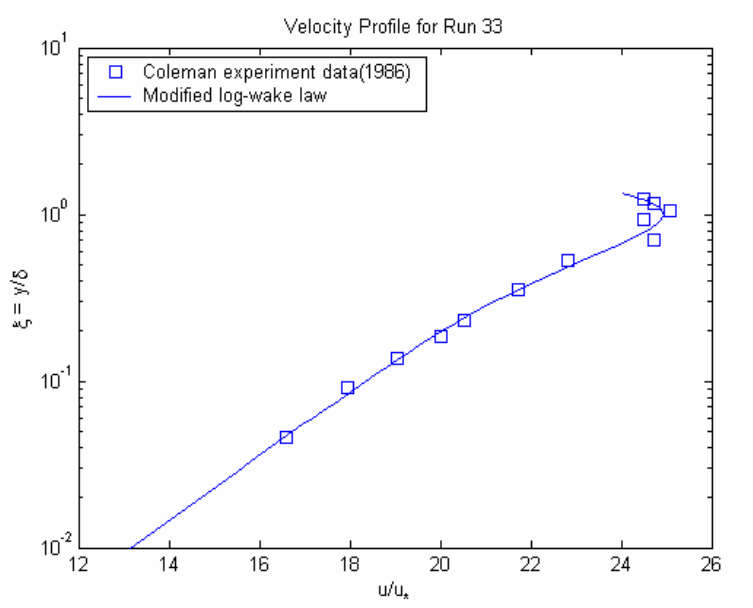
Velocity Profile for Run 33
Coleman experiment data(1986)
Modified log-wake law
ξ = y/δ
u/u*

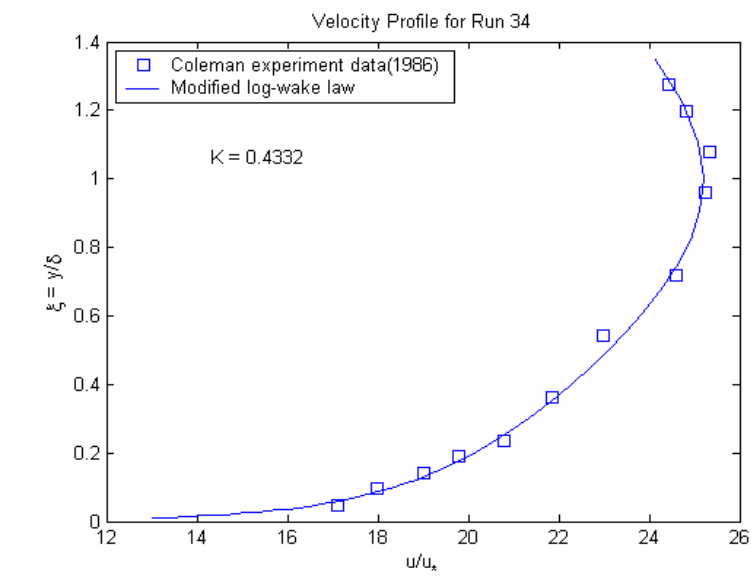
Velocity Profile for Run 34
Coleman experiment data(1986)
Modified log-wake law
K = 0.4332
ξ = y/δ
u/u*

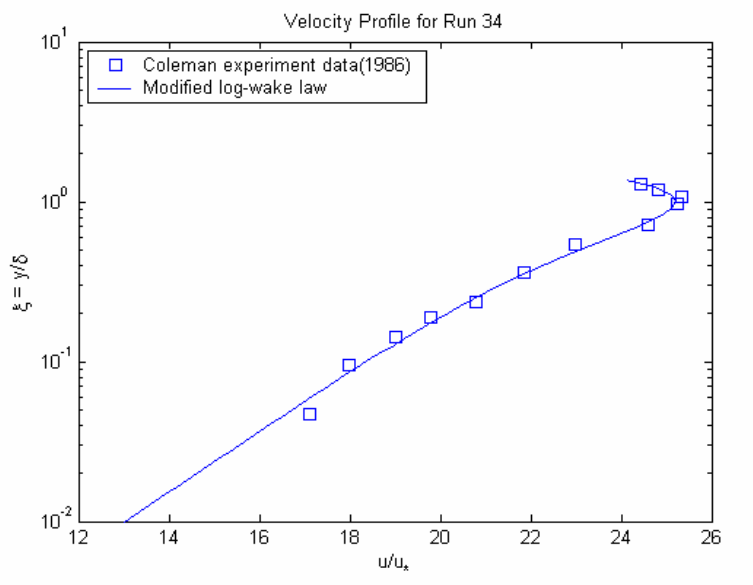
Velocity Profile for Run 34
Coleman experiment data(1986)
Modified log-wake law
ξ = y/δ
u/u*

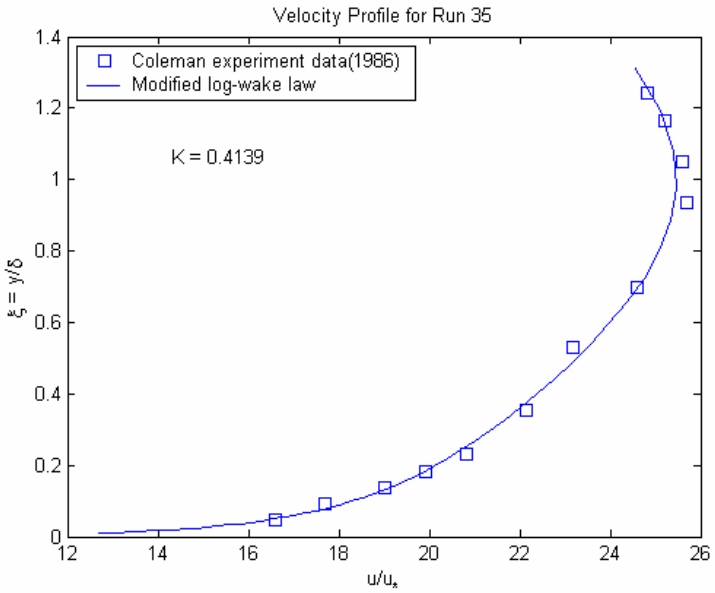
Velocity Profile for Run 35
Coleman experiment data(1986)
Modified log-wake law
K = 0.4139
ξ = y/δ
u/u*

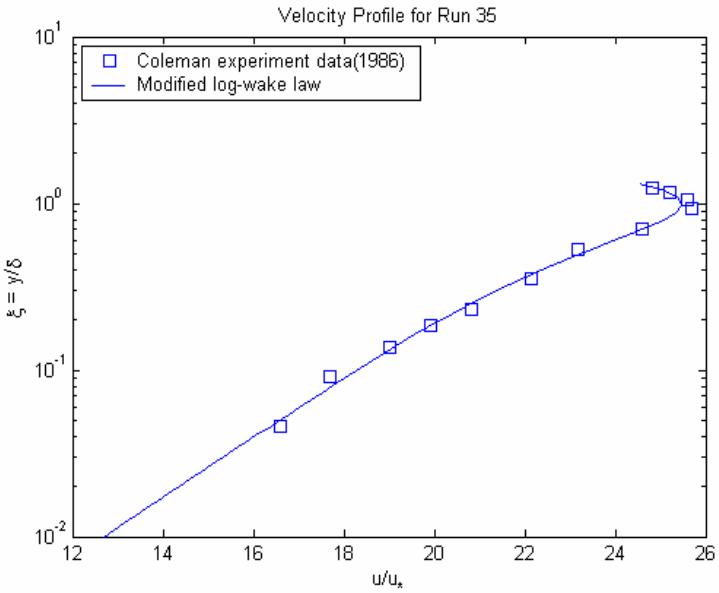
Velocity Profile for Run 35
Coleman experiment data(1986)
Modified log-wake law
ξ = y/δ
u/u*

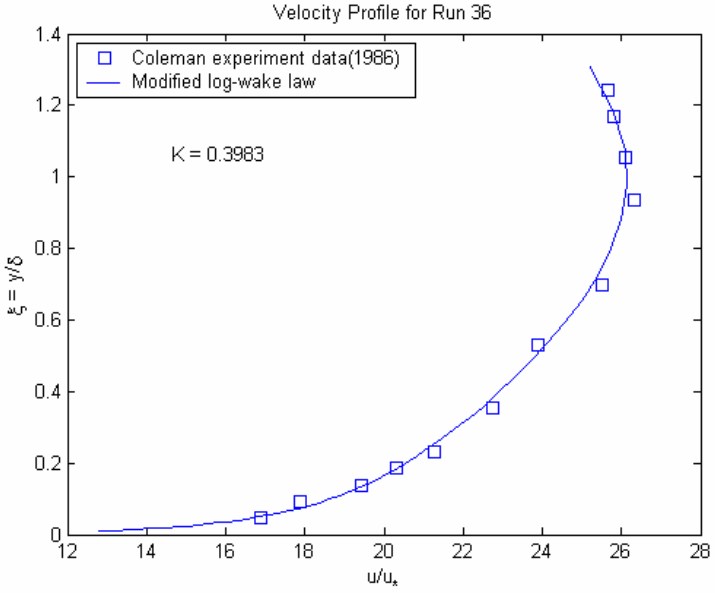
Velocity Profile for Run 36
Coleman experiment data(1986)
Modified log-wake law
K = 0.3983
ξ = y/δ
u/u*

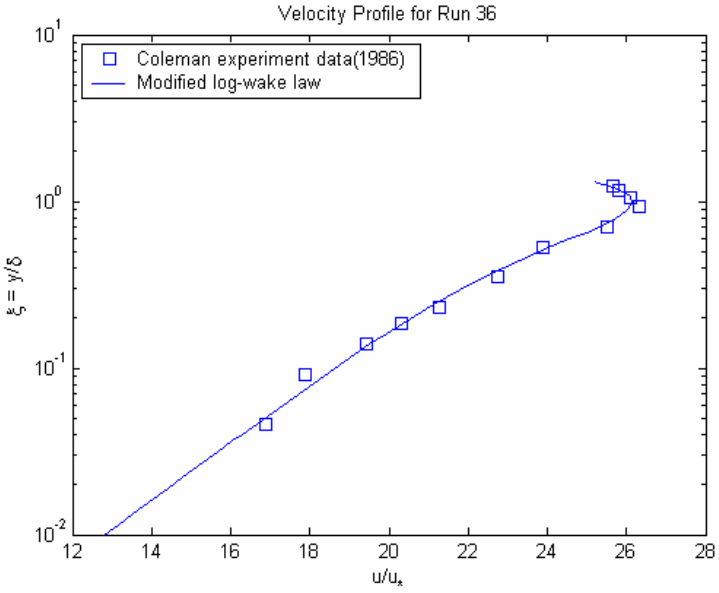
Velocity Profile for Run 36
Coleman experiment data(1986)
Modified log-wake law
ξ = y/δ
u/u*

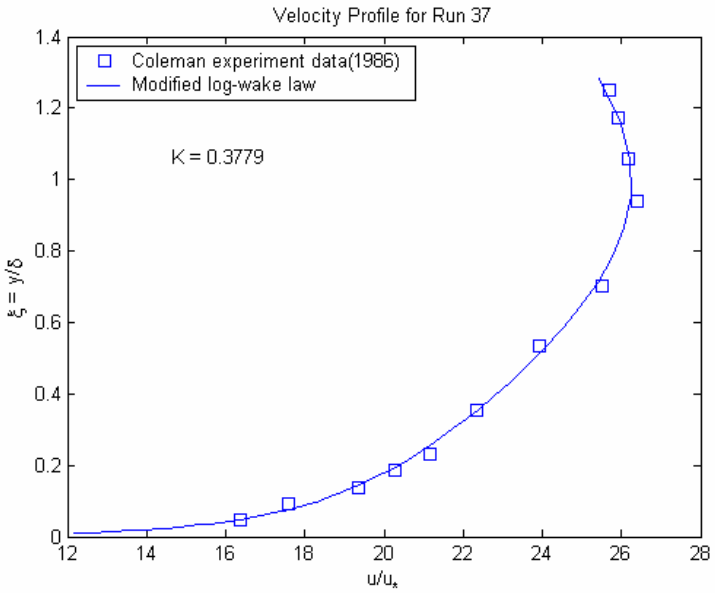
Velocity Profile for Run 37
Coleman experiment data(1986)
Modified log-wake law
K = 0.3779
ξ = y/δ
u/u*

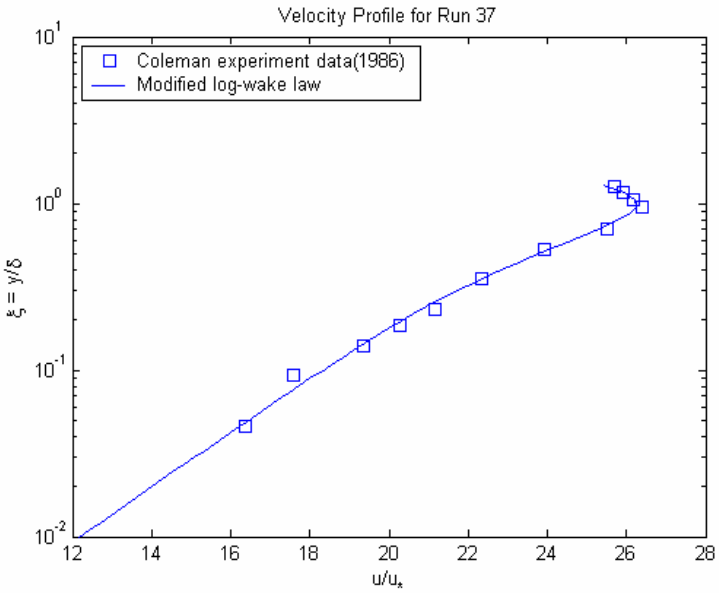
Velocity Profile for Run 37
Coleman experiment data(1986)
Modified log-wake law
ξ = y/δ
u/u*

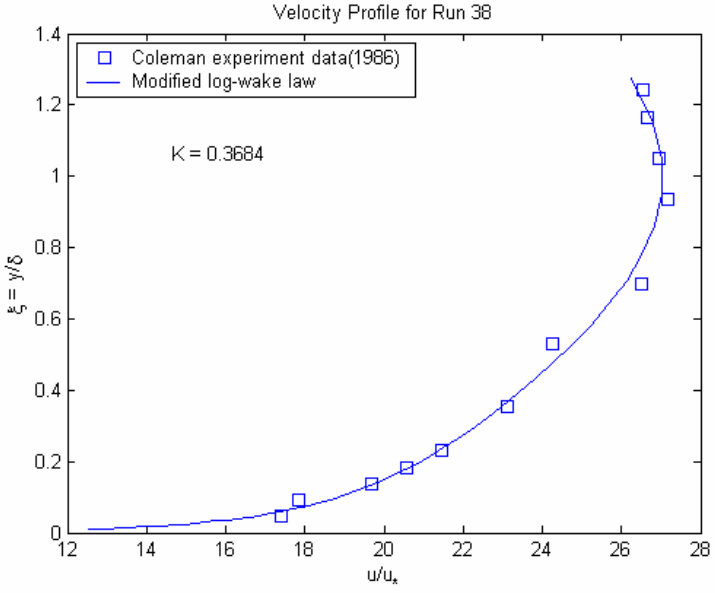
Velocity Profile for Run 38
Coleman experiment data(1986)
Modified log-wake law
K = 0.3684
ξ = y/δ
u/u*

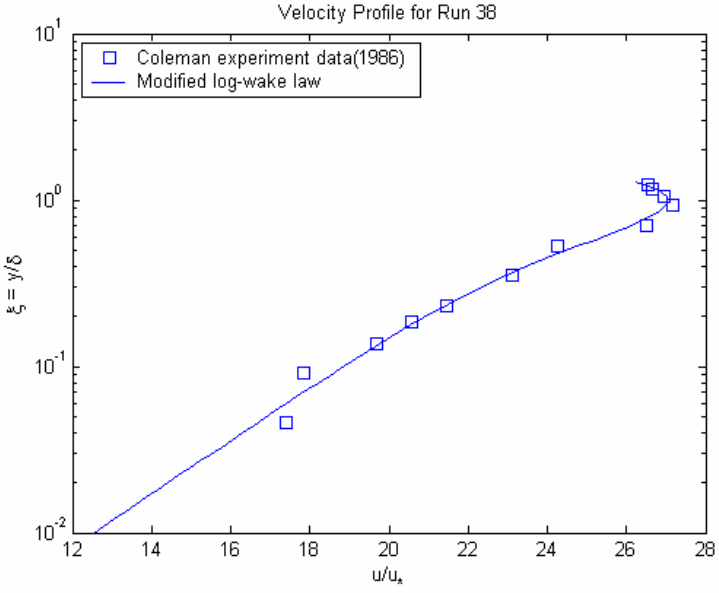
Velocity Profile for Run 38
Coleman experiment data(1986)
Modified log-wake law
ξ = y/δ
u/u*

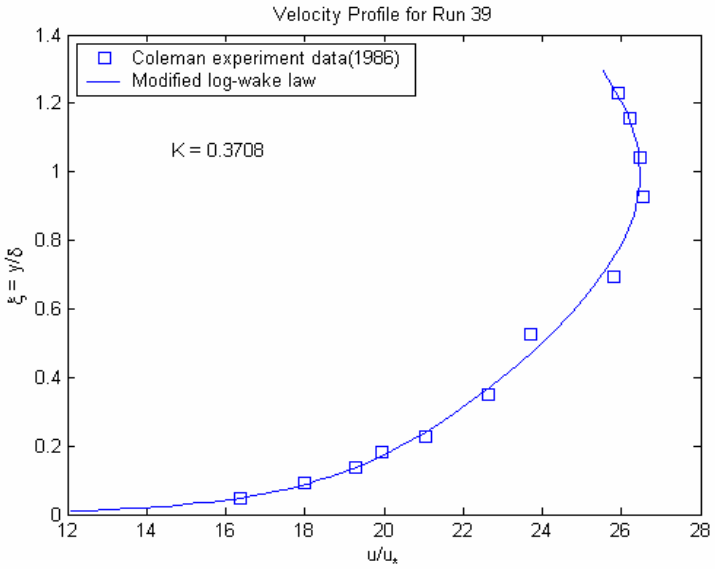
Velocity Profile for Run 39
Coleman experiment data(1986)
Modified log-wake law
K = 0.3708
ξ = y/δ
u/u*

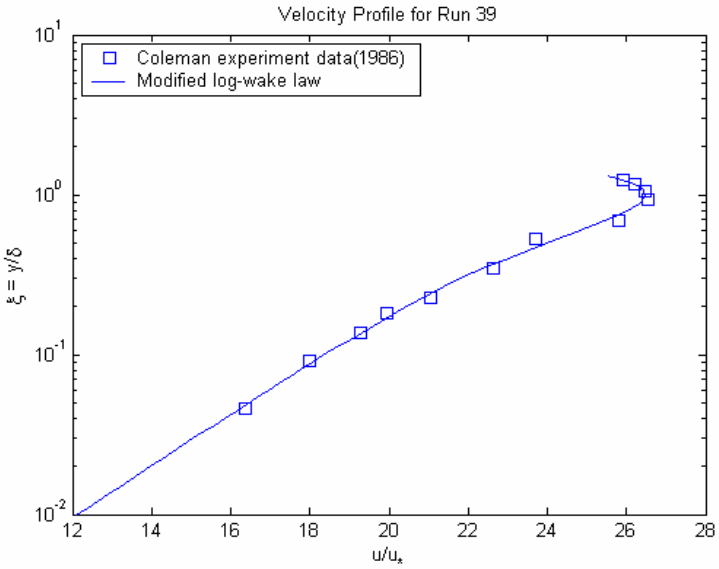
Velocity Profile for Run 39
Coleman experiment data(1986)
Modified log-wake law
ξ = y/δ
u/u*

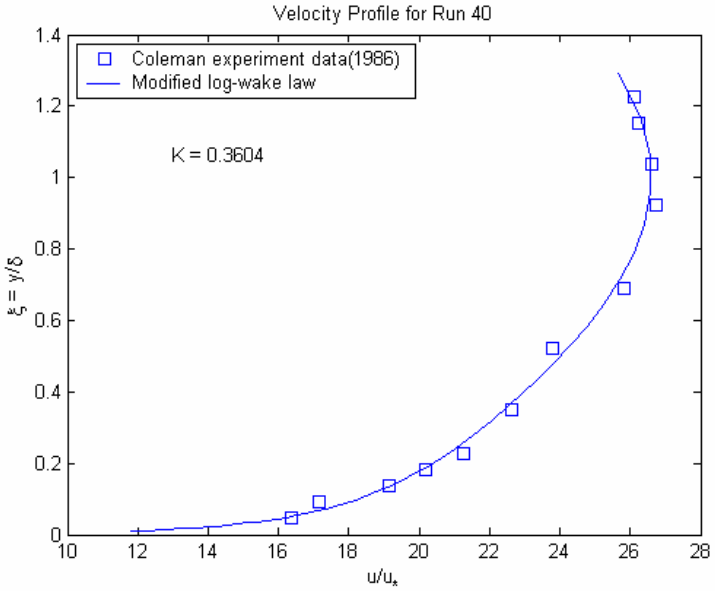
Velocity Profile for Run 40
Coleman experiment data(1986)
Modified log-wake law
K = 0.3604
ξ = y/δ
u/u*

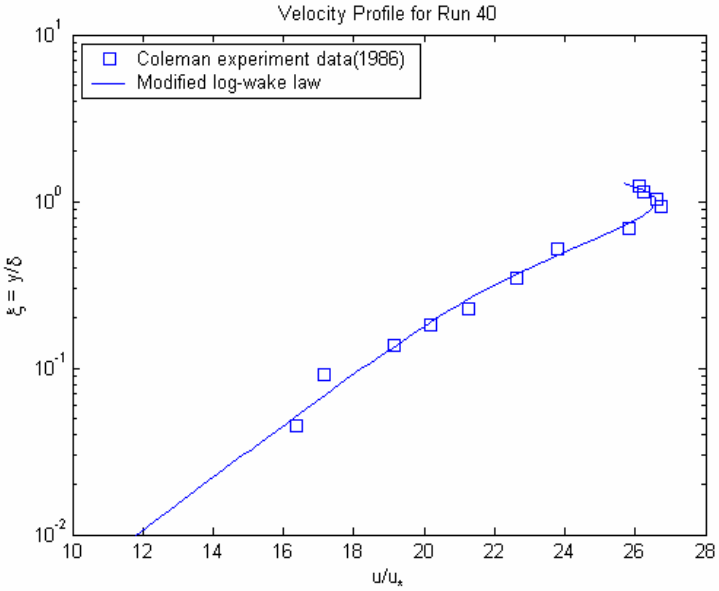
Velocity Profile for Run 40
Coleman experiment data(1986)
Modified log-wake law
ξ = y/δ
u/u*

APPENDIX D RESULTED CONCENTRATION PROFILE FIGURES

For rectangular scale

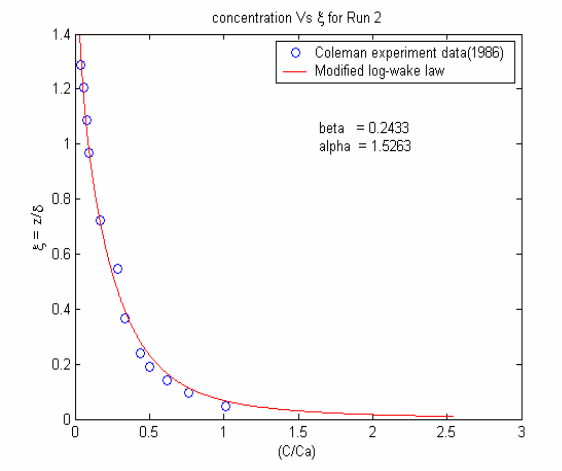

For log-rectangular scale

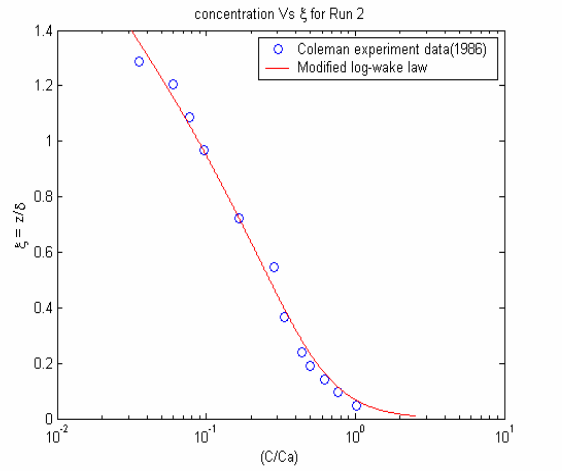

For log-log scale

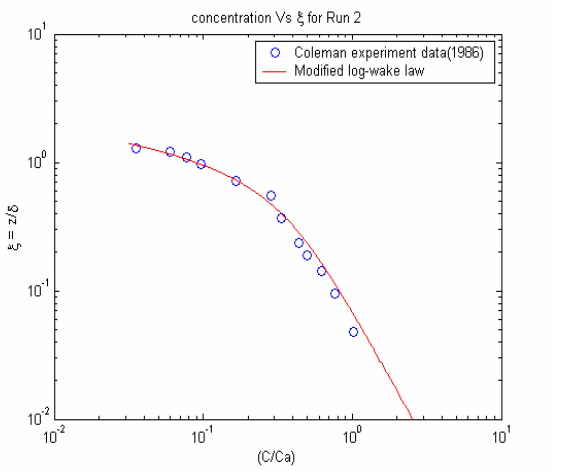

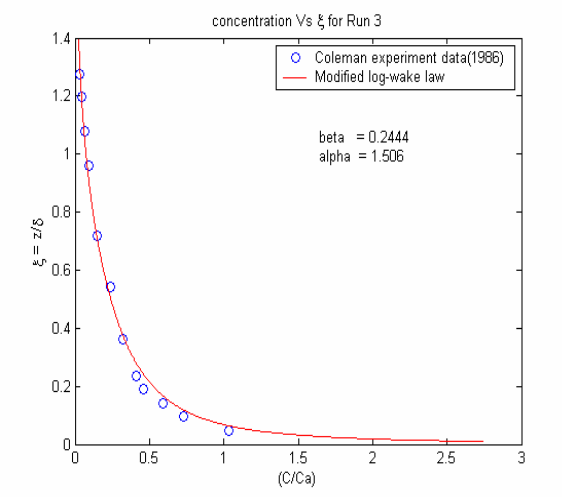

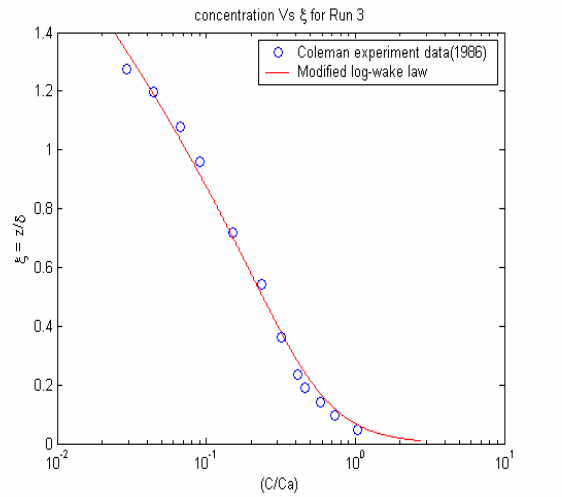

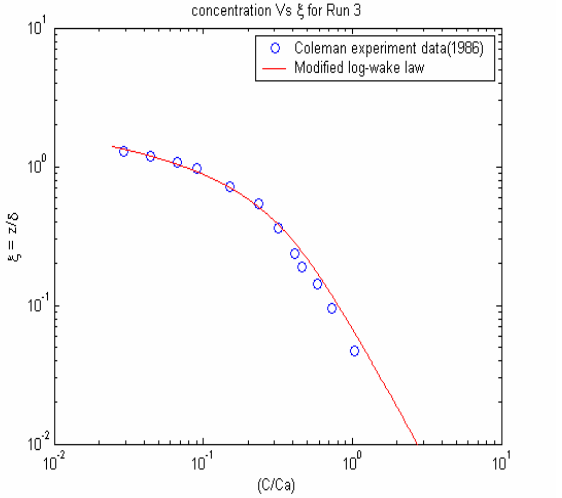

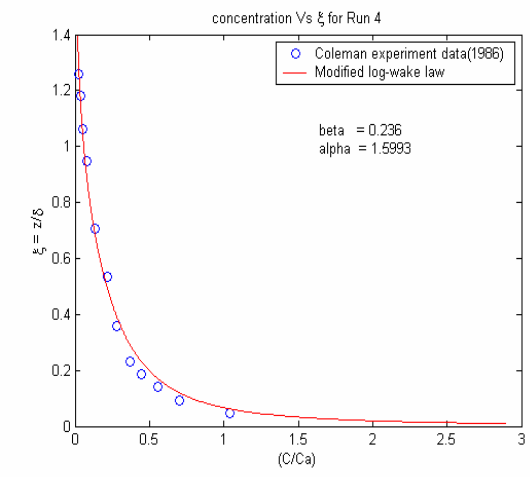
concentration Vs ξ for Run 4
Coleman experiment data(1986)
Modified log-wake law
beta = 0.236
alpha = 1.5993
ξ = z/δ
(C/Ca)

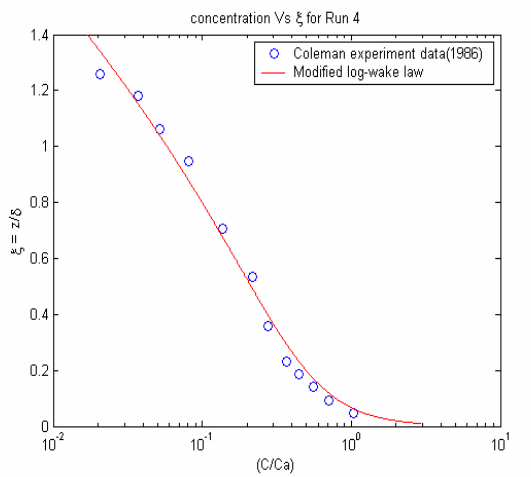
concentration Vs ξ for Run 4
Coleman experiment data(1986)
Modified log-wake law
ξ = z/δ
(C/Ca)

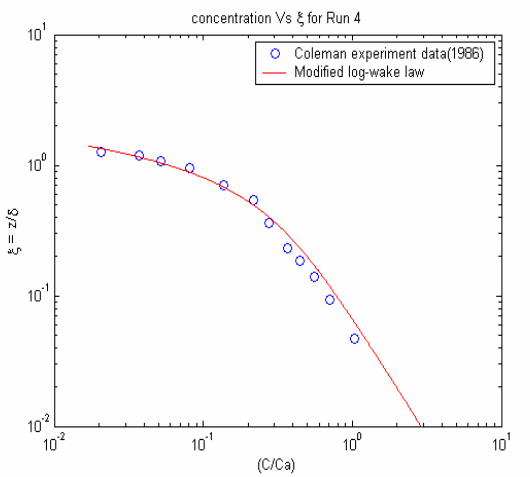
concentration Vs ξ for Run 4
Coleman experiment data(1986)
Modified log-wake law
ξ = z/δ
(C/Ca)

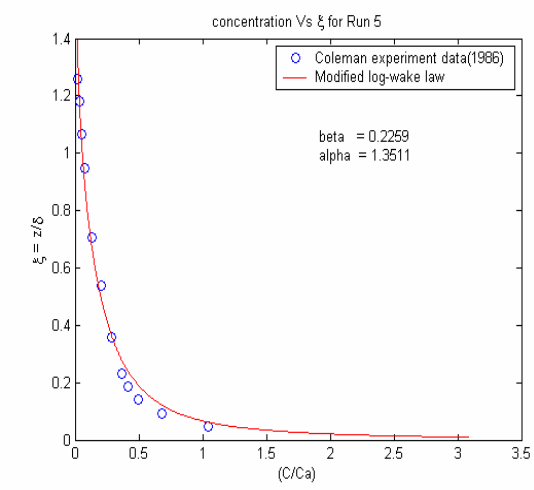
concentration Vs ξ for Run 5
Coleman experiment data(1986)
Modified log-wake law
beta = 0.2259
alpha = 1.3511
ξ = z/δ
(C/Ca)

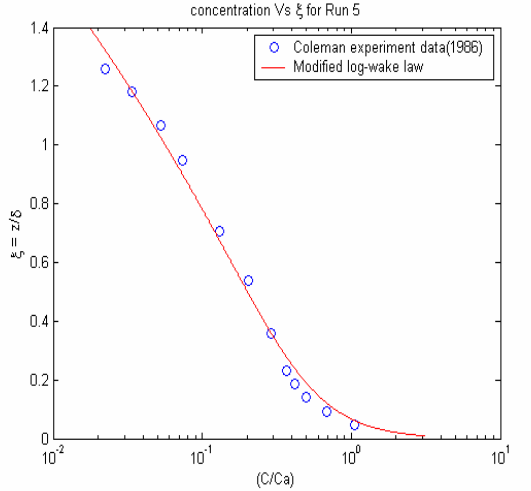
concentration Vs ξ for Run 5
Coleman experiment data(1986)
Modified log-wake law
ξ = z/δ
(C/Ca)

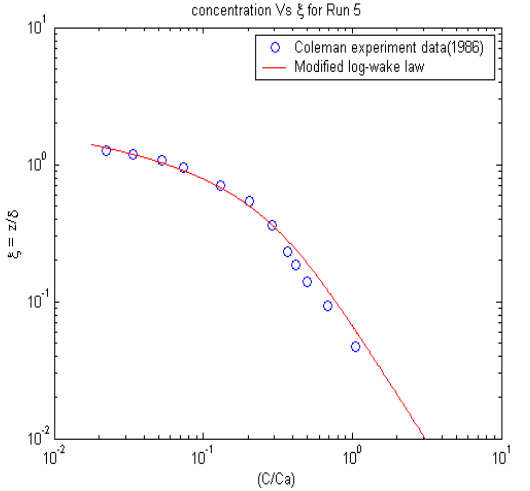
concentration Vs ξ for Run 5
Coleman experiment data(1986)
Modified log-wake law
ξ = z/δ
(C/Ca)

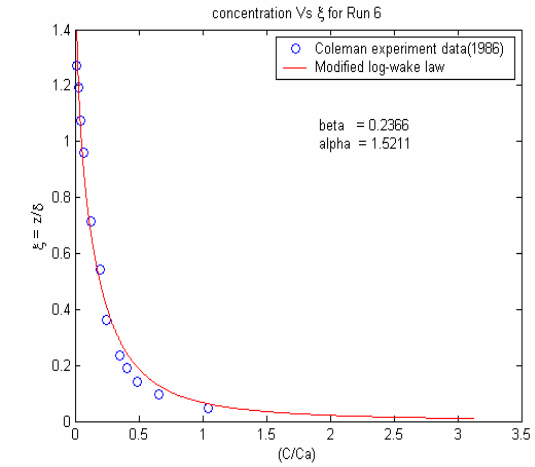
concentration Vs ξ for Run 6
Coleman experiment data(1986)
Modified log-wake law
beta = 0.2366
alpha = 1.5211
ξ = z/δ
(C/Ca)

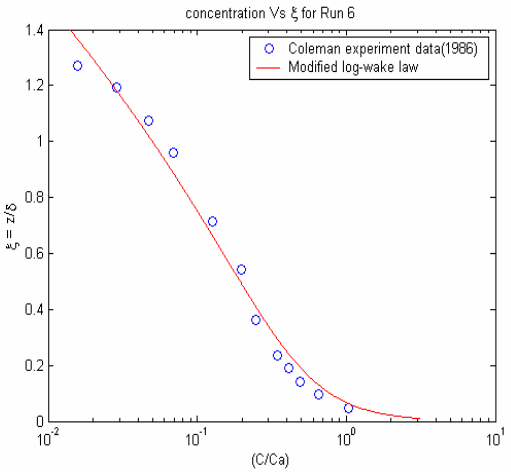
concentration Vs ξ for Run 6
Coleman experiment data(1986)
Modified log-wake law
ξ = z/δ
(C/Ca)

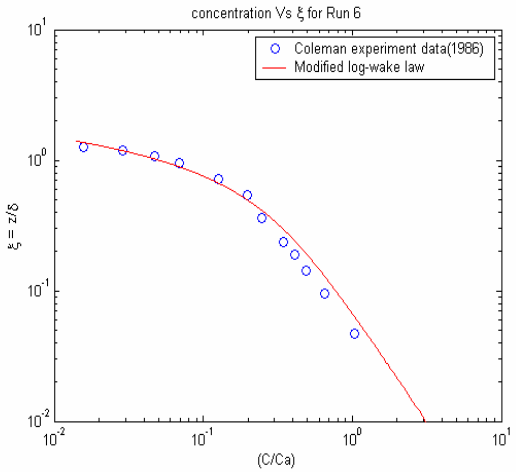
concentration Vs ξ for Run 6
Coleman experiment data(1986)
Modified log-wake law
ξ = z/δ
(C/Ca)

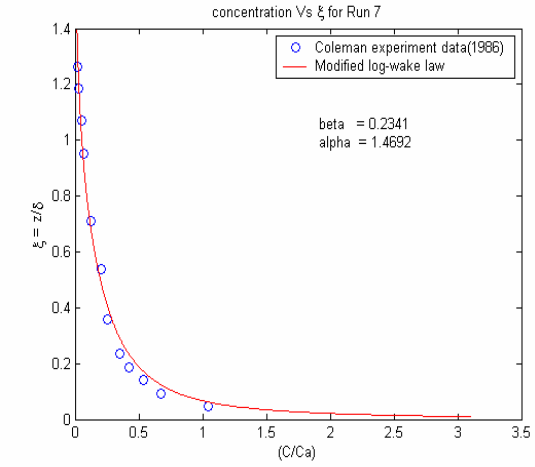
concentration Vs ξ for Run 7
Coleman experiment data(1986)
Modified log-wake law
beta = 0.2341
alpha = 1.4692
ξ = z/δ
(C/Ca)

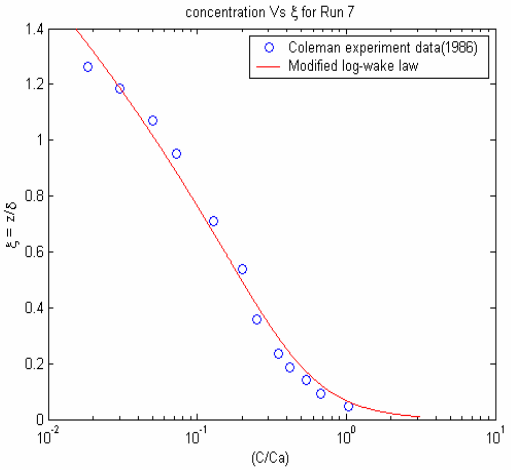
concentration Vs ξ for Run 7
Coleman experiment data(1986)
Modified log-wake law
ξ = z/δ
(C/Ca)

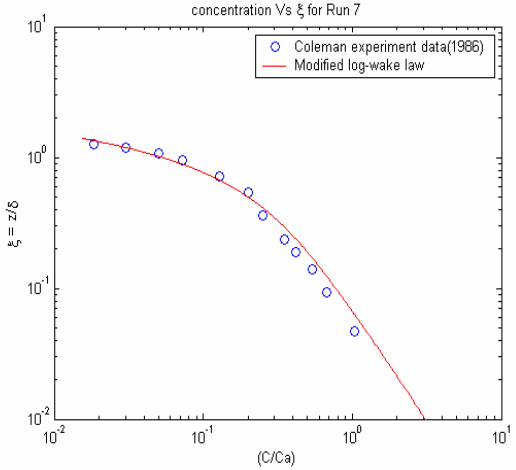
concentration Vs ξ for Run 7
Coleman experiment data(1986)
Modified log-wake law
ξ = z/δ
(C/Ca)

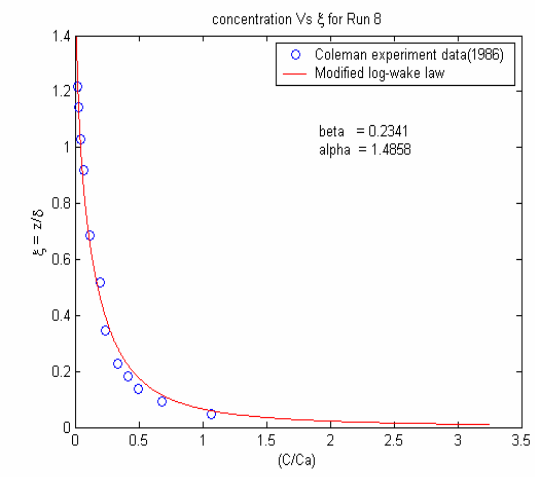
concentration Vs ξ for Run 8
Coleman experiment data(1986)
Modified log-wake law
beta = 0.2341
alpha = 1.4858
ξ = z/δ
(C/Ca)

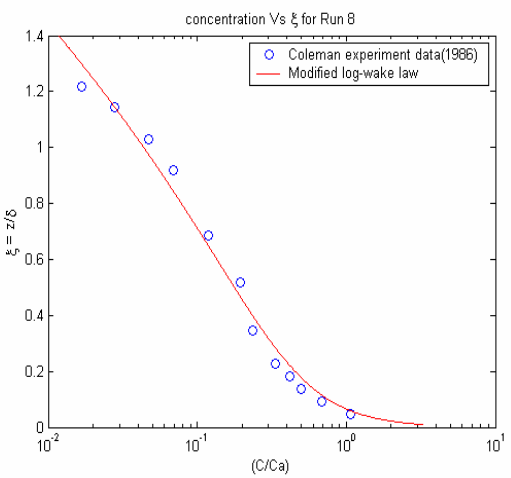
concentration Vs ξ for Run 8
Coleman experiment data(1986)
Modified log-wake law
ξ = z/δ
(C/Ca)

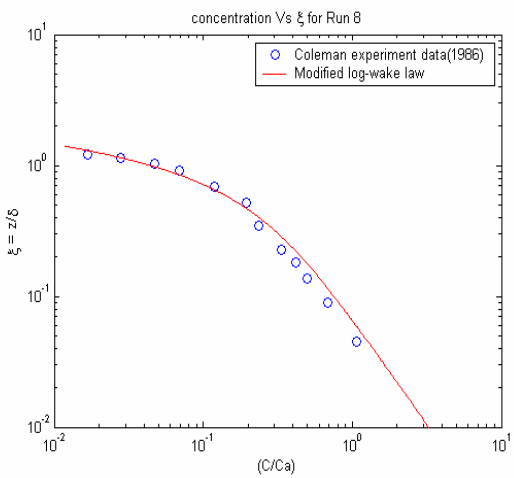
concentration Vs ξ for Run 8
Coleman experiment data(1986)
Modified log-wake law
ξ = z/δ
(C/Ca)

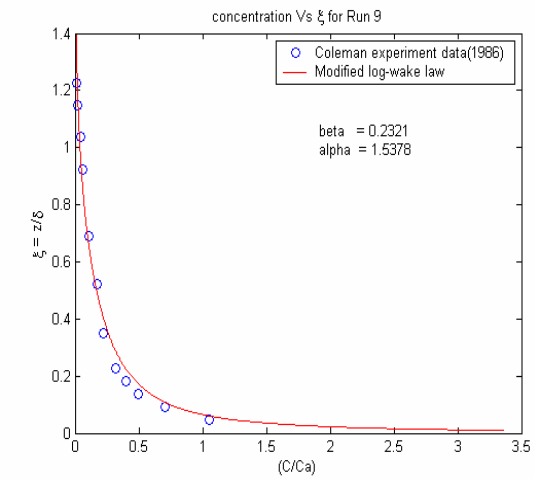
concentration Vs ξ for Run 9
Coleman experiment data(1986)
Modified log-wake law
beta = 0.2321
alpha = 1.5378
ξ = z/δ
(C/Ca)

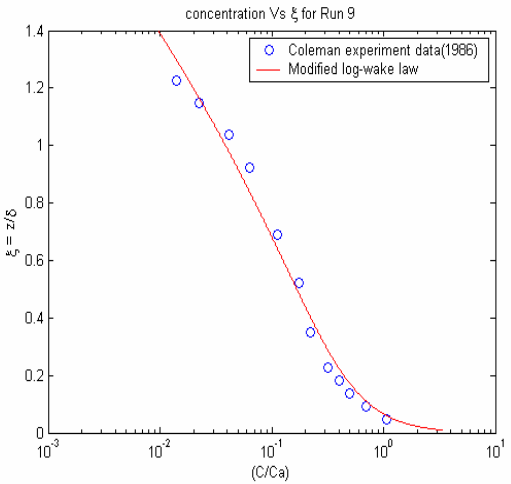
concentration Vs ξ for Run 9
Coleman experiment data(1986)
Modified log-wake law
ξ = z/δ
(C/Ca)

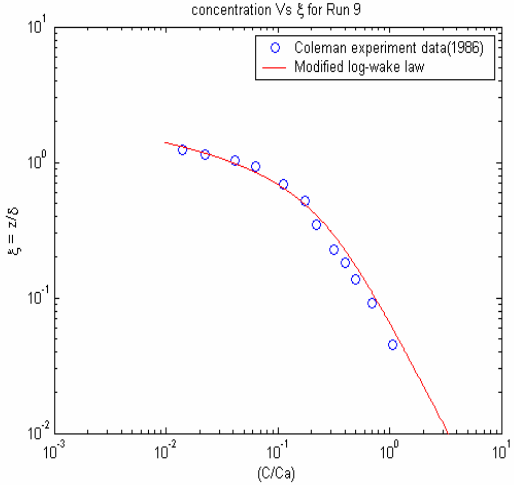
concentration Vs ξ for Run 9
Coleman experiment data(1986)
Modified log-wake law
ξ = z/δ
(C/Ca)

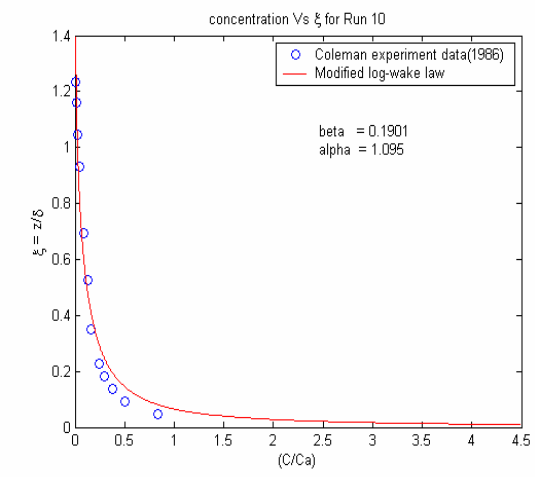
concentration Vs ξ for Run 10
Coleman experiment data(1986)
Modified log-wake law
beta = 0.1901
alpha = 1.095
ξ = z/δ
(C/Ca)

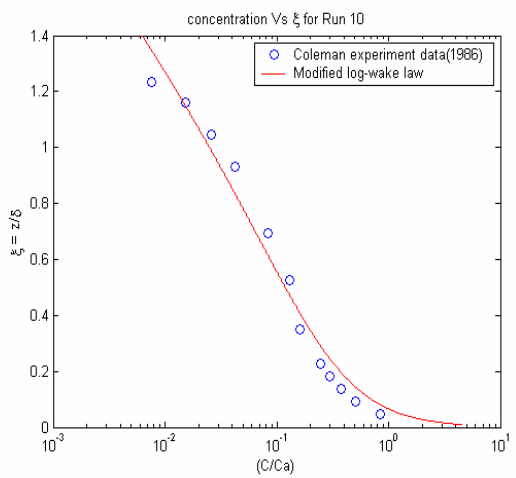
concentration Vs ξ for Run 10
Coleman experiment data(1986)
Modified log-wake law
ξ = z/δ
(C/Ca)

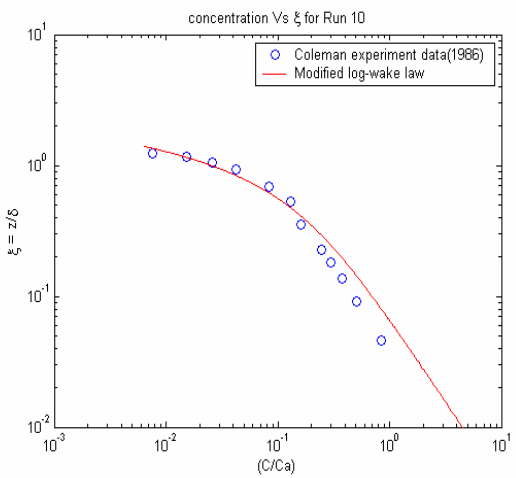
concentration Vs ξ for Run 10
Coleman experiment data(1986)
Modified log-wake law
ξ = z/δ
(C/Ca)

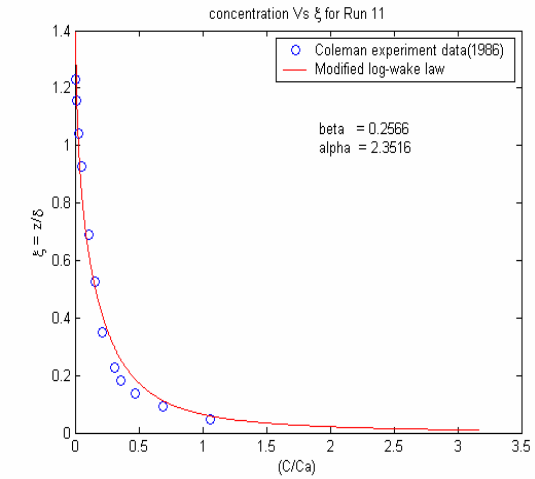
concentration Vs ξ for Run 11
Coleman experiment data(1986)
Modified log-wake law
beta = 0.2566
alpha = 2.3516
ξ = z/δ
(C/Ca)

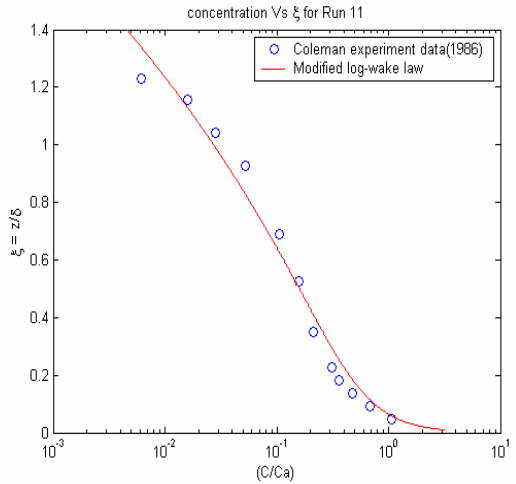
concentration Vs ξ for Run 11
Coleman experiment data(1986)
Modified log-wake law
ξ = z/δ
(C/Ca)

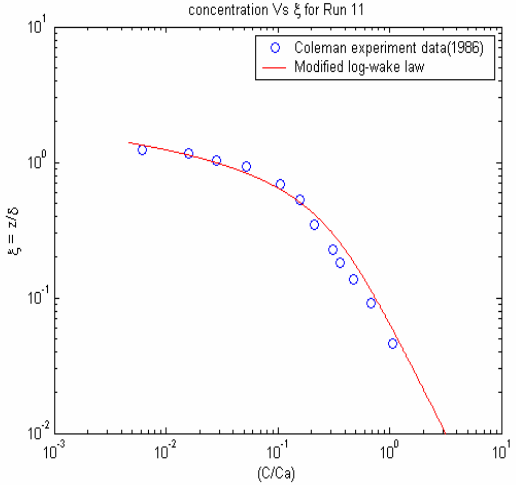
concentration Vs ξ for Run 11
Coleman experiment data(1986)
Modified log-wake law
ξ = z/δ
(C/Ca)

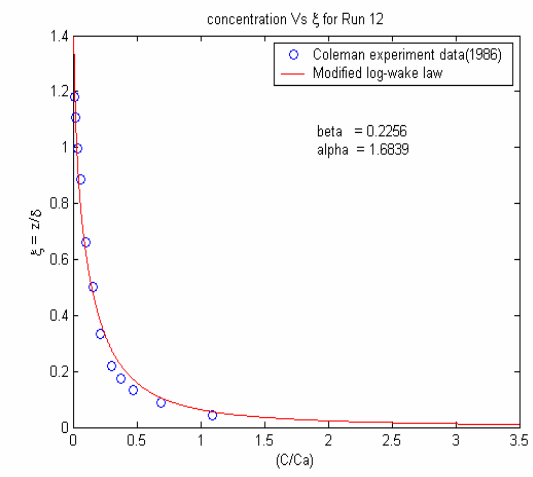
concentration Vs ξ for Run 12
Coleman experiment data(1986)
Modified log-wake law
beta = 0.2256
alpha = 1.6839
ξ = z/δ
(C/Ca)

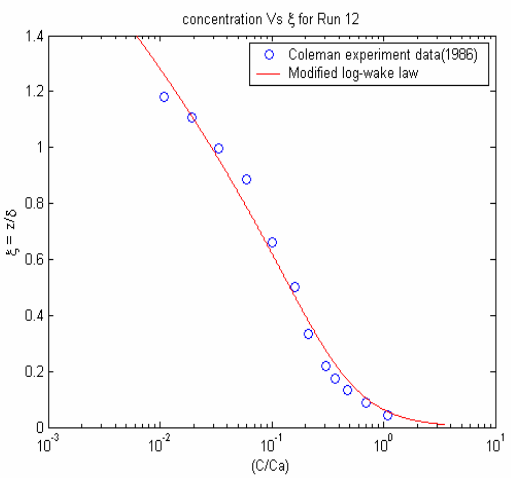
concentration Vs ξ for Run 12
Coleman experiment data(1986)
Modified log-wake law
ξ = z/δ
(C/Ca)

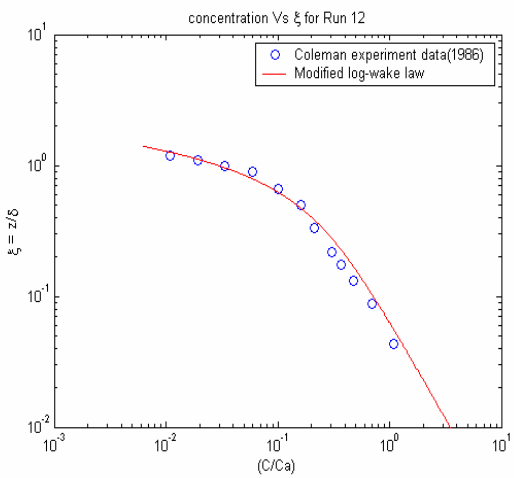
concentration Vs ξ for Run 12
Coleman experiment data(1986)
Modified log-wake law
ξ = z/δ
(C/Ca)

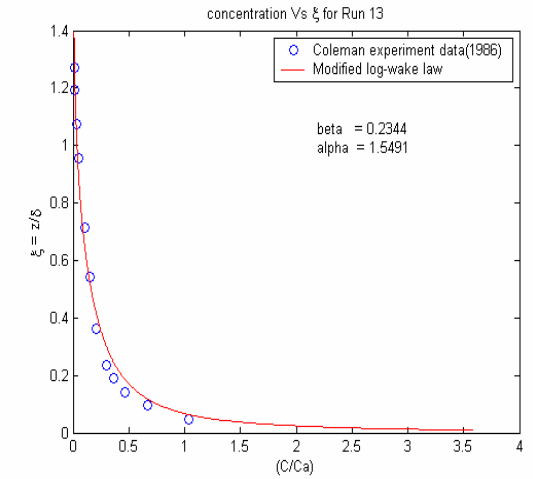
concentration Vs ξ for Run 13
Coleman experiment data(1986)
Modified log-wake law
beta = 0.2344
alpha = 1.5491
ξ = z/δ
(C/Ca)

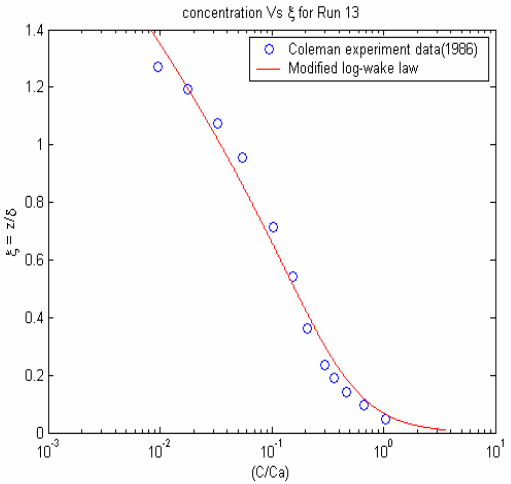
concentration Vs ξ for Run 13
Coleman experiment data(1986)
Modified log-wake law
ξ = z/δ
(C/Ca)

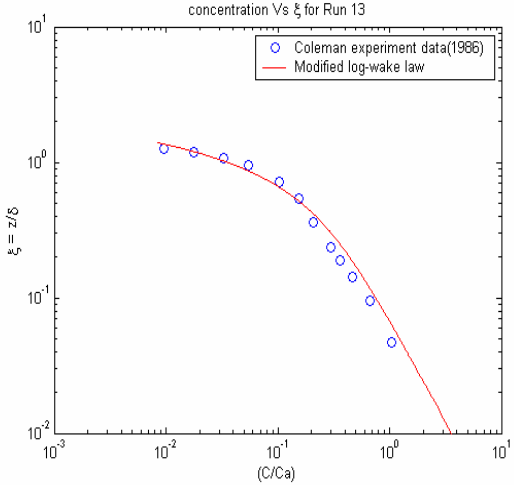
concentration Vs ξ for Run 13
Coleman experiment data(1986)
Modified log-wake law
ξ = z/δ
(C/Ca)

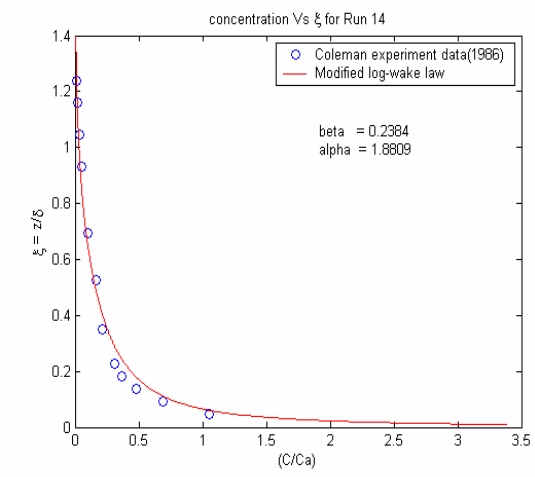
concentration Vs ξ for Run 14
Coleman experiment data(1986)
Modified log-wake law
beta = 0.2384
alpha = 1.8809
ξ = z/δ
(C/Ca)

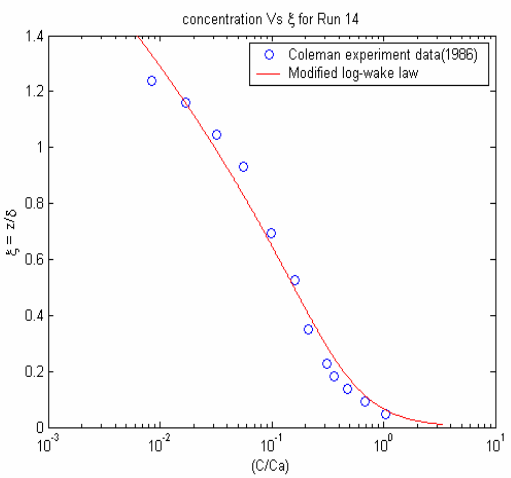
concentration Vs ξ for Run 14
Coleman experiment data(1986)
Modified log-wake law
ξ = z/δ
(C/Ca)

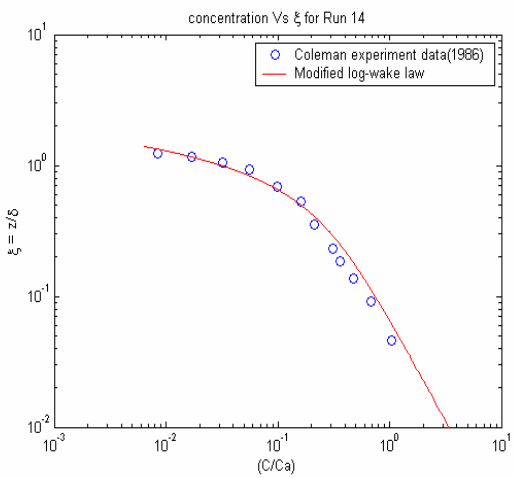
concentration Vs ξ for Run 14
Coleman experiment data(1986)
Modified log-wake law
ξ = z/δ
(C/Ca)

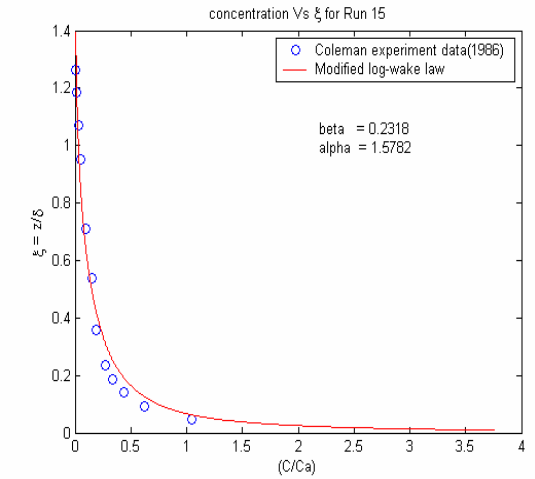
concentration Vs ξ for Run 15
Coleman experiment data(1986)
Modified log-wake law
beta = 0.2318
alpha = 1.5782
ξ = z/δ
(C/Ca)

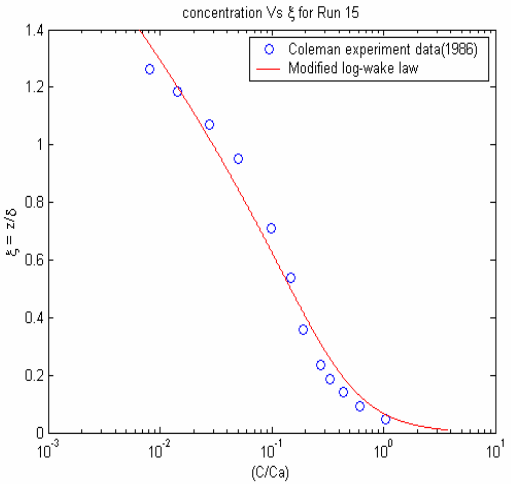
concentration Vs ξ for Run 15
Coleman experiment data(1986)
Modified log-wake law
ξ = z/δ
(C/Ca)

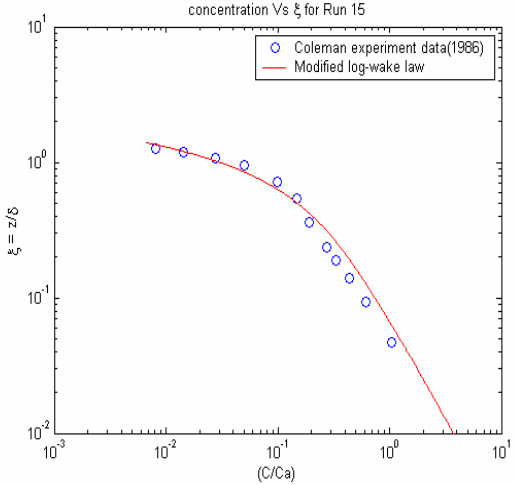
concentration Vs ξ for Run 15
Coleman experiment data(1986)
Modified log-wake law
ξ = z/δ
(C/Ca)

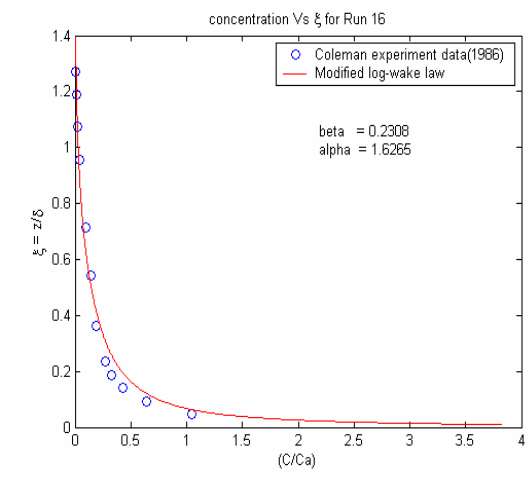
concentration Vs ξ for Run 16
Coleman experiment data(1986)
Modified log-wake law
beta = 0.2308
alpha = 1.6265
ξ = z/δ
(C/Ca)

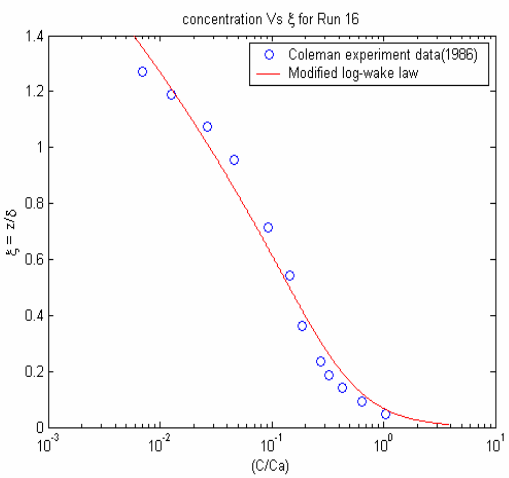
concentration Vs ξ for Run 16
Coleman experiment data(1986)
Modified log-wake law
ξ = z/δ
(C/Ca)

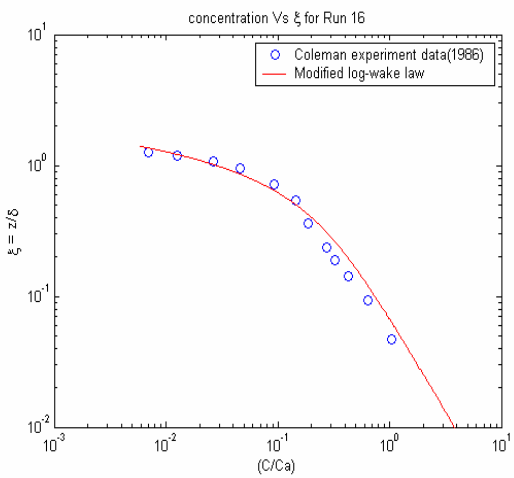
concentration Vs ξ for Run 16
Coleman experiment data(1986)
Modified log-wake law
ξ = z/δ
(C/Ca)

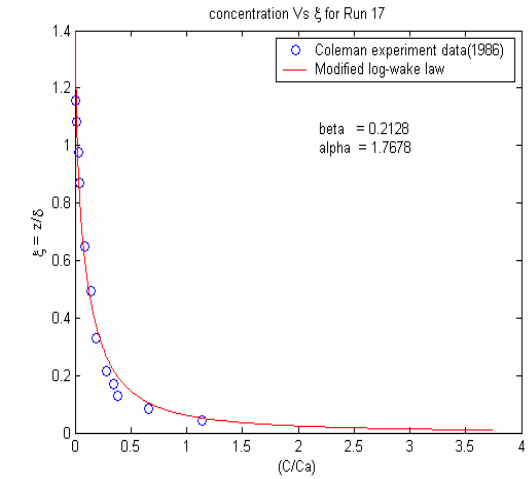
concentration Vs ξ for Run 17
Coleman experiment data(1986)
Modified log-wake law
beta = 0.2128
alpha = 1.7678
ξ = z/δ
(C/Ca)

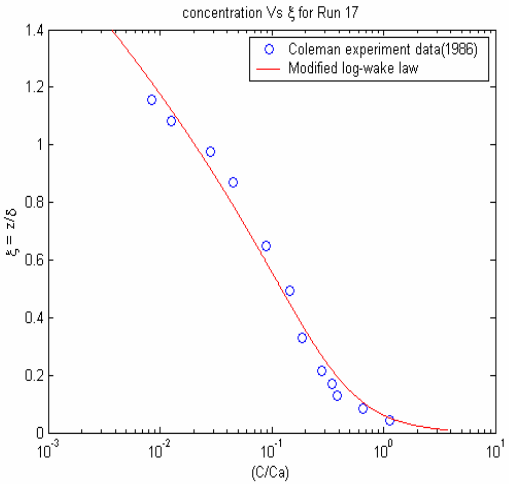
concentration Vs ξ for Run 17
Coleman experiment data(1986)
Modified log-wake law
ξ = z/δ
(C/Ca)

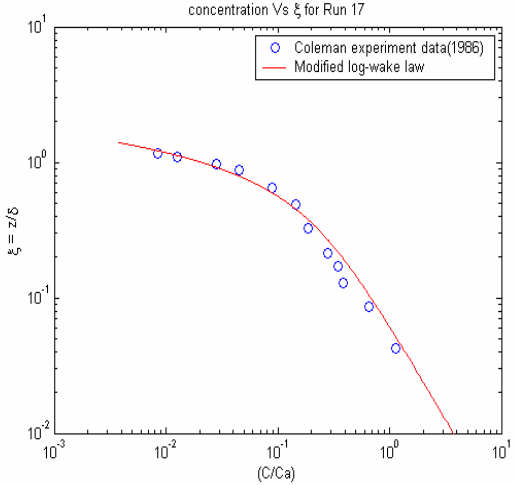
concentration Vs ξ for Run 17
Coleman experiment data(1986)
Modified log-wake law
ξ = z/δ
(C/Ca)

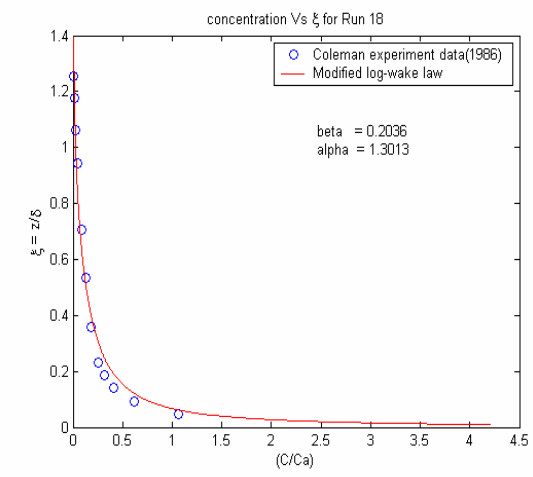
concentration Vs ξ for Run 18
Coleman experiment data(1986)
Modified log-wake law
beta = 0.2036
alpha = 1.3013
ξ = z/δ
(C/Ca)

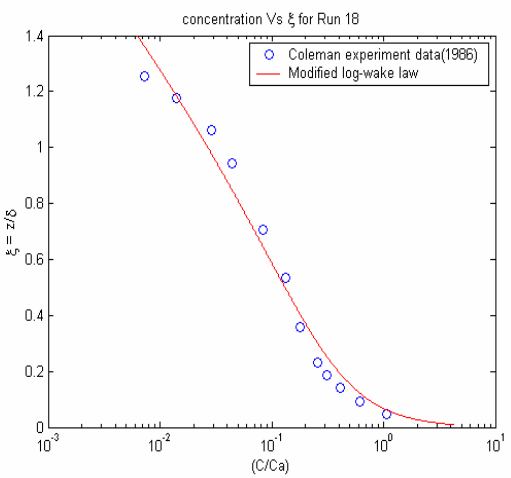
concentration Vs ξ for Run 18
Coleman experiment data(1986)
Modified log-wake law
ξ = z/δ
(C/Ca)

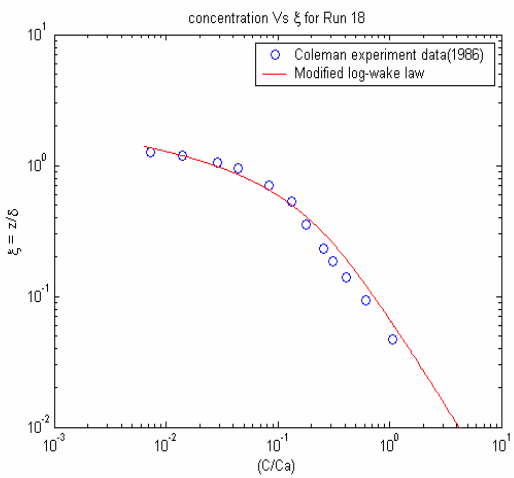
concentration Vs ξ for Run 18
Coleman experiment data(1986)
Modified log-wake law
ξ = z/δ
(C/Ca)

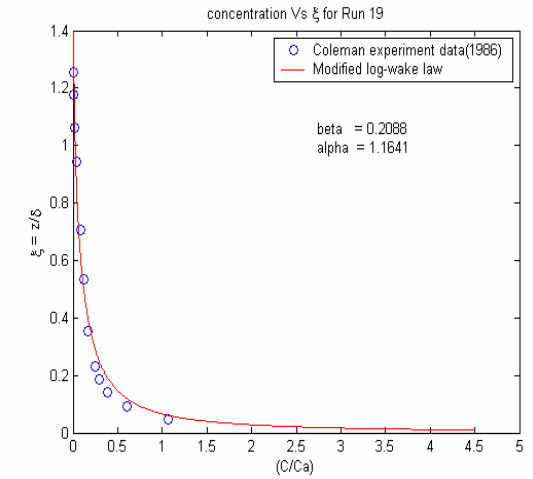
concentration Vs ξ for Run 19
Coleman experiment data(1986)
Modified log-wake law
beta = 0.2088
alpha = 1.1641
ξ = z/δ
(C/Ca)

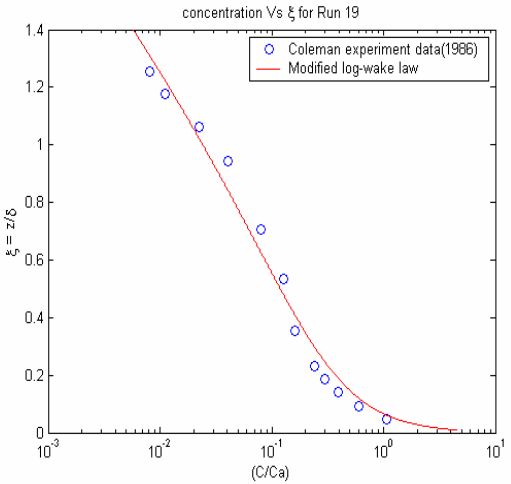
concentration Vs ξ for Run 19
Coleman experiment data(1986)
Modified log-wake law
ξ = z/δ
(C/Ca)

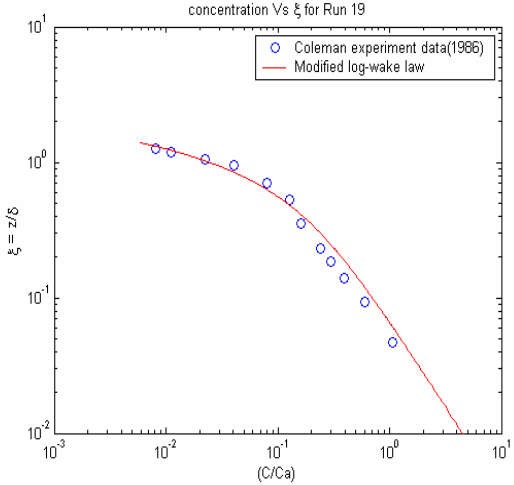
concentration Vs ξ for Run 19
Coleman experiment data(1986)
Modified log-wake law
ξ = z/δ
(C/Ca)

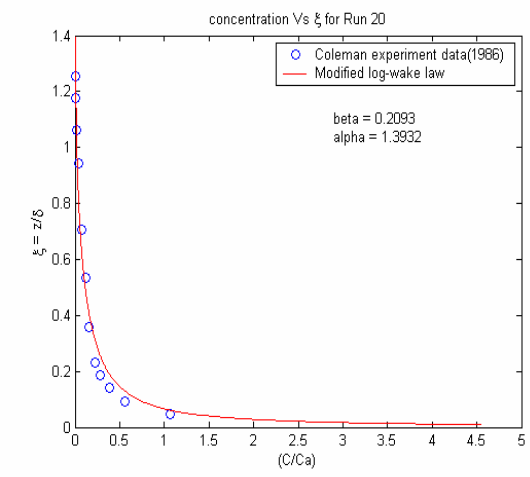
concentration Vs ξ for Run 20
Coleman experiment data(1986)
Modified log-wake law
beta = 0.2093
alpha = 1.3932
ξ = z/δ
(C/Ca)

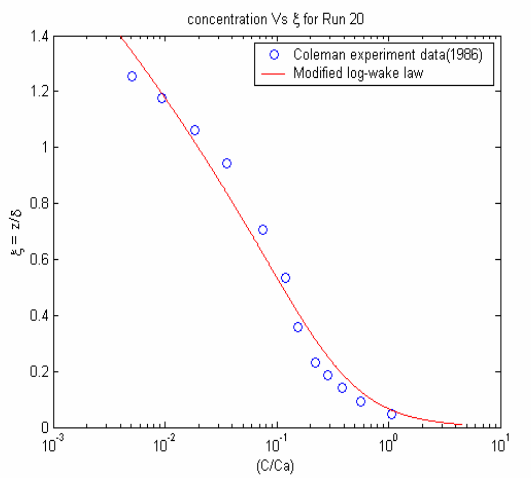
concentration Vs ξ for Run 20
Coleman experiment data(1986)
Modified log-wake law
ξ = z/δ
(C/Ca)

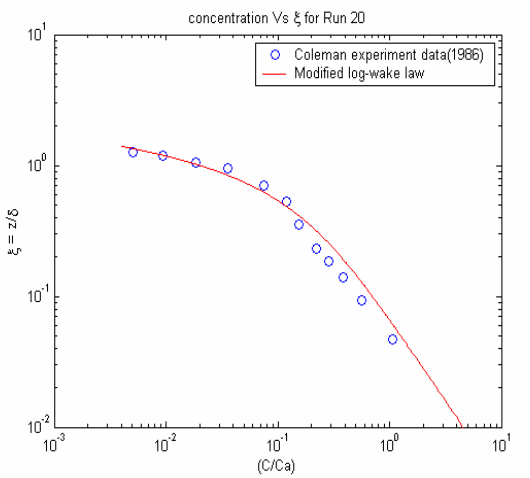
concentration Vs ξ for Run 20
Coleman experiment data(1986)
Modified log-wake law
ξ = z/δ
(C/Ca)

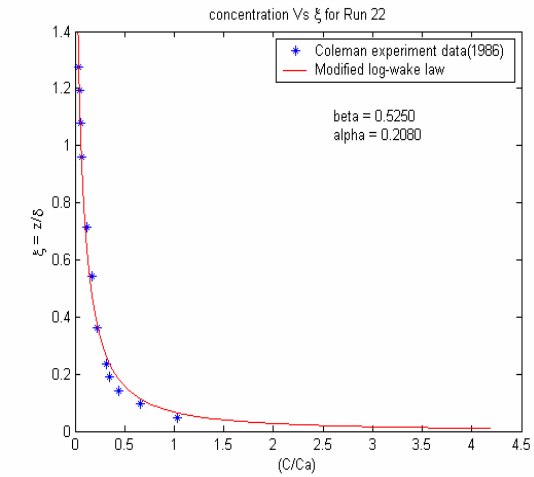
concentration Vs ξ for Run 22
Coleman experiment data(1986)
Modified log-wake law
beta = 0.5250
alpha = 0.2080
ξ = z/δ
(C/Ca)

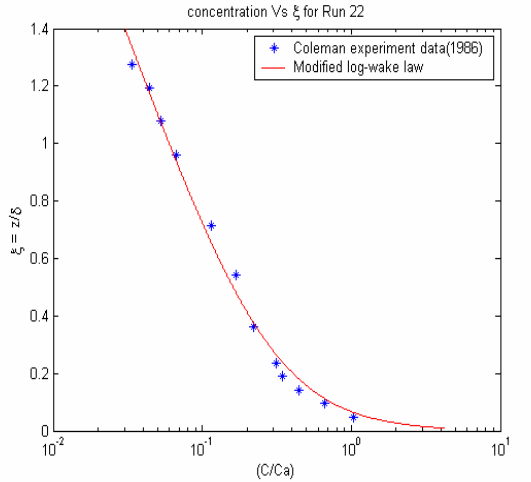
concentration Vs ξ for Run 22
Coleman experiment data(1986)
Modified log-wake law
ξ = z/δ
(C/Ca)

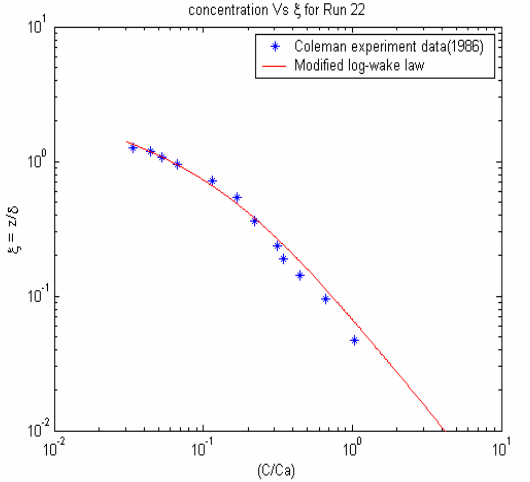
concentration Vs ξ for Run 22
Coleman experiment data(1986)
Modified log-wake law
ξ = z/δ
(C/Ca)

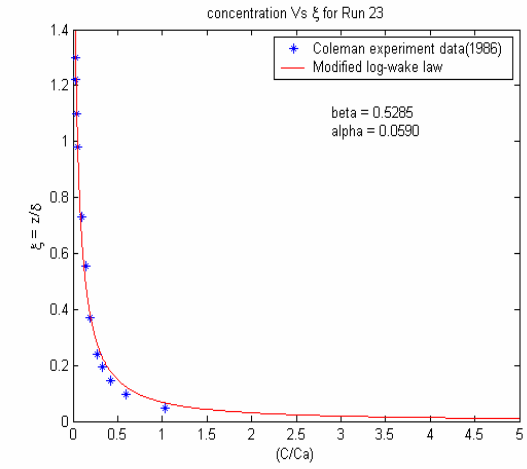
concentration Vs ξ for Run 23
Coleman experiment data(1986)
Modified log-wake law
beta = 0.5285
alpha = 0.0590
ξ = z/δ
(C/Ca)

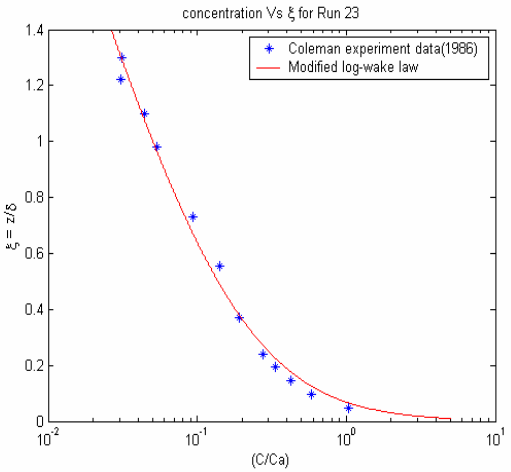
concentration Vs ξ for Run 23
Coleman experiment data(1986)
Modified log-wake law
ξ = z/δ
(C/Ca)

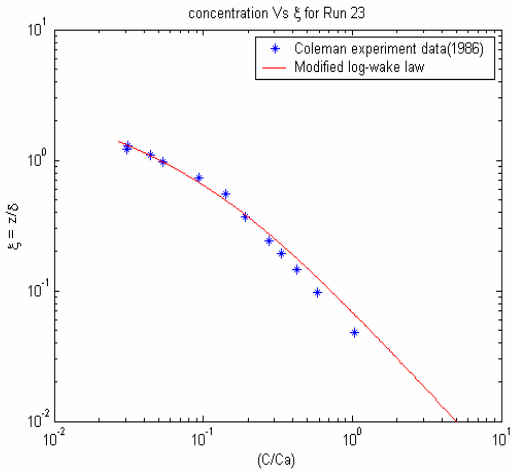
concentration Vs ξ for Run 23
Coleman experiment data(1986)
Modified log-wake law
ξ = z/δ
(C/Ca)

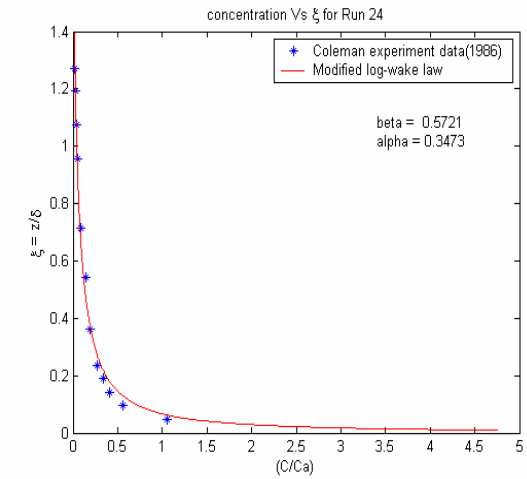
concentration Vs ξ for Run 24
Coleman experiment data(1986)
Modified log-wake law
beta = 0.5721
alpha = 0.3473
ξ = z/δ
(C/Ca)

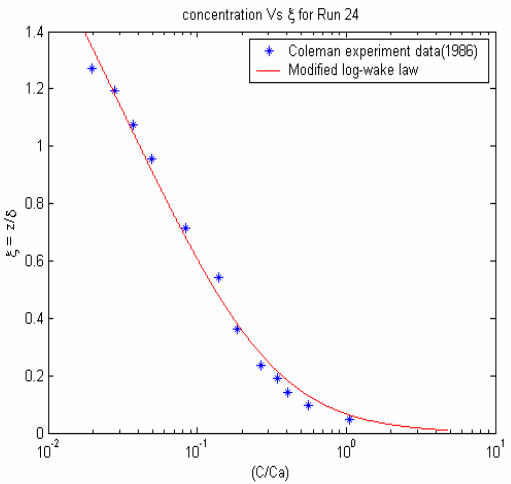
concentration Vs ξ for Run 24
Coleman experiment data(1986)
Modified log-wake law
ξ = z/δ
(C/Ca)

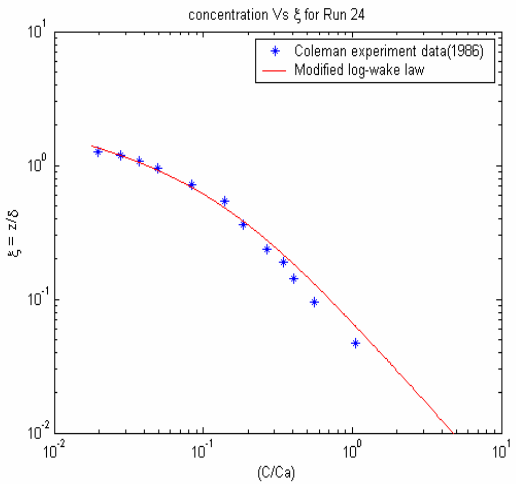
concentration Vs ξ for Run 24
Coleman experiment data(1986)
Modified log-wake law
ξ = z/δ
(C/Ca)

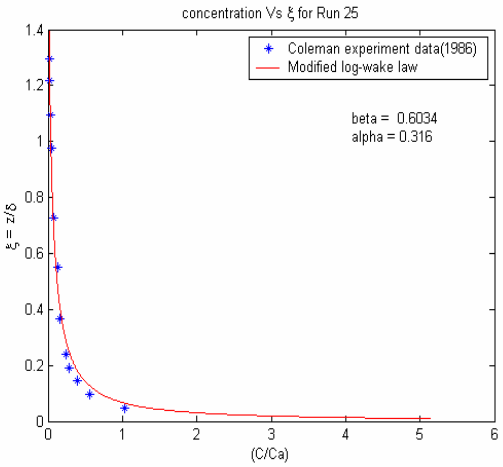
concentration Vs ξ for Run 25
Coleman experiment data(1986)
Modified log-wake law
beta = 0.6034
alpha = 0.316
ξ = z/δ
(C/Ca)

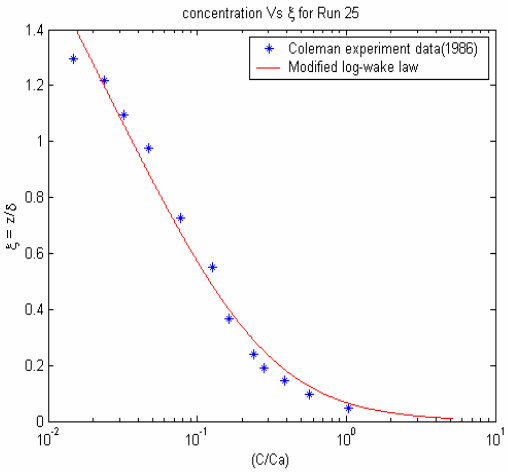
concentration Vs ξ for Run 25
Coleman experiment data(1986)
Modified log-wake law
ξ = z/δ
(C/Ca)

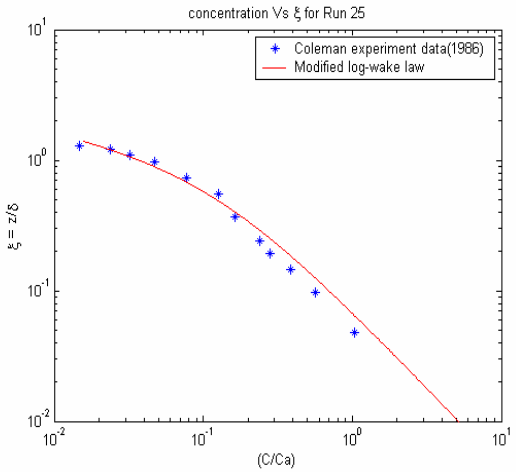
concentration Vs ξ for Run 25
Coleman experiment data(1986)
Modified log-wake law
ξ = z/δ
(C/Ca)

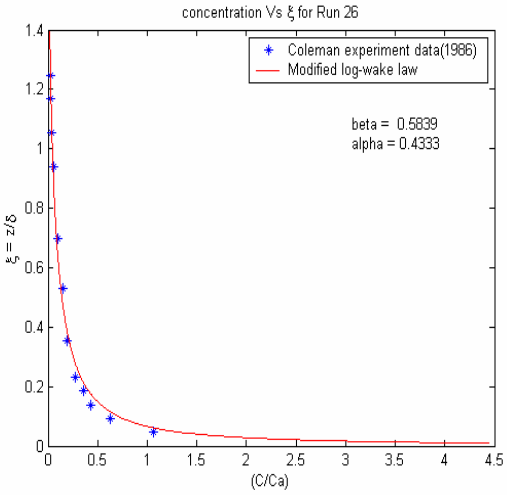
concentration Vs ξ for Run 26
Coleman experiment data(1986)
Modified log-wake law
beta = 0.5839
alpha = 0.4333
ξ = z/δ
(C/Ca)

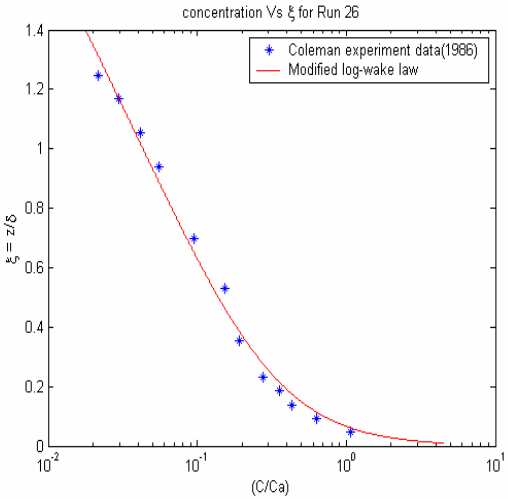
concentration Vs ξ for Run 26
Coleman experiment data(1986)
Modified log-wake law
ξ = z/δ
(C/Ca)

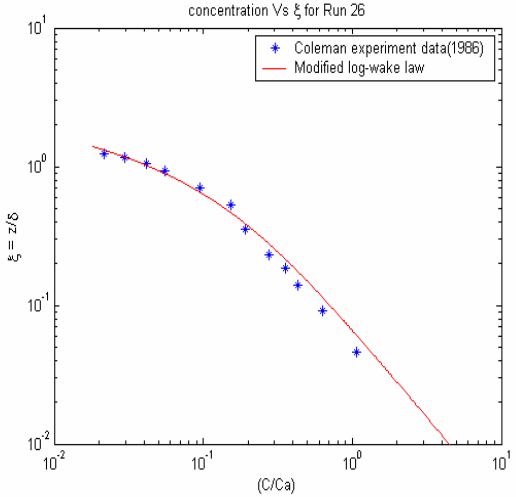
concentration Vs ξ for Run 26
Coleman experiment data(1986)
Modified log-wake law
ξ = z/δ
(C/Ca)

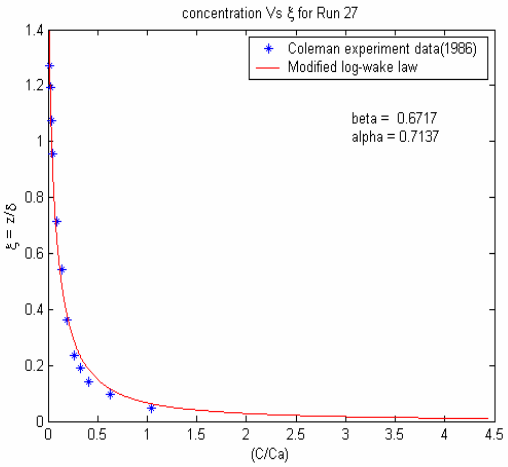
concentration Vs ξ for Run 27
Coleman experiment data(1986)
Modified log-wake law
beta = 0.6717
alpha = 0.7137
ξ = z/δ
(C/Ca)

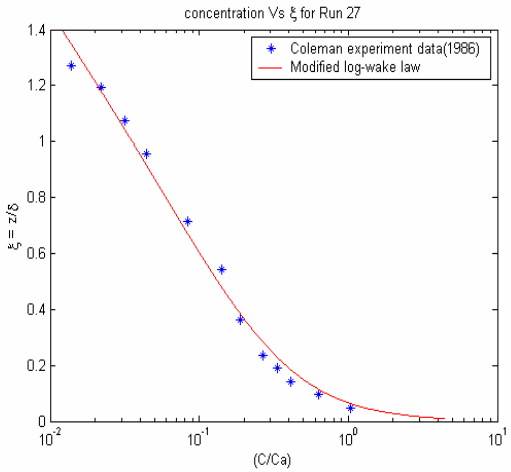
concentration Vs ξ for Run 27
Coleman experiment data(1986)
Modified log-wake law
ξ = z/δ
(C/Ca)

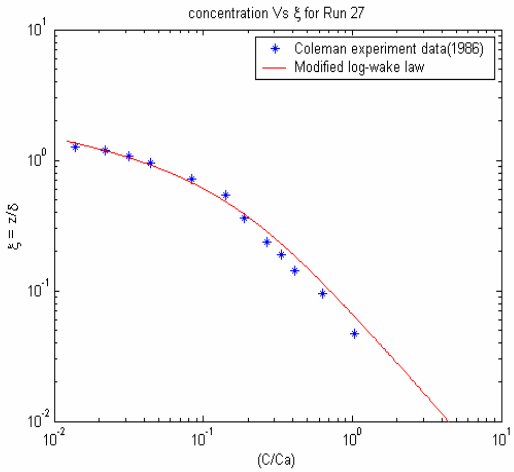
concentration Vs ξ for Run 27
Coleman experiment data(1986)
Modified log-wake law
ξ = z/δ
(C/Ca)

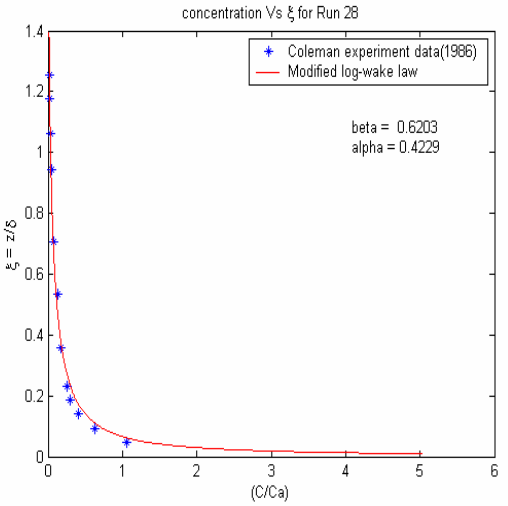
concentration Vs ξ for Run 28
Coleman experiment data(1986)
Modified log-wake law
beta = 0.6203
alpha = 0.4229
ξ = z/δ
(C/Ca)

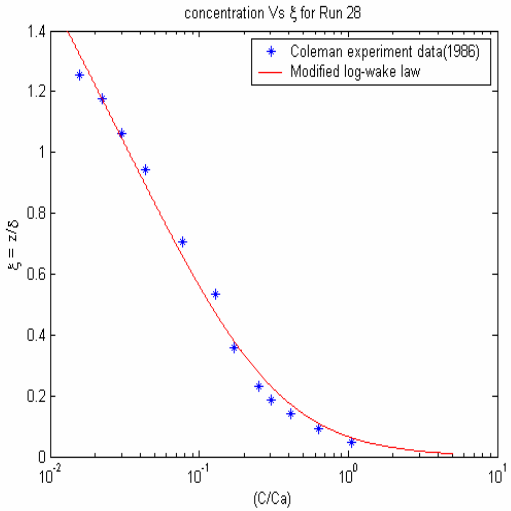
concentration Vs ξ for Run 28
Coleman experiment data(1986)
Modified log-wake law
ξ = z/δ
(C/Ca)

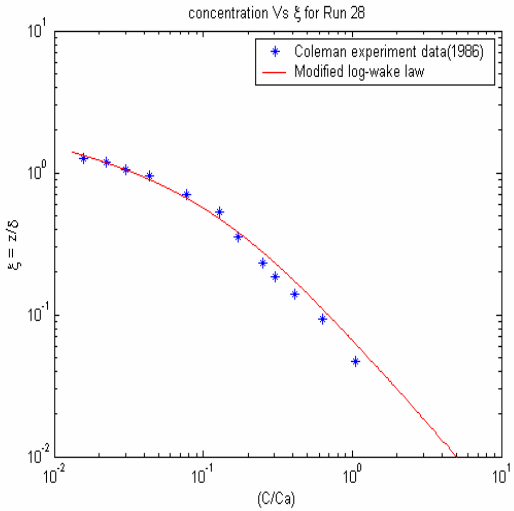
concentration Vs ξ for Run 28
Coleman experiment data(1986)
Modified log-wake law
ξ = z/δ
(C/Ca)

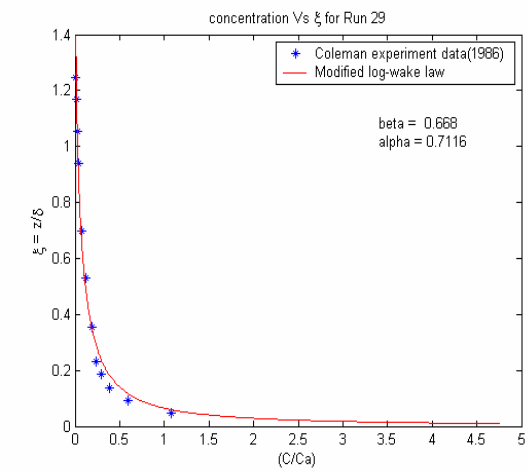
concentration Vs ξ for Run 29
Coleman experiment data(1986)
Modified log-wake law
beta = 0.668
alpha = 0.7116
ξ = z/δ
(C/Ca)

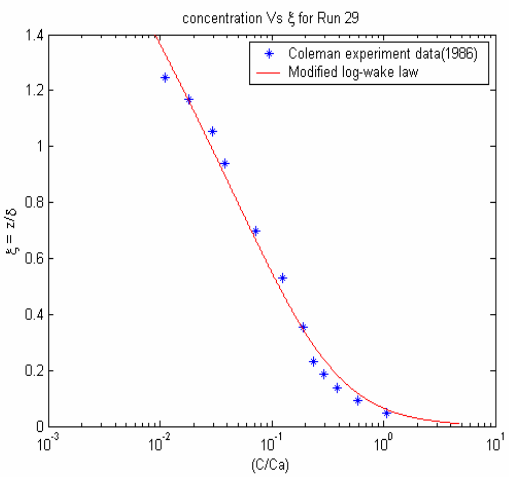
concentration Vs ξ for Run 29
Coleman experiment data(1986)
Modified log-wake law
ξ = z/δ
(C/Ca)

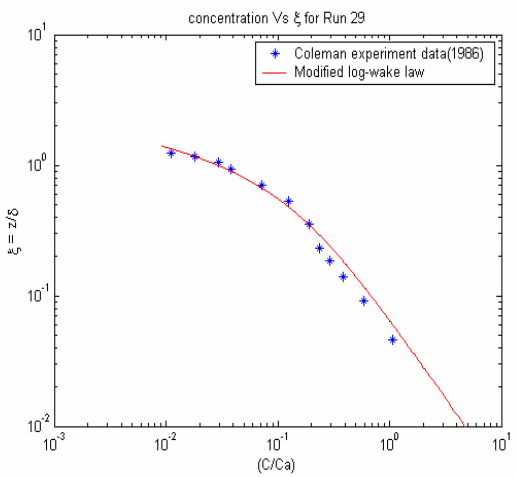
concentration Vs ξ for Run 29
Coleman experiment data(1986)
Modified log-wake law
ξ = z/δ
(C/Ca)

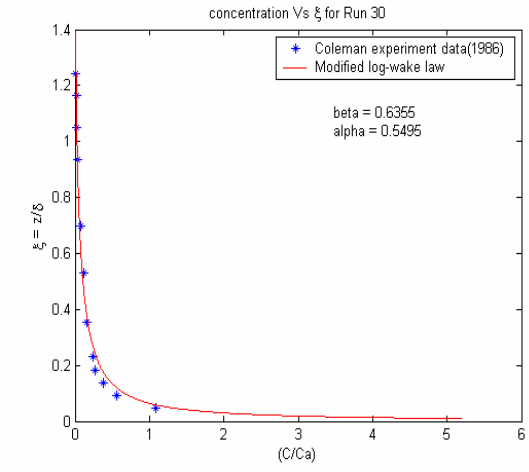
concentration Vs ξ for Run 30
Coleman experiment data(1986)
Modified log-wake law
beta = 0.6355
alpha = 0.5495
ξ = z/δ
(C/Ca)

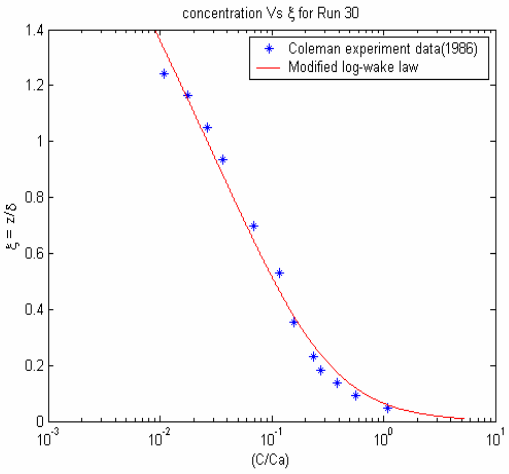
concentration Vs ξ for Run 30
Coleman experiment data(1986)
Modified log-wake law
ξ = z/δ
(C/Ca)

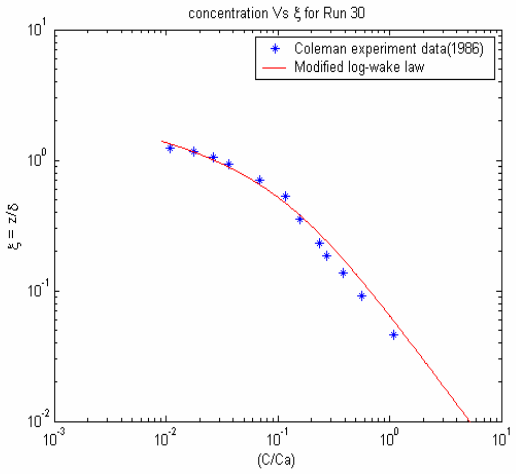
concentration Vs ξ for Run 30
Coleman experiment data(1986)
Modified log-wake law
ξ = z/δ
(C/Ca)

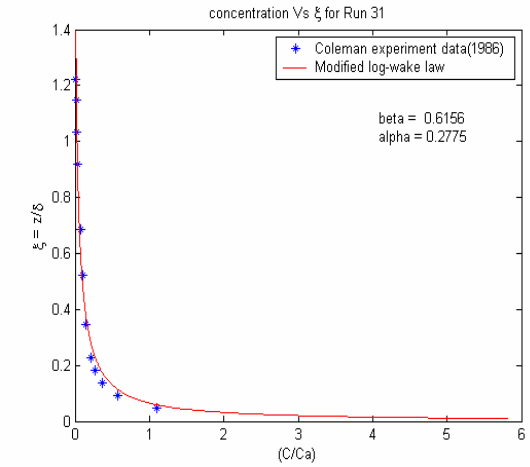
concentration Vs ξ for Run 31
Coleman experiment data(1986)
Modified log-wake law
beta = 0.6156
alpha = 0.2775
ξ = z/δ
(C/Ca)

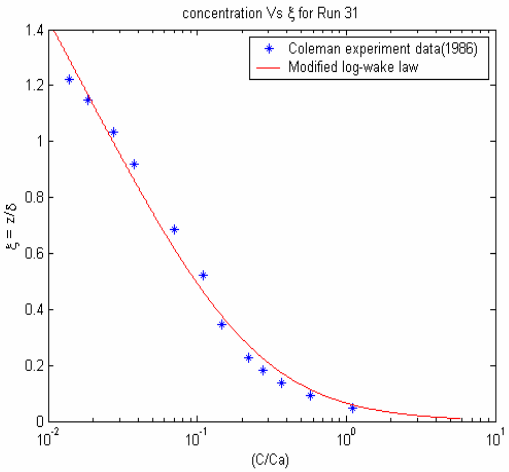
concentration Vs ξ for Run 31
Coleman experiment data(1986)
Modified log-wake law
ξ = z/δ
(C/Ca)

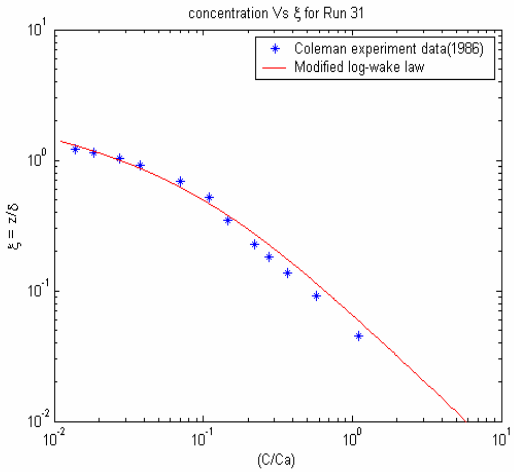
concentration Vs ξ for Run 31
Coleman experiment data(1986)
Modified log-wake law
ξ = z/δ
(C/Ca)

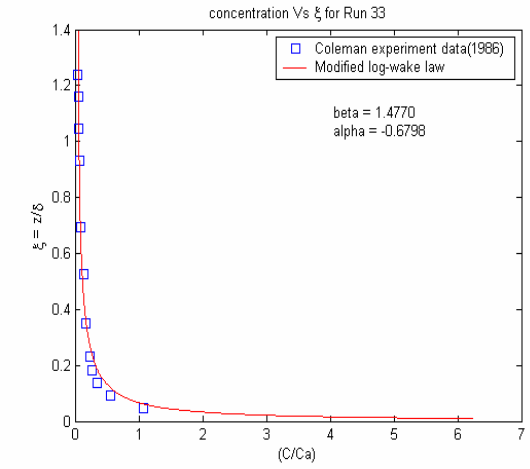
concentration Vs ξ for Run 33
Coleman experiment data(1986)
Modified log-wake law
beta = 1.4770
alpha = -0.6798
ξ = z/δ
(C/Ca)

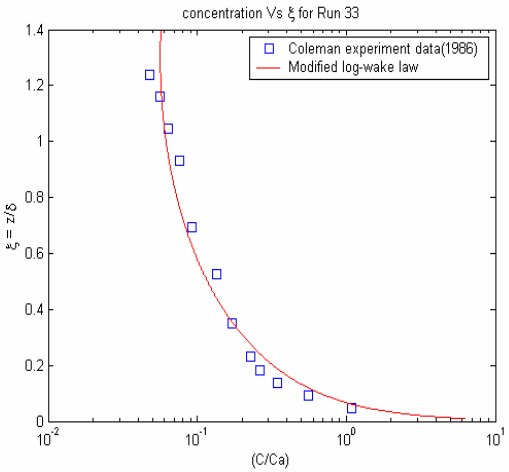
concentration Vs ξ for Run 33
Coleman experiment data(1986)
Modified log-wake law
ξ = z/δ
(C/Ca)

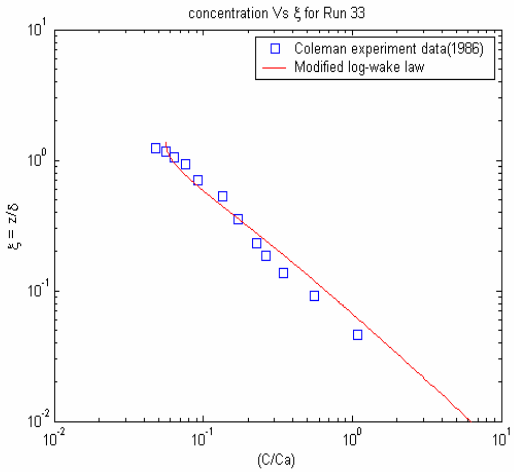
concentration Vs ξ for Run 33
Coleman experiment data(1986)
Modified log-wake law
ξ = z/δ
(C/Ca)

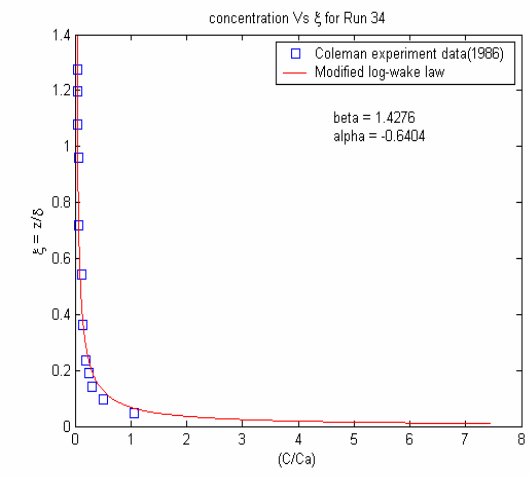
concentration Vs ξ for Run 34
Coleman experiment data(1986)
Modified log-wake law
beta = 1.4276
alpha = -0.6404
ξ = z/δ
(C/Ca)

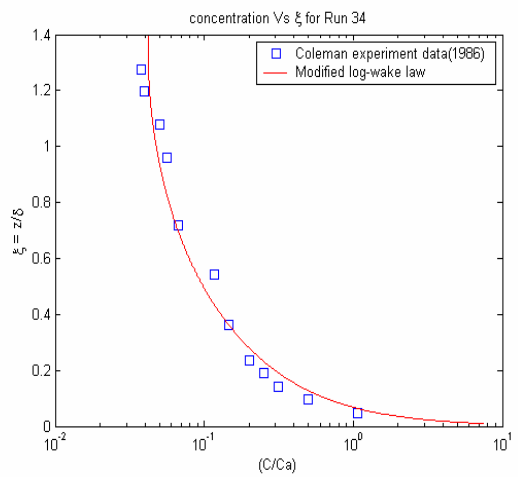
concentration Vs ξ for Run 34
Coleman experiment data(1986)
Modified log-wake law
ξ = z/δ
(C/Ca)

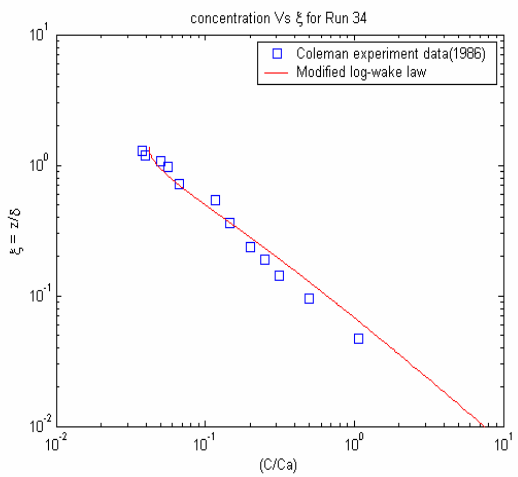
concentration Vs ξ for Run 34
Coleman experiment data(1986)
Modified log-wake law
ξ = z/δ
(C/Ca)

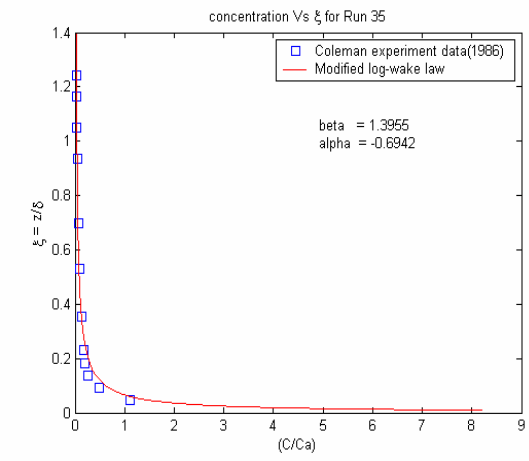
concentration Vs ξ for Run 35
Coleman experiment data(1986)
Modified log-wake law
beta = 1.3955
alpha = -0.6942
ξ = z/δ
(C/Ca)

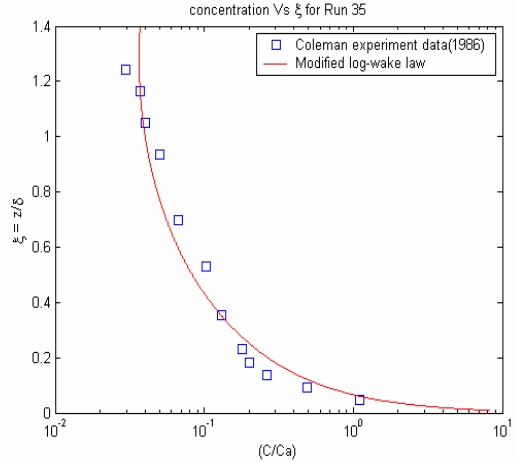
concentration Vs ξ for Run 35
Coleman experiment data(1986)
Modified log-wake law
ξ = z/δ
(C/Ca)

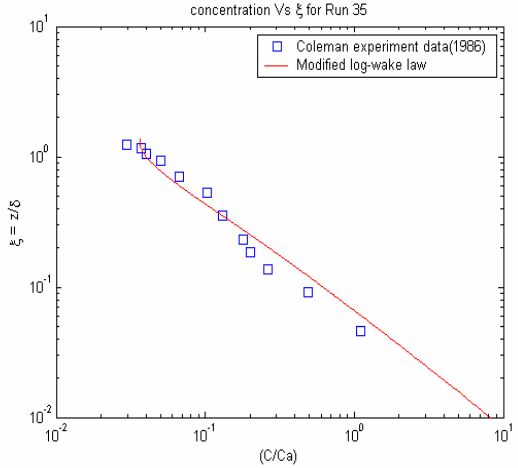
concentration Vs ξ for Run 35
Coleman experiment data(1986)
Modified log-wake law
ξ = z/δ
(C/Ca)

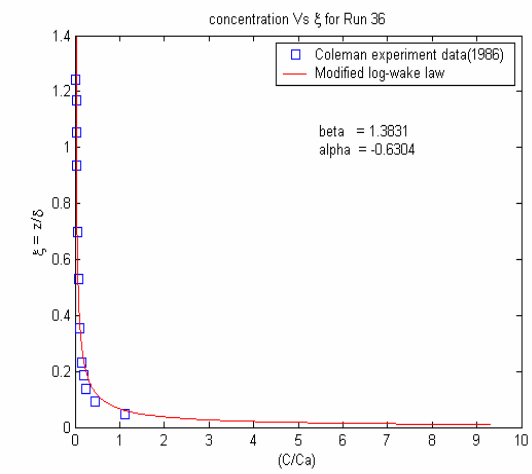
concentration Vs ξ for Run 36
Coleman experiment data(1986)
Modified log-wake law
beta = 1.3831
alpha = -0.6304
ξ = z/δ
(C/Ca)

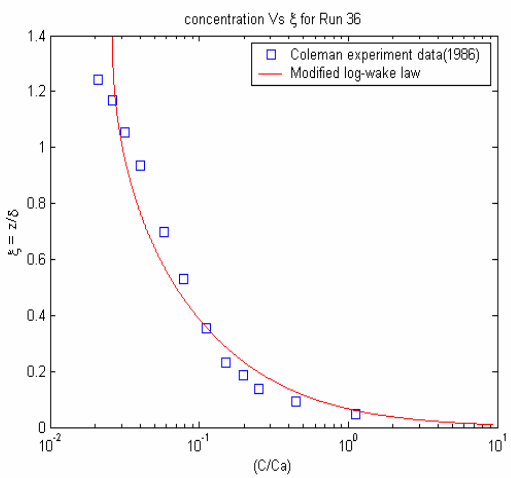
concentration Vs ξ for Run 36
Coleman experiment data(1986)
Modified log-wake law
ξ = z/δ
(C/Ca)

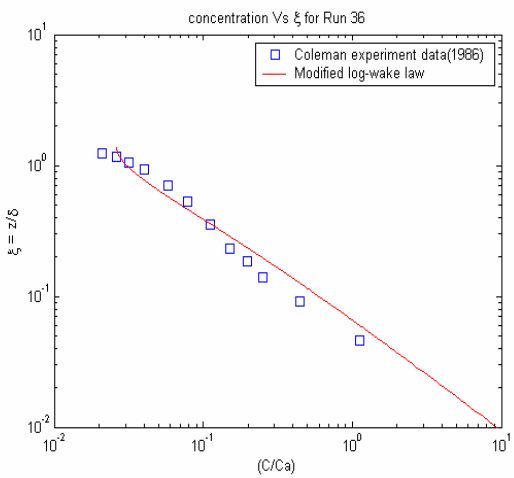
concentration Vs ξ for Run 36
Coleman experiment data(1986)
Modified log-wake law
ξ = z/δ
(C/Ca)

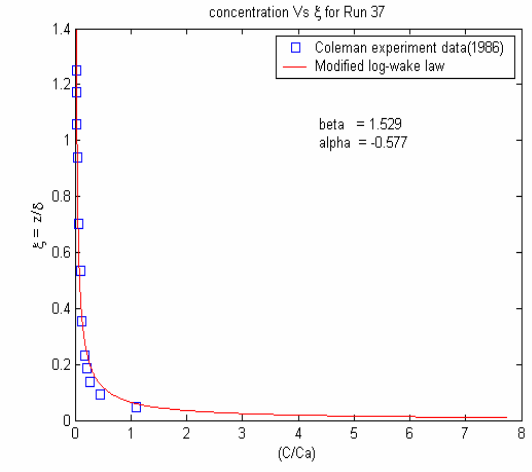
concentration Vs ξ for Run 37
Coleman experiment data(1986)
Modified log-wake law
beta = 1.529
alpha = -0.577
ξ = z/δ
(C/Ca)

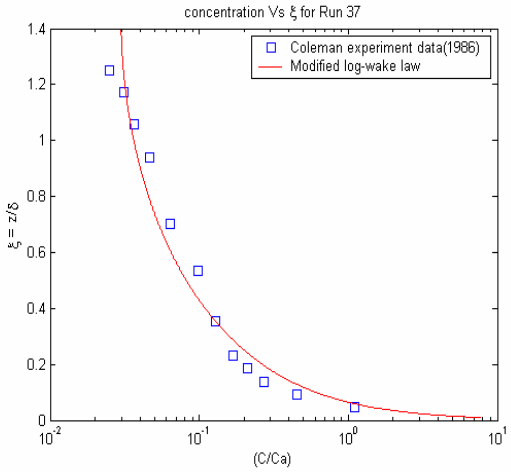
concentration Vs ξ for Run 37
Coleman experiment data(1986)
Modified log-wake law
ξ = z/δ
(C/Ca)

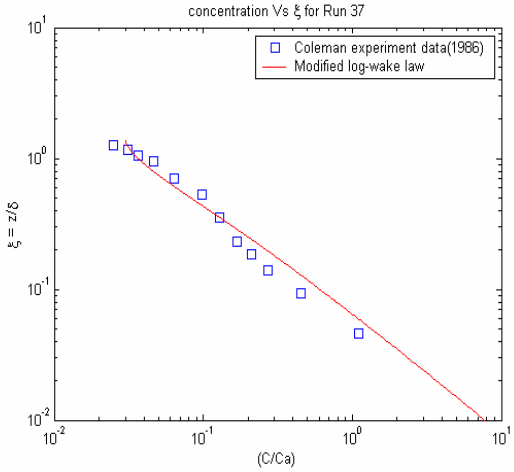
concentration Vs ξ for Run 37
Coleman experiment data(1986)
Modified log-wake law
ξ = z/δ
(C/Ca)

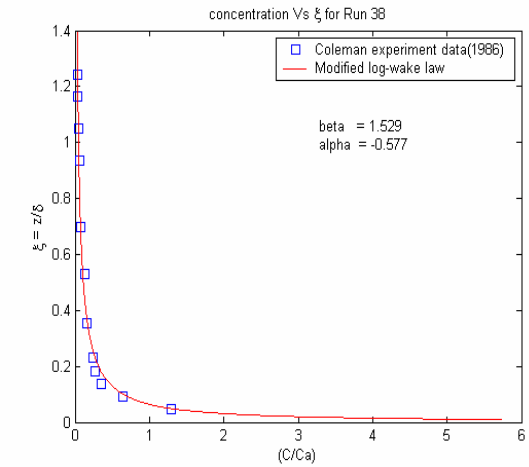
concentration Vs ξ for Run 38
Coleman experiment data(1986)
Modified log-wake law
beta = 1.529
alpha = -0.577
ξ = z/δ
(C/Ca)

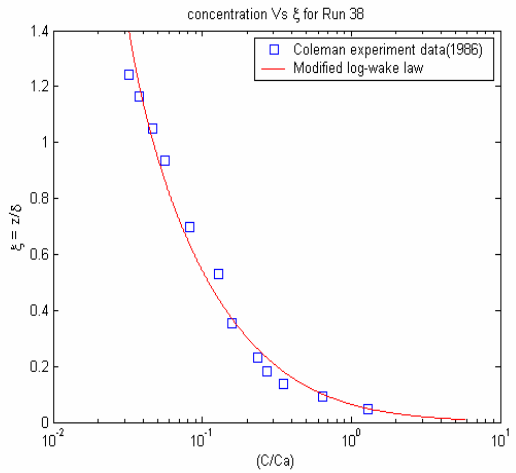
concentration Vs ξ for Run 38
Coleman experiment data(1986)
Modified log-wake law
ξ = z/δ
(C/Ca)

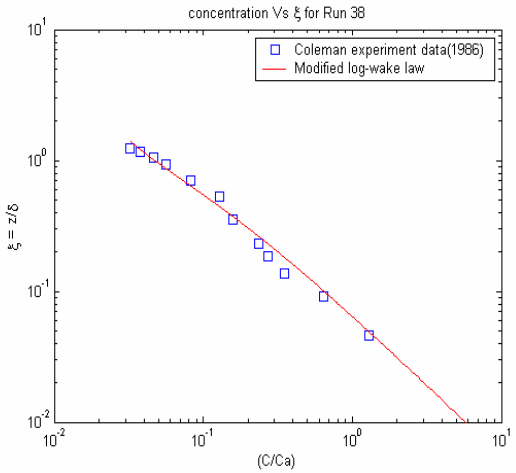
concentration Vs ξ for Run 38
Coleman experiment data(1986)
Modified log-wake law
ξ = z/δ
(C/Ca)

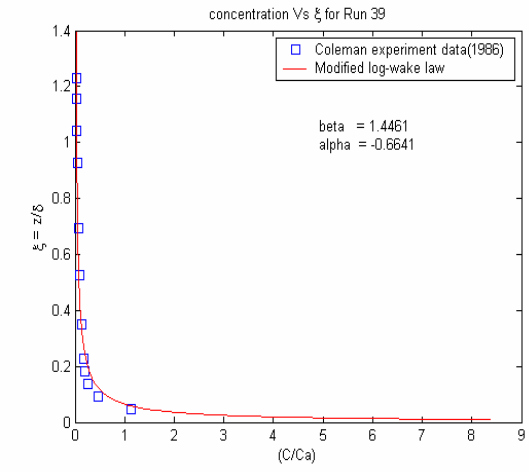
concentration Vs ξ for Run 39
Coleman experiment data(1986)
Modified log-wake law
beta = 1.4461
alpha = -0.6641
ξ = z/δ
(C/Ca)

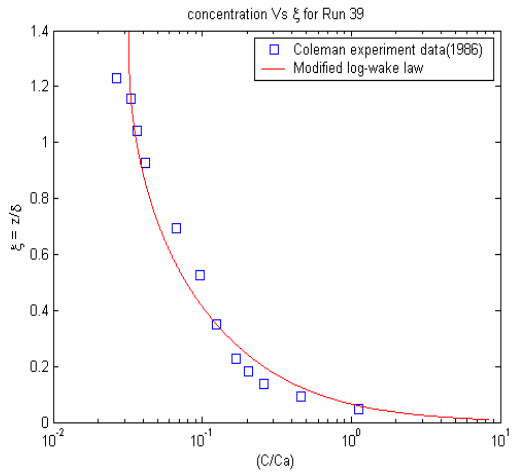
concentration Vs ξ for Run 39
Coleman experiment data(1986)
Modified log-wake law
ξ = z/δ
(C/Ca)

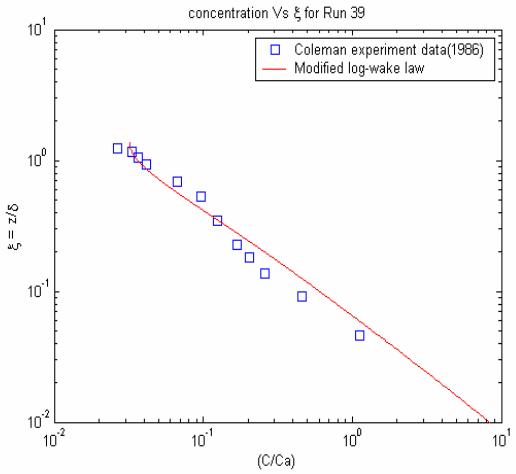
concentration Vs ξ for Run 39
Coleman experiment data(1986)
Modified log-wake law
ξ = z/δ
(C/Ca)

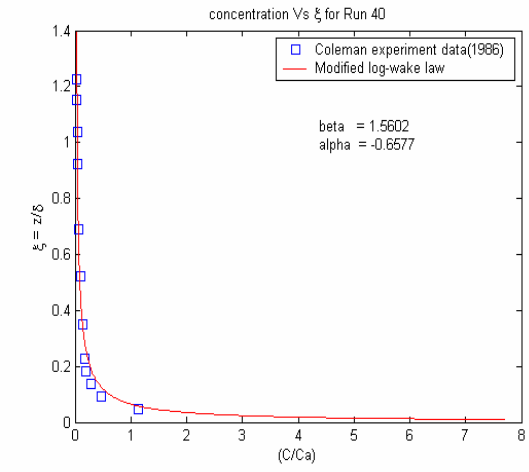
concentration Vs ξ for Run 40
Coleman experiment data(1986)
Modified log-wake law
beta = 1.5602
alpha = -0.6577
ξ = z/δ
(C/Ca)

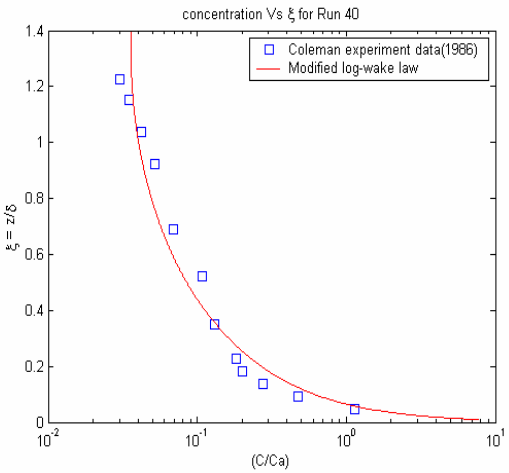
concentration Vs ξ for Run 40
Coleman experiment data(1986)
Modified log-wake law
ξ = z/δ
(C/Ca)

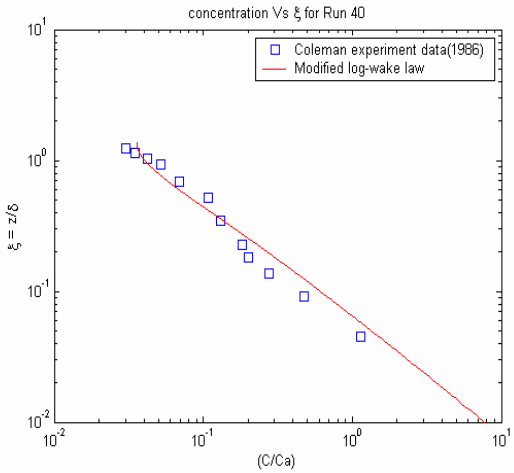
concentration Vs ξ for Run 40
Coleman experiment data(1986)
Modified log-wake law
ξ = z/δ
(C/Ca)